Petrophysics of the Northern Browse Basin

Irma Savitri Widiasri

(B.Sc in Mathematics
Institut Teknologi Bandung, Indonesia)

This thesis is submitted in partial fulfillment of the requirements for the
Master of Science (Petroleum Geoscience)

Australian School of Petroleum
The University of Adelaide

November, 2007

ABSTRACT

The Northern Browse Basin, located on the North West Shelf of Australia, is a gas province with minor oil accumulations. Significant gas discoveries have been made within the Caswell Sub-basin, including the Scott Reef, Brecknock, Brecknock South and Brewster Fields. This area is a focus of exploration for the Chevron Australia Business Unit (Chevron ASBU). With the increasing potential for commercialization of the long-discovered gas in the Northern Browse Basin, Chevron ASBU's interest, and the aim of this project, is to identify any additional unrecognized gas reservoirs in the Late Triassic to Late Cretaceous rocks of the Northern Browse Basin. The section of interest covers the Nome, Plover, Lower Vulcan, Upper Vulcan, Echuca Shoals, Jamieson, Woolaston, Fenelon/Gibson and Puffin Formations. Petrophysical analysis of well logs was undertaken to identify unrecognized potential reservoirs.

A stepwise methodology was undertaken in this study. Log editing, pre-calculation and environmental corrections were first performed. A deterministic method was then used in the petrophysical analysis. The lowest of the estimates from the gamma ray and the density-neutron combination was taken as the shale volume. The Raymer-Hunt-Gardner sonic porosity transform was then used to calculate the porosity, with calibration to core data. Water saturation was determined using the dual water method for shaly sand.

A major uncertainty of this study was the determination of formation water resistivity (*Rw*). Formation water resistivity was determined using Pickett plots and assumed to be the same through the entire Late Triassic-Late Cretaceous sequence analyzed in each well. The resultant *Rw* values describe the salinity distribution within the study area. Salinity generally increases from southwest to northeast, with a range from 12,000 to 80,000 ppm.

Twelve out of the 16 analyzed wells were interpreted to contain potential net pay, which was encountered in the Puffin, Jamieson, Echuca Shoals and Upper Vulcan Formations. In the Puffin Formation, significant potential net pay was interpreted in Gryphaea-1, Discorbis-1 and

Kalyptea-1ST1, with the greatest thickness of 127 m being identified in Kalyptea-1ST1. Potential net pay in this formation has good reservoir quality, with an average of 17% shale volume, 20% porosity and 50% water saturation. Potential net pay in the Jamieson Formation averaged 25 m in thickness and 20% porosity. A half of the wells that encountered the Echuca Shoals Formation are interpreted to contain potential net pay in that unit, with the maximum thickness being 61 m in Adele-1. A very significant potential net pay of 430 m was interpreted in the Upper Vulcan Formation in Heywood-1. The Upper Vulcan Formation has good reservoir quality with an average of 125 m net pay thickness and 10% porosity in five out of seven wells.

This project was a reconnaissance study for possible unrecognized reservoirs in the Northern Browse Basin. It has identified many possible potential reservoirs and follow-up study should focus on re-analyzing the intervals highlighted here. A reservoir by reservoir analysis, especially when picking the parameter, such as *Rw*, would reduce the uncertainties. A probabilistic method of log analysis e.g. Multimin in Geolog (which was briefly attempted here), should be investigated as a replacement for deterministic methods such as the one used in this study.

STATEMENT OF CONFIDENTIALITY

Due to confidentiality agreement between Chevron Company and the Australian School of Petroleum, this thesis is not available for public inspection or borrowing until 5 November 2010.

ACKNOWLEDGEMENTS

I am grateful to the Almighty Allah SWT for all blessing and favor that made this thesis possible.

I would like to express my gratitude to Chevron IBU for supporting this project. A special thanks to Christopher Davin and Randall Cooper for giving me the opportunity to undertake this program. My appreciation is to Chevron ASBU for providing the essential data for this project. Particularly, I thank Justyn Wood and Michael Wilson for their assistance during my internship in Perth and their advice during the project. Many thanks also to Occam Technology Pty Ltd of Adelaide for supplying additional data.

I would particularly like to thank my supervisor, Prof. Richard Hillis and my co-supervisor, Dr. Bruce Ainsworth, for their technical guidance and valuable advice. I would also like to thank Sigit Sutiyono for support. Thanks also to Andy Mitchell and Zuraidah for assistance with Geolog.

Most importantly, I am indebted to my parents, my beloved family, and my great friends in Indonesia and Australia who give me never-ending support, caring and great motivation. Thanks to all the staff and students of the Australian School of Petroleum for a wonderful year and experience.

TABLE OF CONTENTS

LIST OF SYMBOLS

a : Constant, equal to 1
C : Porosity factor
CEC : Cation exchange capacity
C_t : Conductivity of the uninvaded formation
C_w : Conductivity of formation water
C_{wb} : Conductivity of bound water
C_{we} : Equivalent conductivity of the water in the pore space
Δt_{ma} : Sonic matrix
$GR_{\max}$: Gamma ray shale (GAPI)
$GR_{\min}$: Gamma ray matrix (GAPI)
m : Cementation exponent
n : Saturation exponent
ϕ_{cwb} : Porosity of clay bound water
ϕ_e : Effective porosity
$\phi_{e_{\max}}$: The maximum value of effective porosity
ϕ_{fw} : Porosity of free water
ϕ_h : Porosity of hydrocarbon
ϕ_t : Total porosity
ϕ_{tsh} : Shale total porosity, equal to volume of clay bound water
Q_v : CEC of the rock per unit pore volume
R_0 : True formation resistivity where the pore space is 100% water saturated (ohmm)
R_t : True formation resistivity (ohmm)
R_{xo} : Formation resistivity in flushed zone (ohmm)
R_w : Formation water resistivity (ohmm)
S_{wb} : Bound water saturation
S_{we} : Effective water saturation
S_{wt} : Total water saturation
Vsh : Shale volume
V_w : Bulk volumes of formation water
V_{wb} : Bulk volumes of bound water

1 Introduction

1.1 Background

The Northern Browse Basin is located 150-400 km off the northwest coast of Western Australia (Figure 1.1). The area is located on the North West Shelf of Australia in 100 – 600 m of water and immediately north of the giant Gorgon/Ichthys-Brewster gas field (Australian Government, 2004).

The North West Shelf of Australia is predominantly a gas province with relatively minor oil accumulations. Previous studies of this region argued that the probability of oil discovery in this area is low (Longley et al., 2002). However, the probability of gas discovery is high, although their commercial value is determined by the market demand (Longley et al., 2002). Significant discoveries have been made in the Browse Basin within the Caswell Sub-basin, including four large undeveloped gas/condensate fields: Scott Reef, Brecknock, Brecknock South, and Brewster. A number of smaller gas accumulations have also been discovered at Adele, Arquebus, Echuca Shoals, Crux and Argus Fields.

1.2 Study Area

The study encompasses 20 wells within the Northern Browse Basin (Figure 1.1). These wells span an area of approximately 45,000 km^2. Eighteen wells were drilled in the Caswell Sub-basin and the remaining two on the Ashmore Platform. The stratigraphic interval of interest is the Late Triassic to Cretaceous section, comprising the Nome, Plover, Lower Vulcan, Upper Vulcan, Echuca Shoals, Jamieson, Woolaston, Fenelon/Gibson and Puffin Formations.

1.3 Study Objectives

The aim of the project is the petrophysical analysis of the 20 wells located within the study area. Shale volume, porosity and water saturation, were calculated from wireline log and core data over the Late Triassic to Cretaceous interval in the 20 wells.

The study is driven by the increasing commerciality of gas fields in the Northern Browse Basin. The objective of the study was to identify whether any unrecognized gas reservoirs may have been intersected by the existing wells.

1.4 Data

The data used in this study consists of digital wireline log and LWD (Logging While Drilling) data, composite well logs, formation sample (cuttings and core), palynology, petrology, micropaleontology and well summary reports. Most of the data was provided by Chevron Australia Business Unit (ASBU). Occam Technology Pty Ltd supplied digital log data for six of the wells.

1.5 Chevron Interest

This project was sponsored by Chevron IBU (Indonesia Business Unit). Chevron ASBU proposed the study region which is in their current exploration focus area. Chevron interest in this area is witnessed by its participation in the Browse Joint Venture. Chevron and its Browse Joint Venture partners are investigating options for LNG development to process gas from gas fields in the Browse Basin (Chevron, 2007).

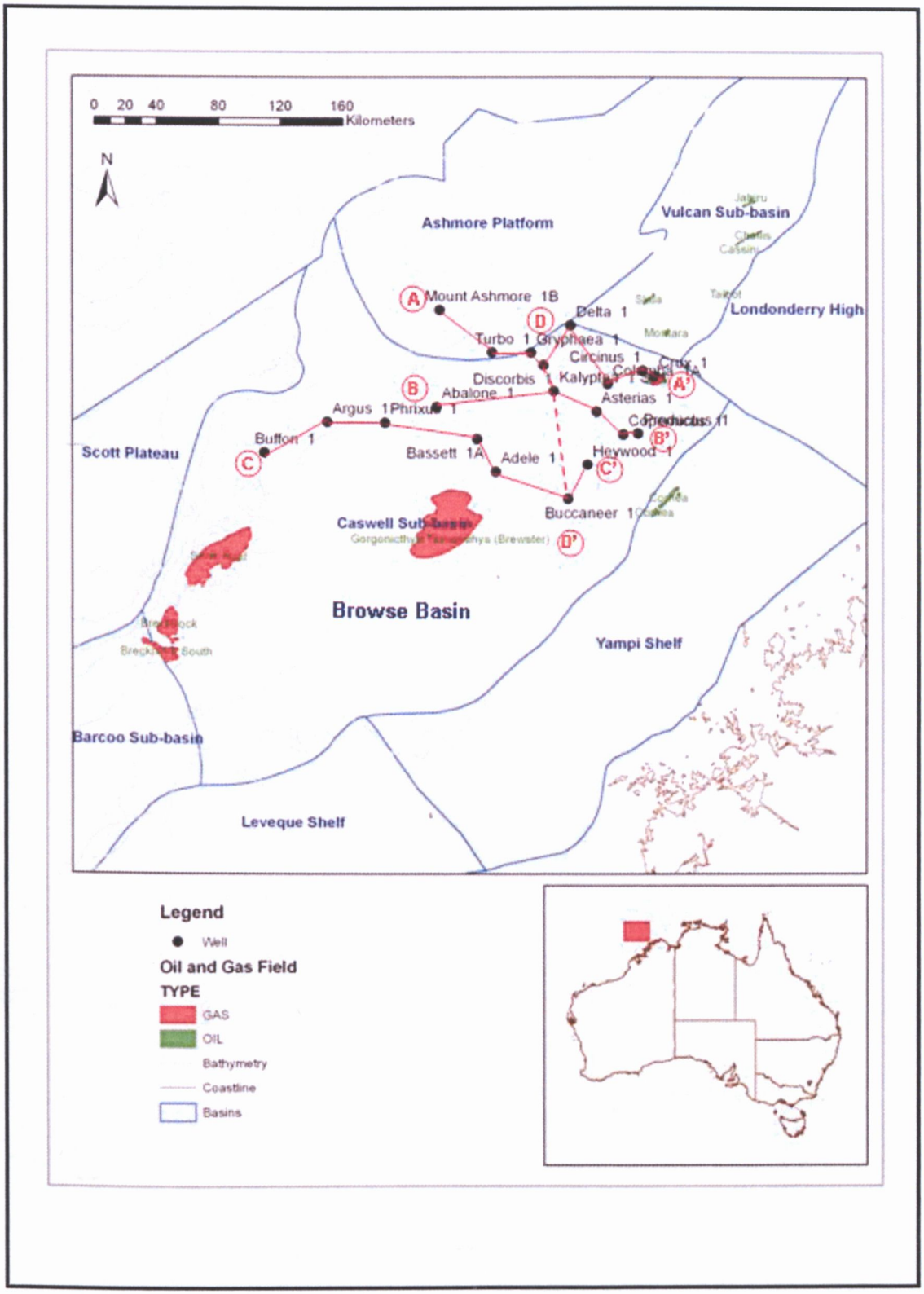

Figure 1.1. The area of study within the Northern Browse Basin. The wells analyzed are shown in black text. A-A', B-B', C-C' and D-D' show the locations of the cross-sections in Figure 3.2 – 3.5 and Figure 4.2 – 4.5.

2 Regional and Petroleum Geology of the Northern Browse Basin

The Browse Basin lies in the southern Timor Sea region of Australia's North West Shelf (Struckmeyer et al., 1998). It is a northeast-southwest trending offshore sedimentary basin and covers approximately 100,000 km^2 (Figure 2.1). It contains over 11 km of Permian to Recent clastic, volcanic, and carbonate sediments deposited during the rifting and separation associated with the breakup of Gondwana in the Mesozoic, and subsequent development of the passive margin (Maung et al., 1994). It is a proven hydrocarbon province with major undeveloped gas and condensate fields (Struckmeyer et al., 1998).

The Browse Basin is divided into four major Sub-basins, the Caswell, Barcoo, Seringapatam and Scott Sub-basins (Struckmeyer et al., 1998). It is bounded to the southeast by a series of shallow basement elements, the Prudhoe Terrace, and the Yampi and Leveque Shelves (Figure 2.1).

The Caswell Sub-basin, the main area of this study, is the northernmost major depocenter of the Browse Basin. The Caswell Sub-basin contains more than 15 km of Paleozoic to Cenozoic sediments (Struckmeyer et al., 1998). It is flanked to the east and southeast by the Prudhoe Terrace and Yampi Shelf, to the west by the Scott Plateau, to the north by the Ashmore Platform, and to the northeast by the Vulcan Sub-basin (Australian Government, 2006). Its northwestern boundary with the Seringapatam Sub-basin is delineated by the Brecknock-Buffon fault, a major structural zone with a north to northeast trend.

The Ashmore Platform, to the north of the Caswell Sub-basin, is an extensive, elevated, and highly structured block. The platform consists of 1500 m of flat-lying Cretaceous and Cenozoic sediments and up to 4500 m of heavily faulted and folded Permian to Triassic sediments (Australian Government, 2007).

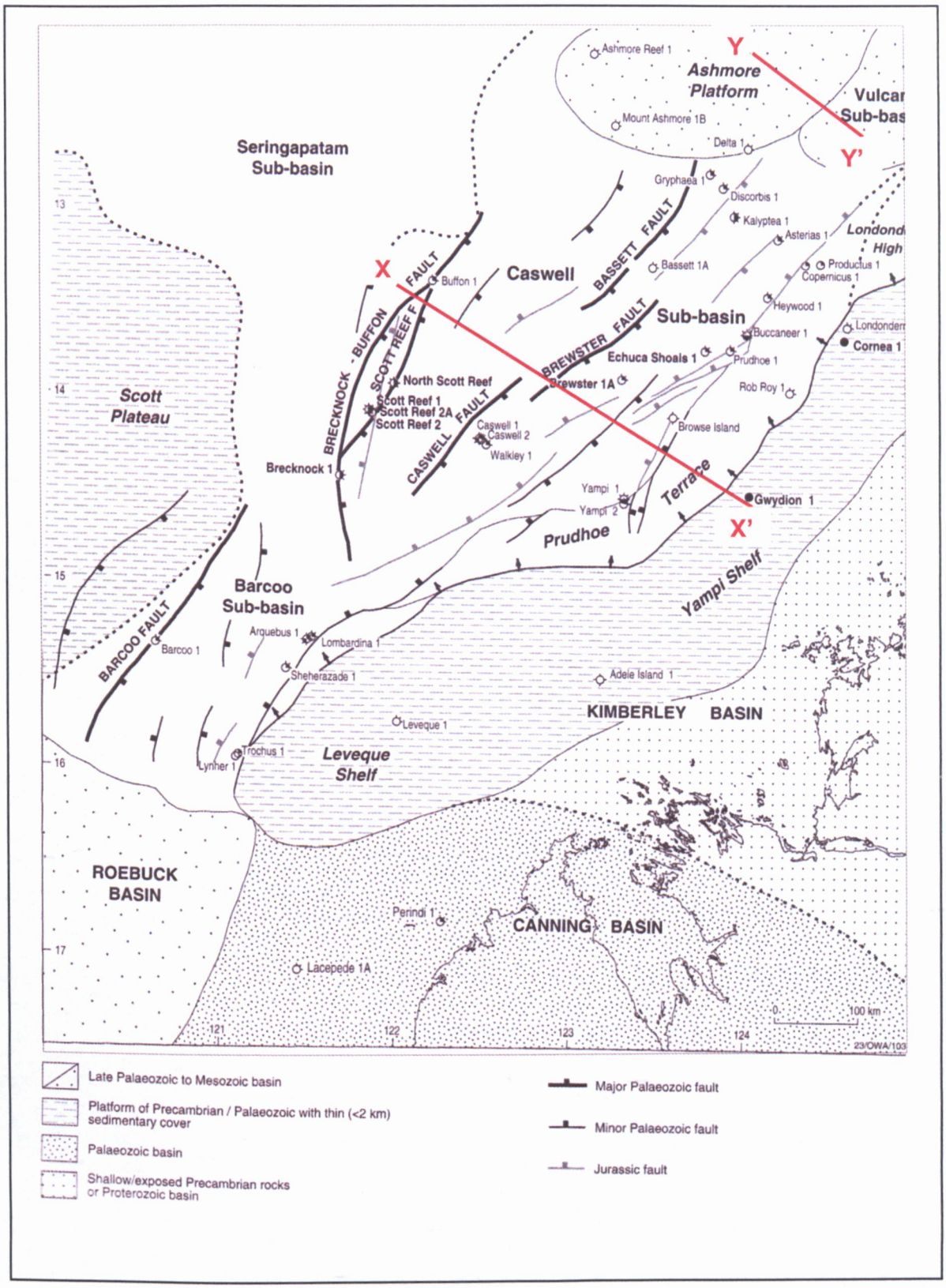

Figure 2.1. Structural elements of the Browse Basin region (modified after Struckmeyer et al., 1998). X-X' and Y-Y' show the locations of the schematic cross-sections illustrated in Figure 2.2.

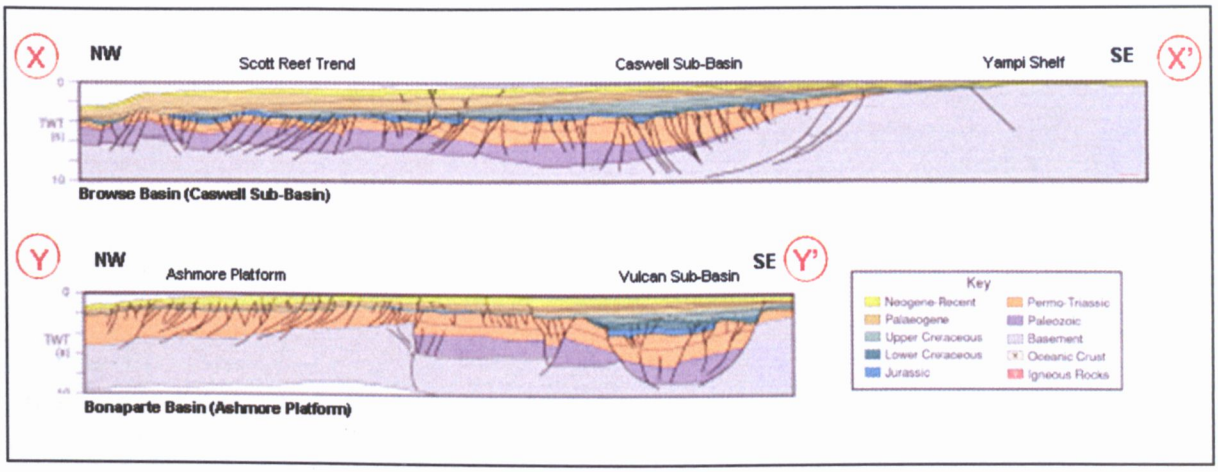

Figure 2.2 Geoseismic sections over the Caswell Sub-basin and Ashmore Platform (modified from Doré and Stewart, 2002). Approximate section locations are shown in Figure 2.1.

2.1 Geological Summary and Stratigraphy

2.1.1 Caswell Sub-basin, Browse Basin

The Browse Basin is a result of six major structural phases (Struckmeyer et al, 1998; Figure 2.2): Late Carboniferous to Early Permian extension, Late Permian to Triassic thermal subsidence, Late Triassic to Early Jurassic inversion, Early to Middle Jurassic extension, Late Jurassic to Cenozoic thermal subsidence and Middle to Late Miocene inversion. Figure 2.3 summarizes the basin stratigraphy, major basin phases, sea level changes and the distribution of hydrocarbon reserves by stratigraphic interval.

The Browse Basin is underlain by approximately 8 to 10 km of Palaeozoic syn-rift and early post-rift succession (Symonds et al., 1994). The initial Palaeozoic phases of extension and subsidence resulted in widespread half-grabens that compartmentalized the basin into northern and southern depocentres, known as the Caswell and Barcoo sub basins respectively (Strukmeyer et al., 1998; Symonds et al., 1994). The Browse Basin was dominated by terrestrial depositional systems and periods of marine influence to a semi-restricted marine basin from the Late Palaeozoic onwards. The Carboniferous section is mainly fluvio-deltaic. The Early Permian section was deposited in a marine environment, and consists of primarily limestones and shales (Blevin et al., 1998).

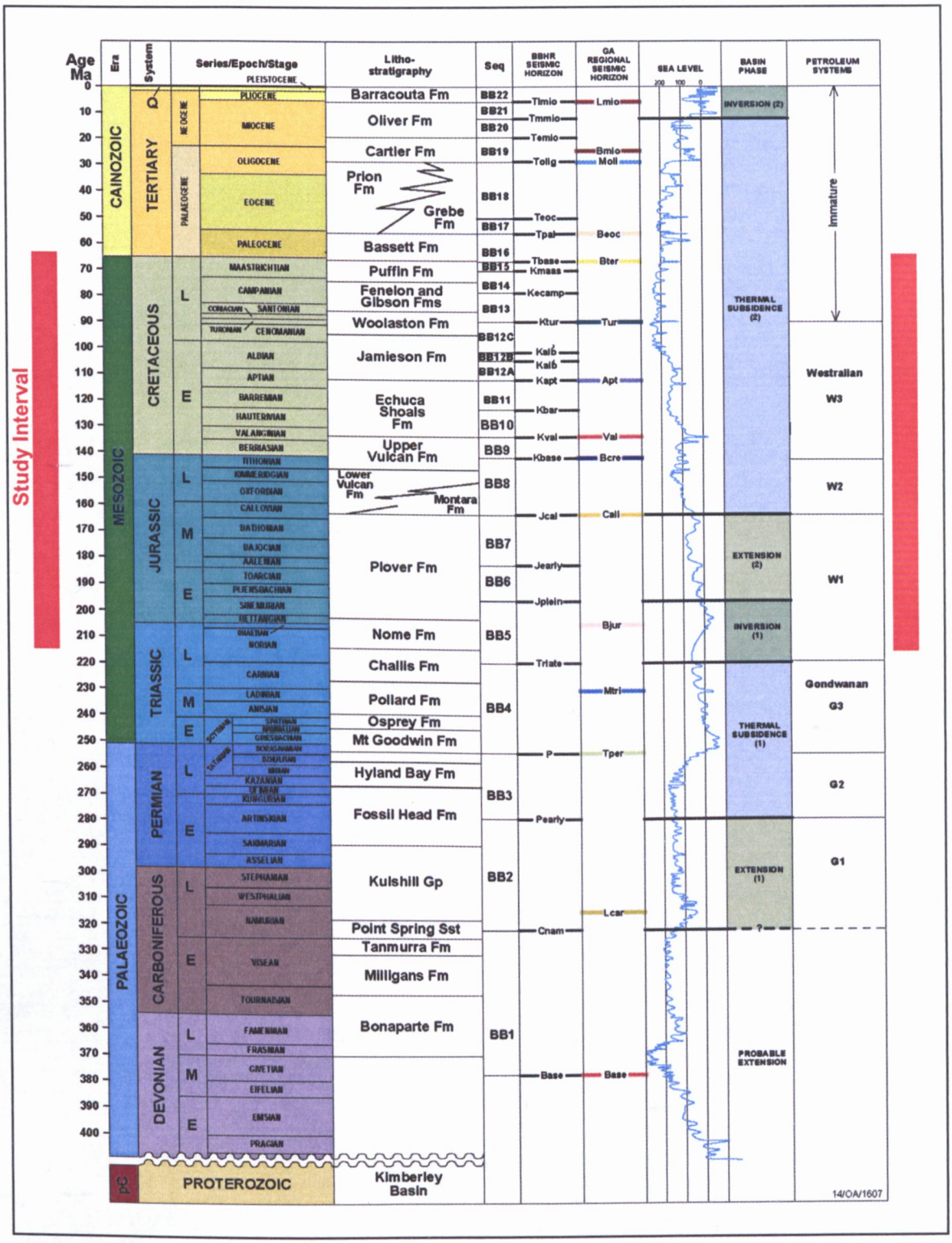

Figure 2.3. Tectonostratigraphy summary and hydrocarbon discoveries of the Browse Basin (modified after Struckmeyer et al., 1998). The section of interest is noted in red bar.

The Late Permian to Triassic succession consists of a transgressive sandstone overlain by claystones with interbeds of siltstones and volcaniclastic sediments. The best reservoirs occur within the transgressive sands in the Hyland Bay Formation (Blevin et al., 1998).

Late Triassic inversion produced syn-inversion deposition in the synclines and erosion on the crests of the anticlines. It resulted in the anticlines, which are associated with the Buffon – Scott Reef - Brecknock anticlinal trends. Overlying reservoir intervals developed as a result of erosion and onlap of the structures in the latest Triassic to Early Jurassic. Seals across the anticlines are expected to range from intra-formational to marine and prodelta shales of the overlying Lower to Middle Jurassic succession (Blevin et al., 1998).

Many of the anticlines that formed during Late Triassic inversion later experienced collapse due to extension that occurred in the Early Jurassic. The Browse Basin was situated in a major volcanic province with evidence of Early to Late Jurassic intrusives (grabbros and tholeiites) and extrusives (basalts). The depositional environment was dominated by fluvio-deltaic systems. The succession contains channel sands and/or coarsening-upward prograding deltaic sands, interbedded with finer-grained beds of prodelta to delta plain siltstone and shale (Blevin et al., 1998). The Early to Late Jurassic was a period of high sediment influx into this basin and these deposits are the primary reservoirs over most of the Browse Basin (Maung et al., 1994).

Thermal subsidence, minor reactivation events, and eustasy controlled the accommodation space from the Late Jurassic to Cenozoic (Australian Government, 2005). The Late Jurassic succession is predominantly fluvio-deltaic and relatively thin across most of the central and western basin. The interbedded fluvio-deltaic and prodeltaic nature of the facies provides multiple stacked reservoir/seal pairs.

The Early Cretaceous succession consists of distinct lowstand, transgressive and highstand depositional packages. The facies within the lowstand system include slope fans, prograding fluvio-deltaic and shoreline to shallow marine facies. The transgressive system contains organic-rich shales, and the overlying highstand package contains shale and siltstone (Blevin et

al., 1998). The Early Cretaceous sediments are predominantly claystone and marl but thin hydrocarbon-bearing turbidite sands of Albian age have also been found (Maung et al., 1994).

The Late Cretaceous sandstones of Maastrichtian-Campanian age have reservoir potential (Maung et al., 1994). The principal reservoir facies are interpreted to be lowstand slope fans, distal turbidites and transgressive, shoreface/shelf sand (Blevin et al., 1998).

The Turonian to lower Campanian succession is characterized by fine-grained pelagic sediments, primarily calcareous claystone, calcareous shale, marl and calcilutite. The terrigenous material was probably sourced from a fluvial system when sea level was relatively high. The depositional environment was shallow shelf and shoreline. A regressive phase occurred in the Early Campanian. It was associated with the lowstand deposition in the Caswell Sub-basin.

Tertiary inversion affected the intensity of structuring during the Miocene and has led to a decrease in trap integrity (Struckmeyer et al., 1998). Probable salt withdrawal structures developed in the northernmost Caswell Sub-basin due to Miocene halokinesis and are related to the anomalously high formation water salinities in this area (Struckmeyer et al., 1998).

2.1.2 Ashmore Platform, Vulcan Sub-basin

Sedimentation in the Ashmore Platform was initiated as a result of Late Carboniferous to Early Permian rifting (Figure 2.4). The depositional environment was shallow marine to fluvio-deltaic during the Permian to Triassic. Uplift and erosion occurred in the Late Triassic. The Plover Formation was deposited during the Early-Middle Jurassic in a fluvio-deltaic environment on the Ashmore Platform. Faulting and uplift occured in the late Middle Jurassic, and rifting in the adjacent Vulcan Sub-basin led to extensive erosion of Triassic-Jurassic strata. The transgression and deposition of the shallow marine Echuca Shoals formation occurred during the Valinginian as a result of post-rift thermal subsidence. Subsidence continued through the Cretaceous which resulted in the deposition of marine siliciclastics (Australian Government, 2007).

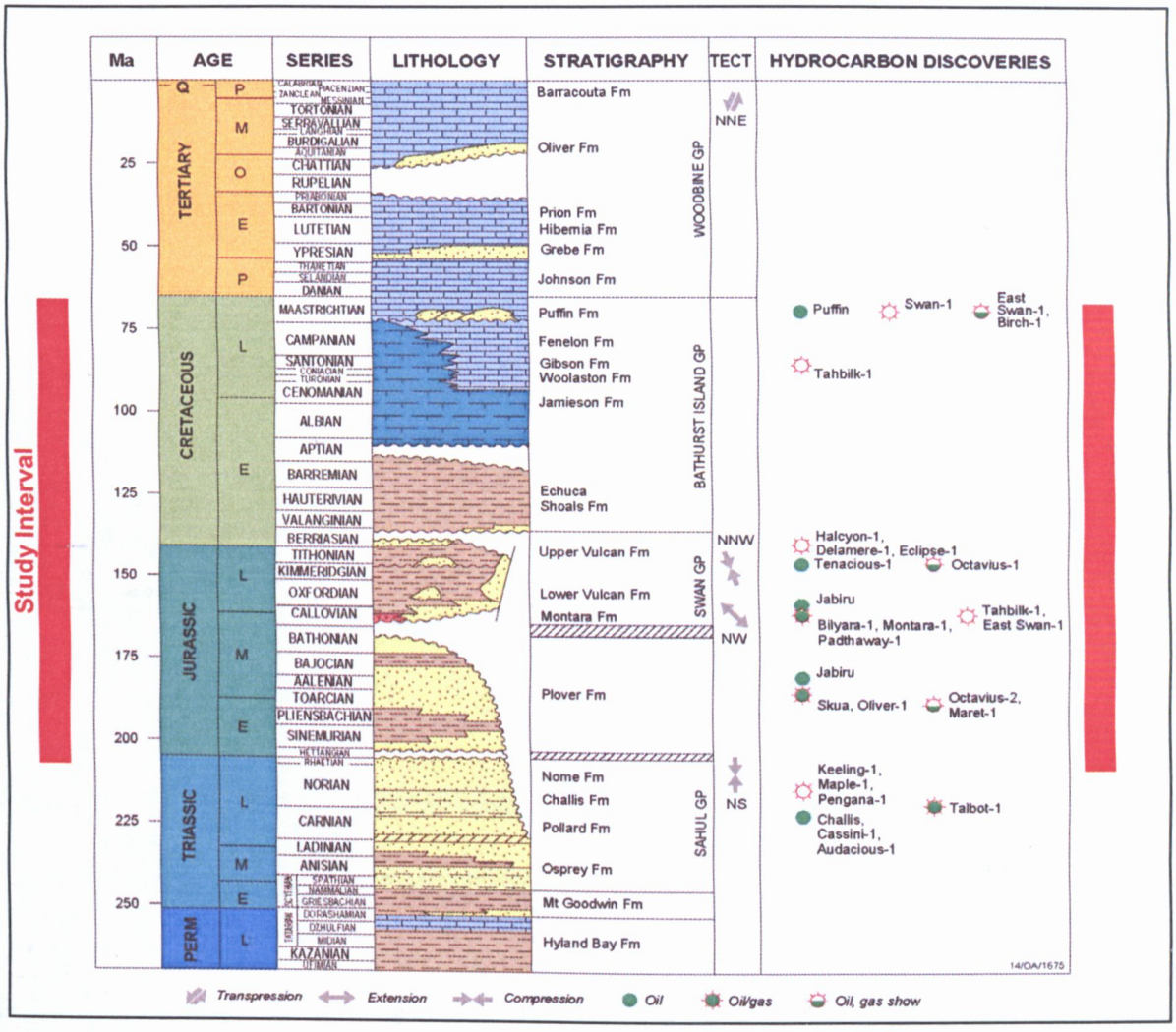

Figure 2.4. Stratigraphic summary of the Vulcan Sub-basin (modified after Edwards et al., 2004). The stratigraphy of the Ashmore Platform is similar to that of the Vulcan Sub-basin, except for the Jurassic sediments which are either thin or absent. The section of interest is noted in red bar.

2.2 Petroleum System

2.2.1 Caswell Sub-basin, Browse Basin

The Browse Basin has all the necessary requirements for a petroleum province. It has good reservoirs, seals, source rocks and suitable structural and stratigraphic traps (Maung et al., 1994).

Potential source rocks in this basin are in the Early-Middle Jurassic (Plover Formation), the Late Jurassic (Vulcan Formation) and within the Early Cretaceous (Echuca Shoals and Jamieson Formations). Fluvio-deltaic facies, with high quality coals and prodelta shales, dominate the Plover Formation, which has significant source potential (Blevin et al., 1998). Thick sections of the Early Cretaceous sediments also contain combined marine and terrestrial organic matter with moderate to good source potential.

Reservoir facies are best developed within the fluvio-deltaic Early-Middle Jurassic Plover Formation, and submarine fans and ponded turbidite mounds of Berriasian, Barremian, Campanian, and Maastrichtian age (Australian Government, 2007). The Middle Campanian ponded turbidite systems have excellent reservoir characteristics in the Carbine and Marabou prospect within the Caswell Sub-basin. Extensional faults were expected to provide vertical conduits for charge from underlying Early Cretaceous source rock (Benson et al., 2004).

The Late Cretaceous claystones of the Puffin Formation give potential seals for Campanian-Maastrichtian ponded turbidites and unconfined fans (Benson et al., 2004). Regional seals are provided by claystones in the Late Jurassic Vulcan Formation and Early Cretaceous Echuca Shoals Formation. Potential intra-formational shale seals occur within the Early-Middle Jurassic Plover Formation (Blevin et al., 1998).

The major trap types within the basin are the Late Triassic faulted anticlines, Jurassic horst/tilted fault blocks and associated drape anticlines, and the Late Cretaceous basin floor fans and ponded turbidite stratigraphic traps (Australian Government, 2007).

2.2.2 Ashmore Platform, Vulcan Sub-basin

The proven Jurassic source rocks of the Browse Basin sediments are thin or absent on the Ashmore Platform. Hence, long distance migration from depocentres in the Cartier Trough and Swan Graben within Vulcan Sub-basin is required for hydrocarbon charge in this area. There are many models of oil migration for the Ashmore Platform which predict little charge.

However, residual oil has been observed in cuttings and sidewall cores from the Miocene Oliver Formation in Warb-1A on the Ashmore Platform (Australian Government, 2007).

The potential reservoirs on the Ashmore Platform are in the Cretaceous Puffin and Triassic Nome Formations. One new possibility is Jurassic/Triassic reef or mound structures (Australian Government, 2007). These features appear to be unfaulted and unaffected by reactivation of the faults in the area. The critical issue is the trap integrity since many of the Late Miocene-Pliocene reactivated faults extend to sea floor (Australian Government, 2007).

2.3 Exploration History

The Browse Basin is one of the most hydrocarbon-rich basins in Australia. The estimated reserves are 13.6 MMbbls of oil, 25.9 TCF of gas, 438.2 MMbbls of LPG, and 543.4 MMbbls of condensate, as at January 2005 (Australian Government, 2007). The Caswell Sub-basin is the largest contributor with major reserves in Scott Reef, Brecknock, Brecknock South, Brewster and Crux.

Gas was discovered in Scott Reef in 1971 within the Early-Middle Jurassic sandstones and Late Triassic-Jurassic sandy dolostone on the Buffon-Scott Reef-Brecknock anticlinal trend. Brecknock-1 tested a broad anticlinal feature 40 km southwest of Scott Reef in 1979 and encountered gas in sandstones of similar age to the reservoir section at Scott Reef. Other significant gas discoveries were made in the Late Jurassic to Early Cretaceous sands in Brewster-1A, Caswell-2 and Echuca Shoals-1.

Exploration in the Northern Browse Basin began in 1978 with the drilling of Basset-1/1A (Table 2.1). The target was a faulted anticline in the central Browse Basin. The well encountered minor shows of gas. Exploration of the Browse Basin was again active between 1984 and 1994 with the drilling of Gryphaea-1, Asterias-1, Discorbis-1 and Kalyptea-1/1ST1. Minor hydrocarbon shows in Asterias-1 and Kalyptea-1ST1 were reported from the Late Jurassic and Early Cretaceous reservoirs (Maung et al., 1994; Table 2.1).

Several major gas accumulations were discovered in the Browse Basin in 2000. Brecknock South-1, located on the Scott Reef-Brecknock trend, intersected a 134 m gross gas column in the Middle Jurassic Plover Formation sandstones. Argus-1 encountered in excess of 240 m of gas-bearing the Late Jurassic (Oxfordian) sandstones. A 280 m gross gas column was intersected in Crux-1 within the Late Triassic to Early Jurassic Nome Formation (Australian Government, 2007).

Exploration in the Ashmore Platform started in 1968 with the drilling of Ashmore Reef-1 by BOC of Australia as stratigraphic test. This well indicated that the Jurassic section is either thin or absent and Triassic sandstones form the potential petroleum reservoirs over much of the Ashmore Platform (Australian Government, 2007). A proven gas zone and oil shows were encountered in Swan-3/3ST1 in 1991. Puffin Field is currently undergoing development for gas zones within the Late Cretaceous sandstones (Australian Government, 2007).

No	Well	Operator	Year	Objectives	Hydrocarbons	Notes
1	Abalone-1	Japan Petroleum Exploration Company, Ltd.	2000	Tested the Late Cretaceous (Maastrichtian) Puffin Formation sandstones	Minor gas shows	Showed in the Puffin Formation
2	Adele-1	Shell Development (Australia) P/L	1998	Tested the Middle Jurassic Plover Formation	Oil and gas accumulation	Thin low-porosity gas-bearing sand was discovered in the Aptian Jamieson Formation. Strong gas readings and fluorescence throughout the Early Cretaceous to Early Jurassic section
3	Argus-1	BHP Petroleum (Australia) Pty. Ltd	2000	Tested the Late Jurassic (Oxfordian) sediments	Oil indications and gas accumulation	In excess of 240 m gas column encountered from the Late Jurassic sediments.
4	Astenas-1	BHP Petroleum	1987	Targeted sandstones within the Early Cretaceous Echuca Shoals and Upper Vulcan Formations and the Maastrichtian Puffin Formation; Tested a faulted anticline	Oil show and gas indications	Hydrocarbon indications from the Aptian to Tithonian age; Residual hydrocarbons encountered in the Tithonian sands.
5	Basset-1A	Woodside Petroleum Ltd.	1978	Tested the Late Cretaceous (Maastrichtian and Campanian) sands on a large, faulted anticline	No significant hydrocarbon shows; Gas indications	
6	Buccaneer-1	Shell Development (Australia) P/L	1990	Tested the Middle-Late Jurassic Plover and Lower Vulcan Formation	Oil show and gas indications	Fair hydrocarbon shows were encountered in the Upper Vulcan Formation and the Middle Triassic ages
7	Buffon-1	B.O.C of Australia Ltd.	1963	Tested a large anticlinal feature in the Early to Middle Jurassic and Triassic sandstones	High gas reading	Showed from the objective sections
8	Circinus-1ST1	Nippon Oil Exploration (Vulcan) Pty. Ltd.	1999	Tested the prospectivity of the Plover Formation within an interpreted horst block	No hydrocarbon shows	
9	Columba-1AST1	Nippon Oil Exploration (Vulcan) Pty. Ltd.	1999	Tested the Plover Formation sandstones in a tilted fault block	Oil and gas indications	Two thin gas sands were intersected in the Upper Vulcan Formation, but no structural closure exists at the well location.
10	Copernicus-1	Mobil Exploration and Production Australia P/L	1993	Targeted braid delta sand packages of the Late Jurassic Lower Vulcan Formation	Oil shows	Oil shows were noted in the Echuca Shoals and Pollard Formation sandstones
11	Crux-1	Nippon Oil Exploration (Vulcan) Pty. Ltd.	2000	Tested the Plover Formation within an interpreted horst structure	Gas shows	Intersected a gross gas column of 280 m within the Late Triassic Nome Formation
12	Delta-1	Elf Aquitane	1988	Tested the Maastrichtian Puffin Formation in an unfaulted drape anticline over a deeper horst block	Gas indications	Good reservoir quality sandstones were encountered.
13	Discorbis-1	BHP Petroleum	1989	Targeted sandstones within the Early Cretaceous Echuca Shoals and Upper Vulcan Formations and the Maastrichtian Puffin Formation	Oil shows and residual hydrocarbon indications	Good oil shows were encountered in the Puffin Formation within a faulted anticline. Residual hydrocarbons were encountered in the Late Cretaceous Woolaston Formation.
14	Gryphaea-1	BHP Petroleum	1987	Tested the Late Jurassic sandstones	Oil and gas indications	Oil and gas shows were encountered in sandstones of Maastrichtian, Valinginian and Triassic ages
15	Heywood-1	Woodside/Burmah Oil NL	1974	Tested Permo/Triassic-Middle Jurassic horst block	Oil and gas indications	High gas readings and traces of live oil were encountered in the Early Cretaceous to Early Jurassic sequence. Good oil shows in the Middle-Early Jurassic section.
16	Kalyptea-1ST1	BHP Petroleum	1989	Targeted sandstones within the Early Cretaceous Echuca Shoals and Upper Vulcan Formations and the Maastrichtian Puffin Formation; Tested the crestal location of a large anticlinal structure	Oil, gas and condensate indications	Gas and condensate were recovered from the tight Upper Vulcan Formation
17	Mt Ashmore-1B	Woodside Petroleum Ltd.	1980	Tested the sandstones of the Middle-Lower Jurassic to Triassic ages within closure on alarge dome-shaped structure	No significant shows of hydrocarbon	The potential reservoirs were water-bearing
18	Phrixus-1	BHP Petroleum (Australia) Pty. Ltd	2001	Targeted the Late Cretaceous Puffin Formation	Hydrocarbon indications	Encountered in the targeted sandstones
19	Productus-1	Mobil Exploration and Production Australia P/L	1991	Tested the Permian Hyland Bay Fromation	No hydrocarbon	All reservoirs were water saturated
20	Turbo-1	Japan Petroleum Exploration Company, Ltd.	2000	Tested the Puffin Formation; Excellent reservoir quality	No hydrocarbon	Could be caused by the lack of charge

Table 2.1 Summary of the exploration wells within the Northern Browse Basin utilized in this study (Australian Government, 2004; Well Completion Reports of Buffon-1 and Mt Ashmore-1B).

3 Methodology

The objective of the project was to calculate the petrophysical parameters; shale volume, porosity and water saturation from the log data over the target section in each of the 20 wells in the study area. These parameters and the other well data were examined to detect any previously gas reservoirs in the wells. The workflow for this project is shown in Figure 3.1. This chapter discusses the methodology utilized.

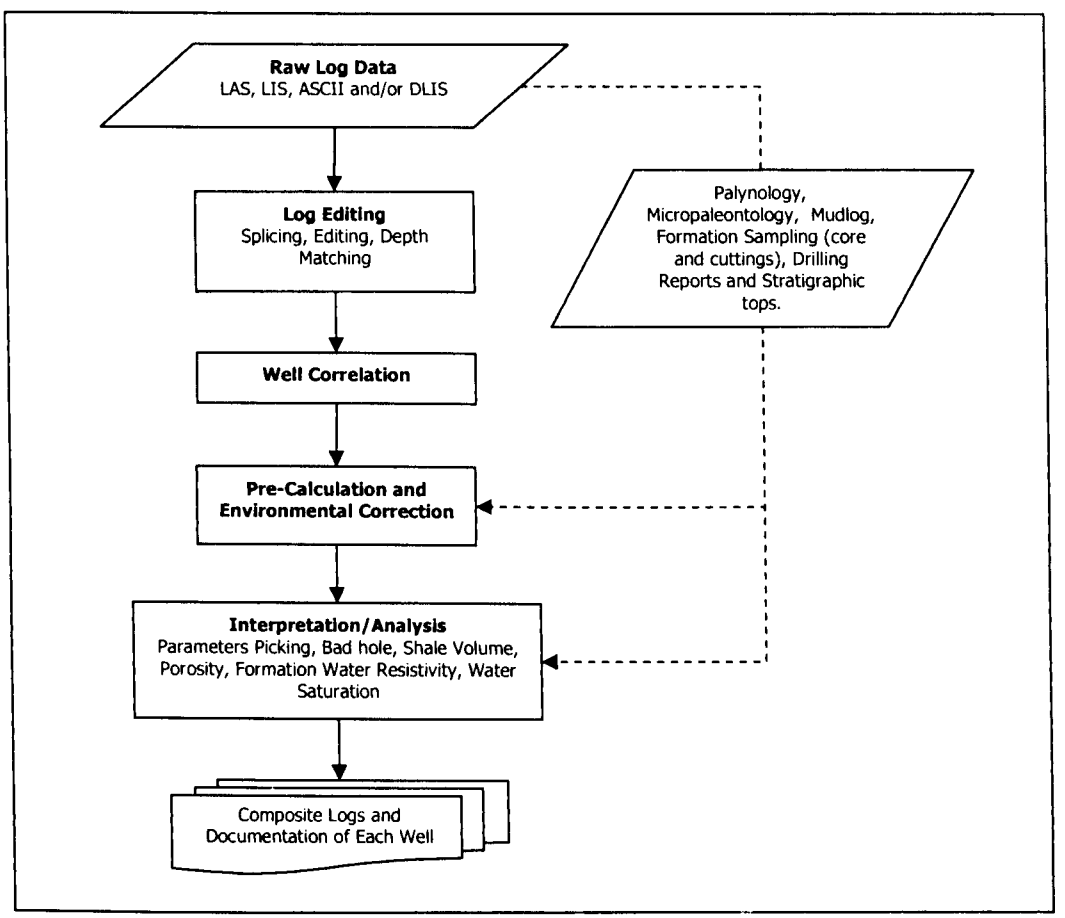

Figure 3.1. Overview of the workflow applied in this study.

3.1 Raw Data

The logs utilized in this project were raw wireline and LWD (Logging While Drilling) data. The log formats were LAS, DLIS and ASCII. The software used for the interpretation was Paradigm's Geolog 6.6.

The formation tops were provided by Chevron from their database. However, tops were not available for Delta-1 and Mount Ashmore-1B, hence the tops for these wells were obtained from palynology and micropaleontology reports and log correlation.

Mudlog and formation sampling reports, including cuttings, sidewall core and core, were needed to calibrate the results. These data were not always available for each well (Table 3.1). Drilling data such as mud properties and borehole temperature are necessary for environmental corrections. These data were usually found in the log header. Some drilling parameters were assumed where data were not available.

Although there are twenty wells within the area, only sixteen wells were analyzed quantitatively due to the lack of data. No mud property data were available for Buccaneer-1 and Copernicus-1. No supporting data i.e. mud properties, cuttings description and well completion reports were provided for Circinus-1ST1 and Columba-1ST1. Those four wells were included in the correlative cross sections, but excluded from the quantitative log analysis.

3.2 Log Editing

Curve splicing and data editing were applied to the logs to prepare them for petrophysical analysis.

The aim of splicing is to merge logs from multiple runs such that all runs in a well are combined to form a single continuous log. Splicing is also done to combine two sets of data such as wireline and LWD.

Occasional bad log values need to be manually edited. For example, erroneous data can be found over casing at the top of the logging run or in hole washouts. Such invalid data were manually deleted. A summary of log editing applied to the wells in this study is shown in Appendix 3.

No	Well Name	Core	Sidewall Cores	Tops	Composite Well Log	Drilling Data	Formation Sampling	Logging	Surveys	Micropal-aeontology	Mudlog	Palynology	Petrology Report	Reservoir and Fluid Analysis	Well Summary	Data Sources
1	Abalone-1	N	Y	Y	Y	Y	Y	Y	Y	Y	Y	Y	N	Y	Y	Chevron ASBU (Geoscience Australia)
2	Adele-1	N	Y	Y	N	Y	N	Y	Y	Y	Y	Y	N	N	Y	Chevron ASBU (Geoscience Australia)
3	Argus-1	N	Y	Y	Y	Y	Y	Y	Y	Y	Y	Y	Y	N	Y	Chevron ASBU (Geoscience Australia) and Occam Technology Pty Ltd
4	Asterias-1	N	Y	Y	Y	Y	Y	Y	N	Y	Y	Y	Y	N	Y	Chevron ASBU (Geoscience Australia) and Occam Technology Pty Ltd
5	Basset-1A	N	Y	Y	Y	Y	Y	Y	Y	Y	Y	Y	Y	N	Y	Chevron ASBU (Geoscience Australia)
6	Buccaneer-1	N	Y	Y	Y	Y	Y	Y	Y	N	Y	Y	Y	N	Y	Chevron ASBU (Geoscience Australia)
7	Buffon-1	Y	Y	Y	Y	Y	Y	Y	Y	Y	Y	Y	Y	Y	Y	Chevron ASBU (Geoscience Australia)
8	Circinus-1ST1	N	N	Y	N	N	N	Y	N	N	N	N	N	N	N	Chevron ASBU (Geoscience Australia) and Occam Technology Pty Ltd
9	Columba-1ST1	N	N	Y	N	N	N	Y	N	N	N	N	N	N	N	Chevron ASBU (Geoscience Australia) and Occam Technology Pty Ltd
10	Copernicus-1	N	Y	Y	Y	Y	Y	Y	Y	Y	Y	Y	Y	N	Y	Chevron ASBU (Geoscience Australia)
11	Crux-1	Y	Y	Y	Y	Y	Y	Y	Y	Y	Y	Y	Y	Y	Y	Chevron ASBU (Geoscience Australia)
12	Delta-1	N	Y	N	Y	Y	Y	Y	N	Y	Y	Y	N	N	Y	Chevron ASBU (Geoscience Australia)
13	Discorbis-1	N	Y	Y	Y	Y	Y	Y	N	Y	Y	Y	Y	N	Y	Chevron ASBU (Geoscience Australia)
14	Gryphaea-1	N	Y	Y	Y	Y	Y	Y	Y	Y	Y	Y	Y	N	Y	Chevron ASBU (Geoscience Australia)
15	Heywood-1	N	Y	Y	Y	Y	Y	Y	N	Y	Y	Y	Y	N	Y	Chevron ASBU (Geoscience Australia)
16	Kalyptea-1ST1	Y	Y	Y	Y	Y	Y	Y	N	N	Y	N	Y	N	Y	Chevron ASBU (Geoscience Australia)
17	Mt Ashmore-1B	N	Y	N	Y	Y	Y	Y	Y	Y	Y	Y	N	N	Y	Chevron ASBU (Geoscience Australia)
18	Phrixus-1	N	Y	Y	N	N	Y	Y	Y	Y	Y	N	Y	N	Y	Chevron ASBU (Geoscience Australia) and Occam Technology Pty Ltd
19	Productus-1	N	Y	Y	Y	Y	Y	Y	Y	Y	Y	Y	N	Y	Y	Chevron ASBU (Geoscience Australia)
20	Turbo-1	N	Y	Y	Y	Y	Y	Y	Y	Y	Y	Y	N	N	Y	Chevron ASBU (Geoscience Australia) and Occam Technology Pty Ltd

Table 3.1. Data availability summary

3.3 Well Correlation

Cross-sections were created through the wells in order to recognize and correlate the reservoir intervals and to facilitate subsequent petrophysical analysis. Three cross-sections were generated: northern, central and southern. The northern cross-section encompasses Mount Ashmore-1B, Turbo-1, Gryphaea-1, Discorbis-1, Delta-1, Columba-1ST1, Circinus-1ST1 and Crux-1 (Figure 3.2). The central cross-section covers Abalone-1, Kalyptea-1ST1, Asterias-1, Copernicus-1 and Productus-1 (Figure 3.3). The southern cross-section contains Buffon-1, Argus-1, Phrixus-1, Basset-1A, Adele-1, Heywood-1 and Buccaneer-1 (Figure 3.4). An additional cross-section from north to south, connecting the three cross-sections, was constructed (Figure 3.5). The location of the cross-sections is shown in Figure 1.1.

The sequence of interest in this study is from the Late Triassic to Late Cretaceous, covering nine formations from the Nome Formation to the Puffin Formation (Figure 2.3). The correlation was made based on the formation tops (Table 3.2) supplied by Chevron, well completion reports and log character. The top of the Puffin Formation was picked as the datum.

3.4 Pre-Calculation and Environmental Corrections

The pre-calculation and environment/borehole corrections need to be undertaken before quantitative interpretation because tool performance is influenced by the borehole conditions at the time of the measurement.

Pre-Calculation

The objective of the pre-calculation process is to create logs of borehole and formation condition used in the environmental corrections and petrophysical analysis. The required data are the tool type, temperature data, mud properties, top and bottom depths of the logged intervals.

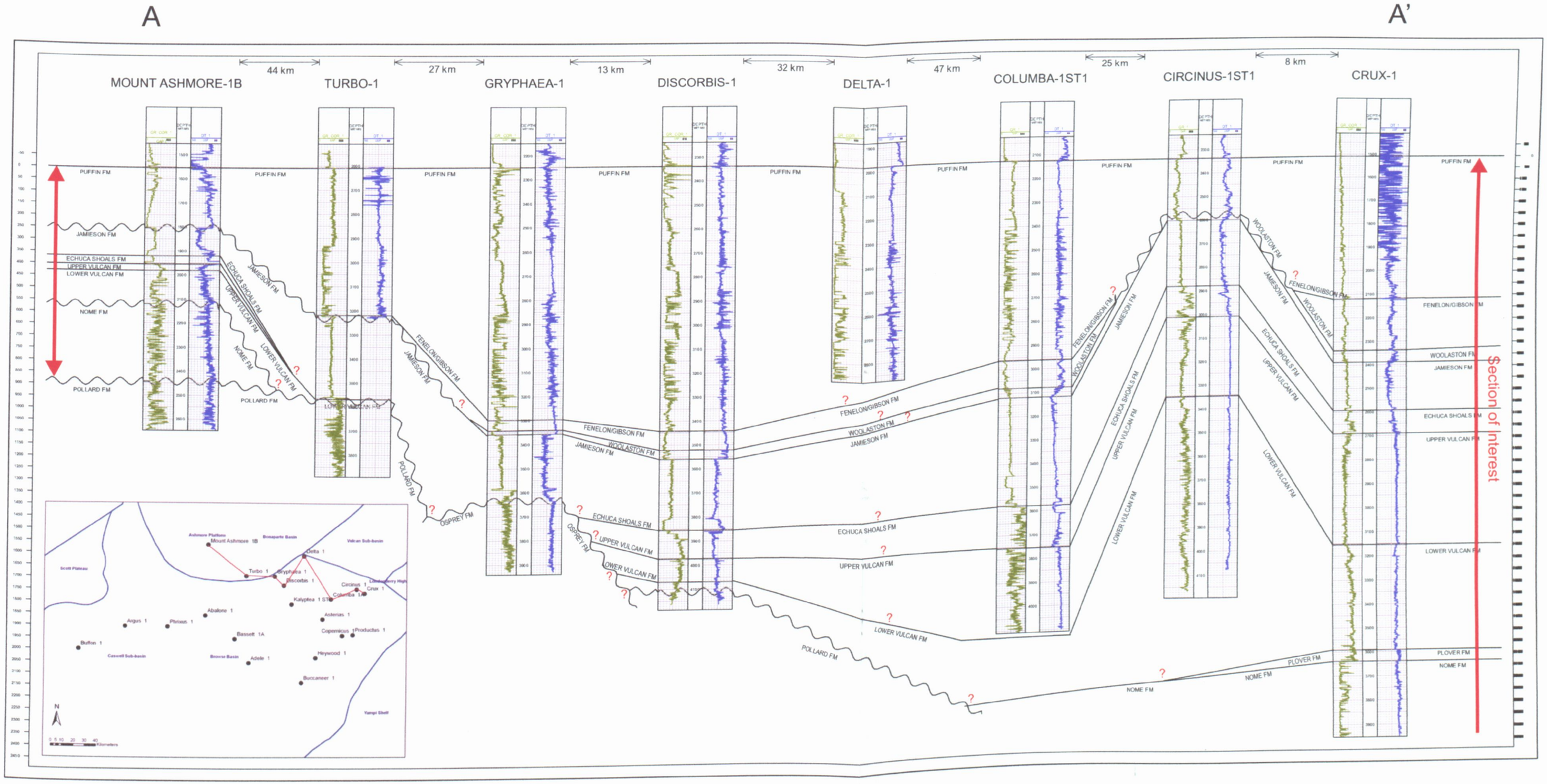

Figure 3.2. Log cross-section through the northern part of the study area, showing lithostratigraphic correlation. The data shown are:
track 1 - green curves : gamma ray logs (scale : 0 - 150, unit : GAPI)
track 2 - measured depth annotated at 100 m interval
track 3 - blue curves : sonic logs (scale: 140 - 40, unit : us/ft).

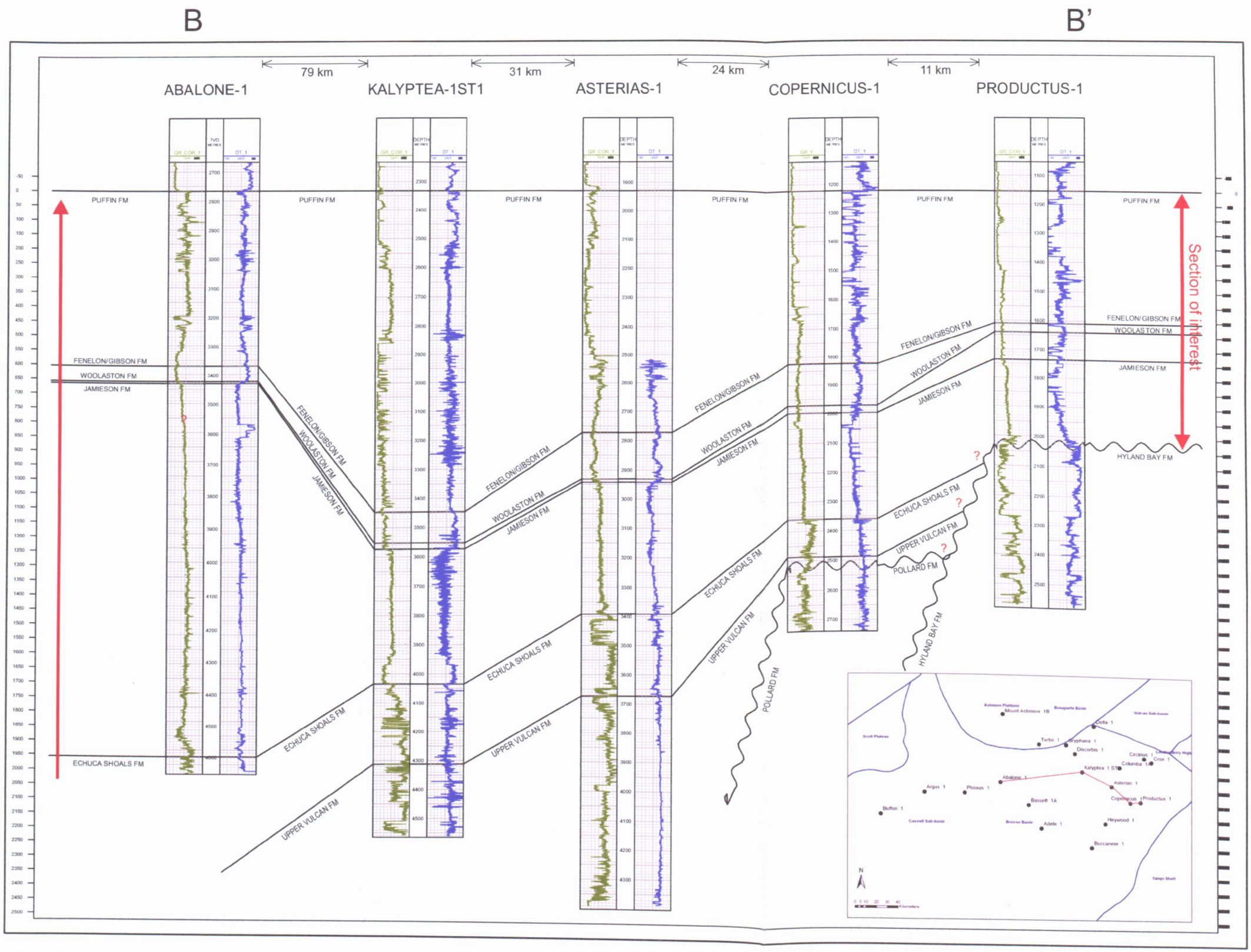

Figure 3.3. Log cross-section through the central part of the study area, showing lithostratigraphic correlation. The data shown are:
track 1 - green curves : gamma ray logs (scale : 0 - 150, unit : GAPI)
track 2 - measured depth annotated at 100 m interval, except for Abalone-1 in TVD
track 3 - blue curves : sonic logs (scale: 140 - 40, unit : us/ft).

C

C'

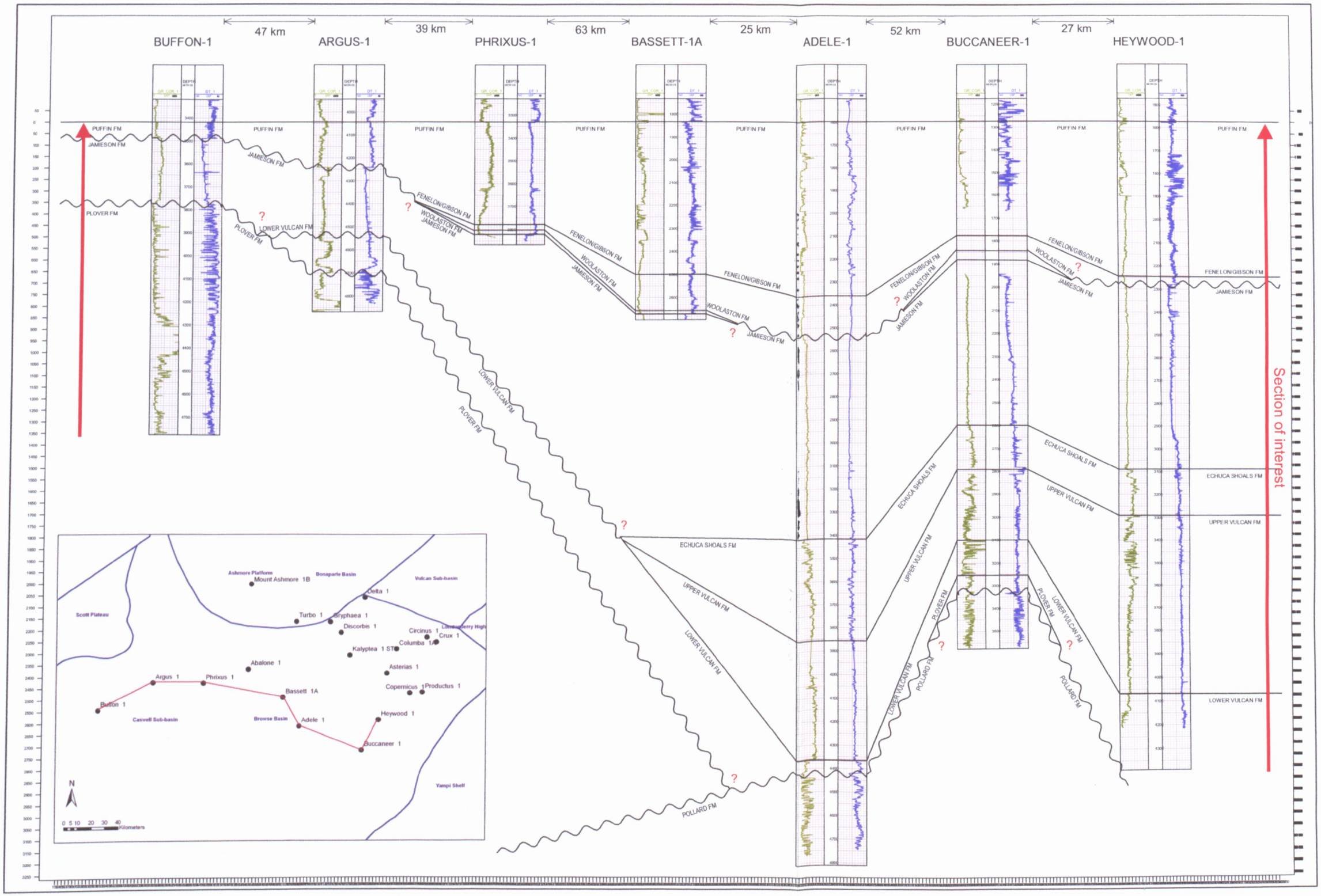

Figure 3.4. Log cross-section through the southern part of the study area, showing lithostratigraphic correlation. The data shown are:
track 1 - green curves : gamma ray logs (scale : 0 - 150, unit : GAPI)
track 2 - measured depth annotated at 100 m interval
track 3 - blue curves : sonic logs (scale: 140 - 40, unit : us/ft).

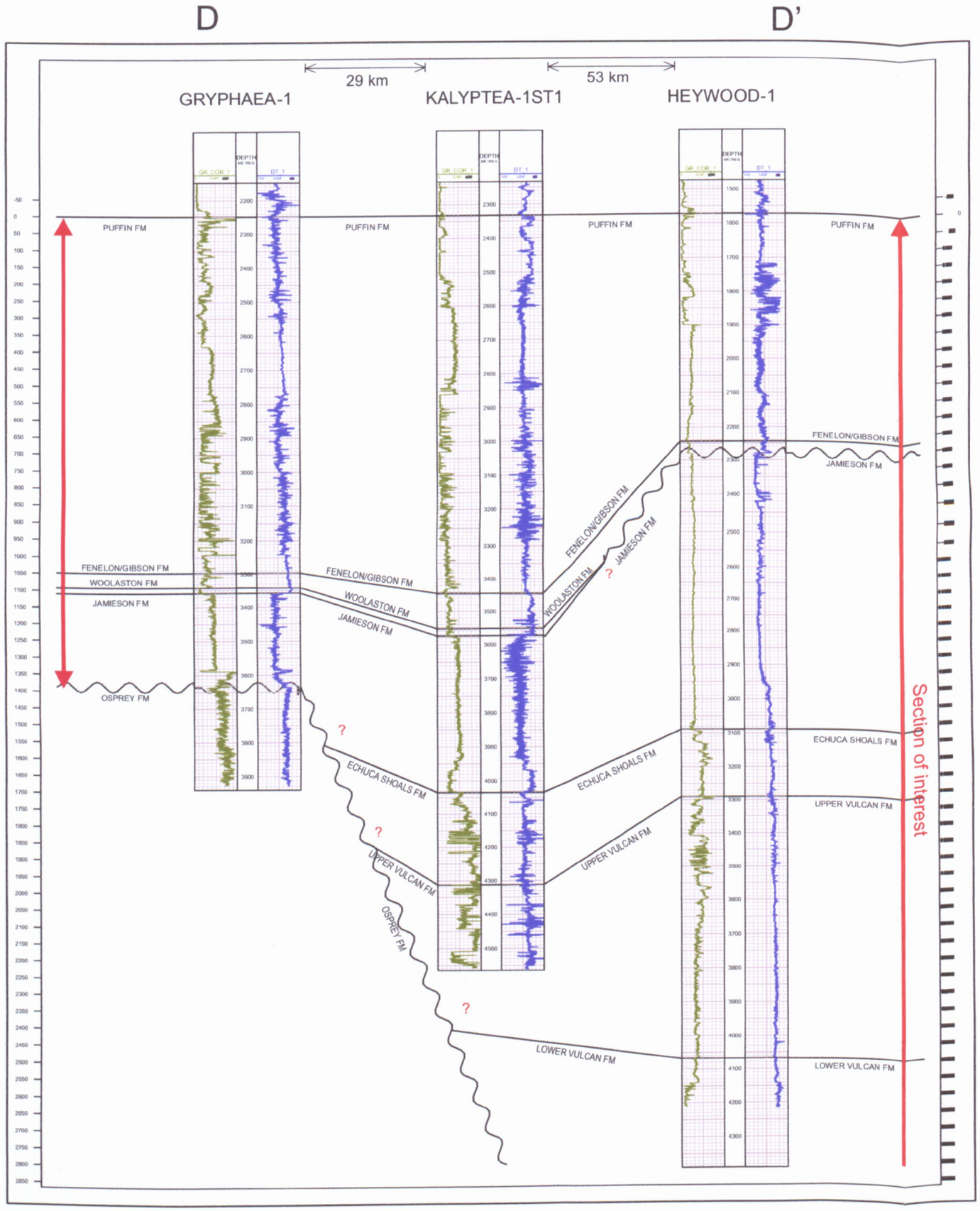

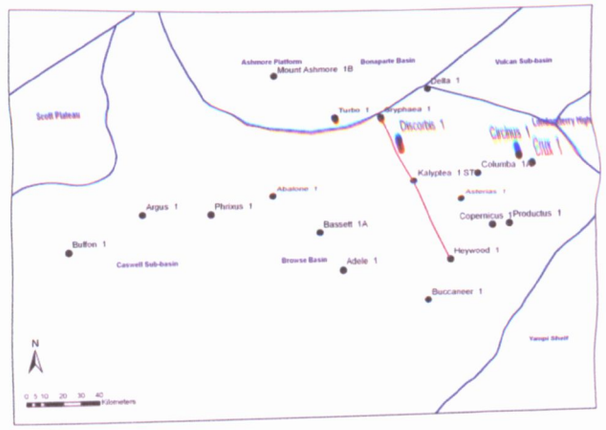

Figure 3.5. Log cross-section from north to south of the study area, showing lithostratigraphic correlation. The data shown are:
track 1 - green curves : gamma ray logs (scale : 0 - 150, unit : GAPI)
track 2 - measured depth annotated at 100 m interval
track 3 - blue curves : sonic logs (scale: 140 - 40, unit : us/ft).

No	Well Name	Cretaceous						Jurassic		Triassic
		Puffin Fm	Fenelon/Gibson Fm	Woolaston Fm	Jamieson Fm	Echuca Shoals Fm	Upper Vulcan Fm	Lower Vulcan Fm	Plover Fm	Nome Fm
1	Abalone-1	2767	3370	3424	3431	4724				
2	Adele-1	1597	2361		2540	3415	3858	4365		
3	Argus-1	4044			4242			4536	4700	
4	Asterias-1	1929	2773	2931	2942	3392	3674			
5	Bassett-1A	1832	2499.5	2656	2670					
6	Buccaneer-1	1274	1776	1842	1882	2599	2792	3100	3254	
7	Buffon-1	3419			3488				3776	
8	Circinus-1	2336		2579	2600	2880	3010	3446		
9	Columbia-1A	2125	2964	3080	3120	3578	3754			
10	Copernicus-1	1222	1824	1972	1998	2360	2488			
11	Crux-1	1509	2043	2337	2388	2591.5	2690	3154.5	3591	3640
12	Delta-1	1980								
13	Discorbis-1	2339	3443	3521	3560	3855	3974	4070		
14	Gryphaea-1	2249	3297.5	3342	3359					
15	Heywood-1	1572	2244		2279	3089	3290	4068		
16	Kalyptea-1ST1	2333	3446	3553	3574	4035	4312			
17	Mount Ashmore-1B	1553			1805	1921	1954	1981		2120
18	Phrixus-1	3330	3779	3803	3822					
19	Productus-1	1153	1610	1640	1736					
20	Turbo-1	2609	3220		3232			3567		

Table 3.2. Formation tops (m MD).

From this input data, the pre-calculation module in the Geolog 6.6 software computed the following data over the logging intervals: formation temperature, formation pressure, resistivities of the mud, mud filtrate and mud cake, mud cake thickness, salinity of mud and mud filtrate, conductivities of flushed and unflushed zones and photo-electric cross section. The equations used in these calculations are given in Table 3.3.

The formation temperature was determined assuming a linear variation through the logged interval. However, temperature data were not available for the top and bottom of the logged interval for all wells. Regional data on seabed temperature as a function of water depth (Figure 3.6) and bottom hole temperature as a function of depth below seabed (Figure 3.7) were used to estimate these temperatures, where temperature log data were not available.

Formation Temperature	$FTEMP = TLT + \frac{(Depth - TLI)(BLT - TLT)}{(BLI - TLI)}$
Formation Pressure	$FPRESS = Depth * DFD * 0.00980665$
Mud Resistivity	$RM = RMS \frac{MST + 21.5}{FTEMP + 21.5}$
Mud Filtrate Resistivity	$RMF = RMFS \frac{MFST + 6.77}{FTEMP + 6.77}$
Mudcake Resistivity	$RMC = RMCS \frac{MCST + 6.77}{FTEMP + 6.77}$
Photoelectric Cross Section	$rhoe = \frac{RHOB + 188.3}{1.0704}$, converting to electronic density $U = rhoe \frac{PEF}{1000}$
Mud Salinity	$rm75 = RMS \frac{MST + 21.5}{23.9 + 21.5}$ $xm = \frac{3.562 - \log 10(rm75 - 0.0123)}{0.955}$ $SALM = 10^{xm}$
Mud Filtrate Salinity	$rmf75 = RMFS \frac{MFST + 21.5}{23.9 + 21.5}$ $xmf = \frac{3.562 - \log 10(rmf75 - 0.0123)}{0.955}$ $SALMF = 10^{xmf}$
Flushed Zone Conductivity	$Ct = \frac{1}{Rt}$
Unflushed Zone Conductivity	$Cxo = \frac{1}{Rxo}$
BLI : Bottom log interval (m) *BLT : Bottom log interval temperature(degC)* *DFD : Drilling fluid density(g/cc)* *MCST : Mudcake sample temperature (degC)* *MFST : Mud filtrate sample temperature (degC)* *MST : Mud sample temperature (degC)* *PEF : Photo-electric factor (B/E)*	*RMCS : Resistivity of mudcake sample (ohmm)* *RMFS : Resistivity of filtrate sample (ohmm)* *RMS : Resistivity of mud sample (ohmm)* *Rt : True formation resistivity (ohmm)* *Rxo : Flushed zone resistivity (ohmm)* *TLI : Top log interval (m)* *TLT : Top log interval temperature (degC)*

Table 3.3. The formulae used in the pre-calculation procedure (Paradigm, 2006).

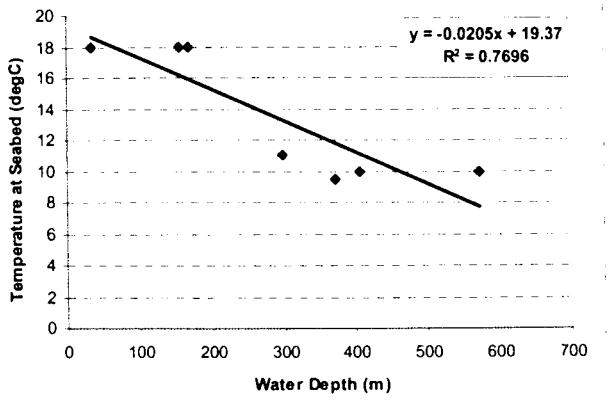

Well	Water Depth (m)	Temperature (degC)
Abalone-1	406	10
Argus-1	572	10
Bassett-1A	372	9.5
Crux-1	168	18
Discorbis-1	156	18
Heywood-1	35	18
Turbo-1	299	11

Figure 3.6. Plot of temperature at seabed against water depth. The fitted equation was used in calculating the temperature-depth relationship for the wells with no temperature data.

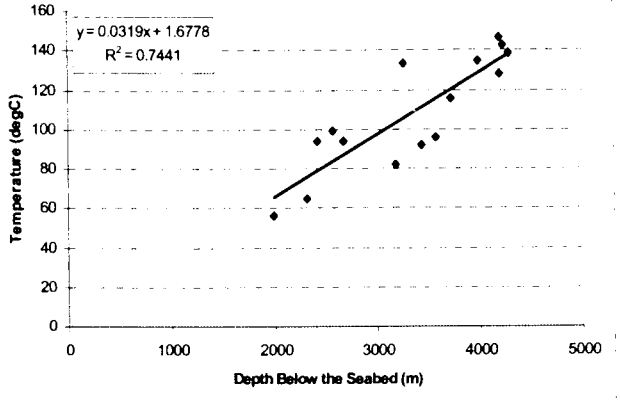

Well	Depth below the Seabed (m)	Temperature (degC)
Abalone-1	3174	82
Argus-1	4282.5	139
Asterias-1	4188.6	147
Bassett-1A	2320	65
Buffon-1	4233.64	143
Copernicus-1	2571	99
Crux-1	3255.5	133.5
Delta-1	2670	94
Discorbis-1	3987	135
Gryphaea-1	3723	116
Heywood-1	4195	128
Mount Ashmore-1B	1994.4	56
Phrixus-1	3433	92
Productus1	2422	94
Turbo-1	3576	96

Figure 3.7. Plot of bottomhole temperature against depth below the seabed. The fitted equation was used in calculating the temperature-depth relationship for the wells with no temperature data.

Environmental Corrections

The environment when logs are recorded affects the measurement. This measurement is influenced by factors such as temperature, pressure, borehole size, mud properties and depth of the invaded zone. Environmental corrections are performed in order to correct the raw wireline

log data for the effects of borehole conditions. These corrections were undertaken using the environmental correction algorithms coded into Geolog 6.6.

Borehole corrections are applied to the gamma ray curve in order to correct for the effects of mud weight and hole size. Environmental corrections revise the density and neutron logs for a variety of borehole conditions. The Micro Spherically Focused Log (MSFL) log is corrected for the effects of borehole conditions to derive the true resistivity of the flushed zone, *Rxo*. The dual laterolog curves are corrected for borehole conditions and invasion corrections are applied to derive true formation resistivity, *Rt*. The data used for both pre-calculation and environmental corrections are summarized in Appendix 2.

3.5 Interpretation/Analysis

This project involves the determination of reservoir rock properties i.e. shale volume, porosity, and water saturation. A deterministic approach is used here. Within Geolog 6.6, the petrophysical parameters were interpreted using a traditional, stepwise methodology. First, the shale volume was calculated, then the porosity was determined and finally the water saturation was computed. Results from the previous step are required for the subsequent one. Petrophysics definitions (e.g. of porosity and saturation types) vary somewhat and Figure 3.8 shows the definition used by the Geolog 6.6 software and followed here.

A probabilistic approach was also undertaken to investigate an alternative methodology. This was performed using the Multimin module within Geolog software. Multimin is an integrated petrophysical analysis which reflects the flexibility of the probabilistic modeling approach (Paradigm, 2006). However, the porosity results when compared to the core data are very pessimistic. A further study using Multimin is needed to compile the fluid properties package, mineral response parameters and other information from the well itself. A brief discussion of Multimin experiment is presented in section 5.2.

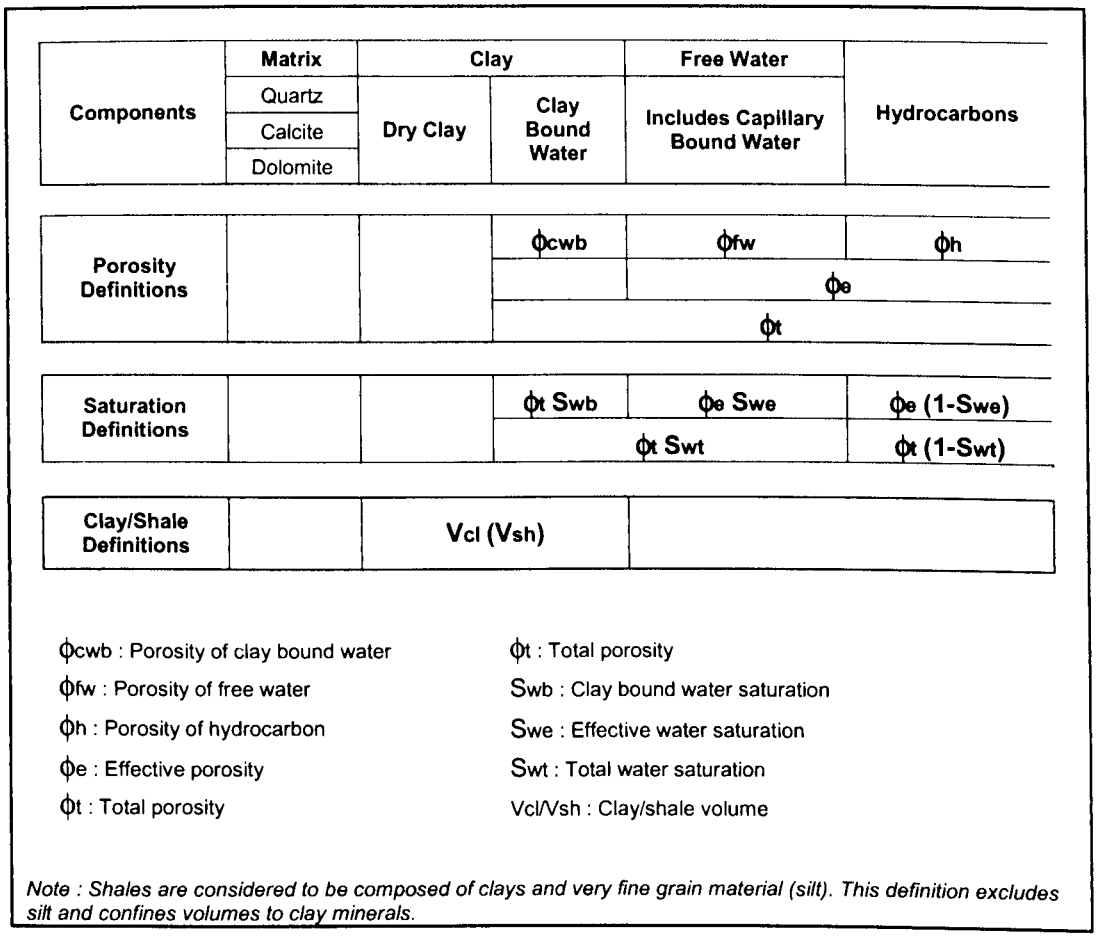

Figure 3.8. The definitions and terminologies (modified from Paradigm, 2006)

3.5.1 Parameter Picking

The objective of parameter picking is to interactively pick the petrophysical parameters that will be used in the petrophysical analysis. This process encompasses picking shale point from a cross plot, picking minimum and maximum of gamma ray values from a histogram, and interactively determining the water resistivity, *Rw*, from Pickett plots. Summaries of the parameters picked in the study are shown in Appendix 4.

In order to pick parameters such as shale points, and sand and shale baselines, it was first necessary to decide into what intervals the analyzed section should be split. The same parameters could be applied to the entire sequence to be analyzed (up to 2 km) or each formation could be analyzed separately. The former was considered too coarse a division and

the latter too fine. If the analysis was undertaken on each individual formation, for example, clean units would be erroneously assigned 100% shale at the shaliest point. It was decided to split the sequence analyzed into two units for parameter picking. One, the Late Cretaceous section which comprises the Puffin, Fenelon/Gibson and Wooalston Formations, is carbonate-dominated. The second, the Early Cretaceous – Late Triassic section which encompasses the Jamieson, Echuca Shoals, Upper Vulcan, Lower Vulcan, Plover and Nome Formations, is clastic-dominated.

Gamma ray histograms were created for each of the two sections in each well in order to define the matrix and shale baselines (Figure 3.9). Density-neutron cross plots were used to determine shale points (Figure 3.10). The shale point is taken as the extreme southeast value within the supposed shale field (Rider, 2002). The gamma ray-sonic cross plot was used to examine the sonic values of the shale point (Figure 3.11).

The Pickett plot is a log-log cross plot of porosity versus resistivity. It was used for estimating formation water resistivity (Figure 3.12). A detailed explanation of this plot is given in section 3.5.5.

3.5.2 Bad Hole Identification

Bad hole was identified from the caliper and density correction logs. The cutoffs used in this project to identify bad hole were $0.2\,gr/cm^3$ for the density correction log and *1.5 inch* for the absolute difference between caliper and bit size. A bad hole flag was set to mark intervals thus identified. Summaries of the bad hole within each well are shown in Appendix 2.

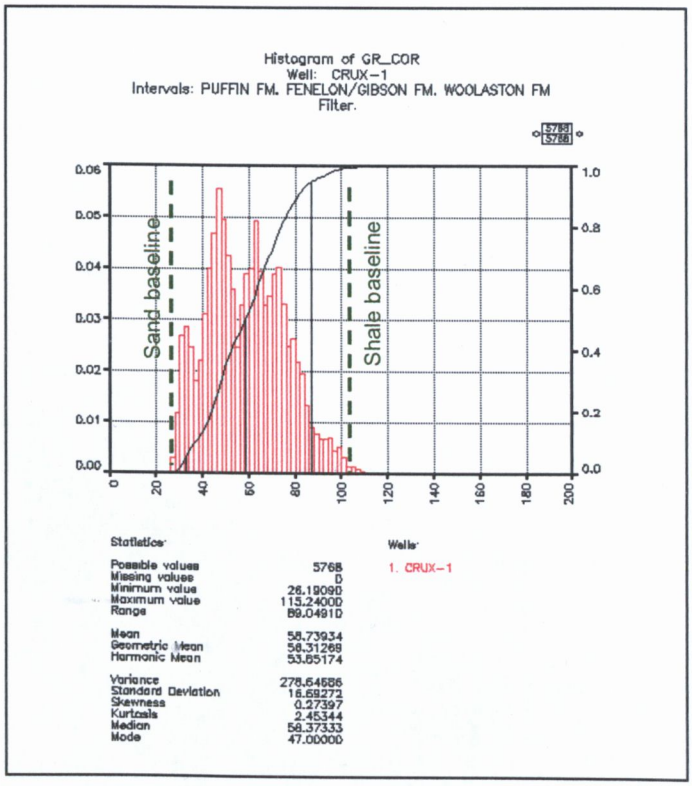

Figure 3.9. Example of shale and sand baselines defined on gamma ray histogram: Upper section, Crux-1.

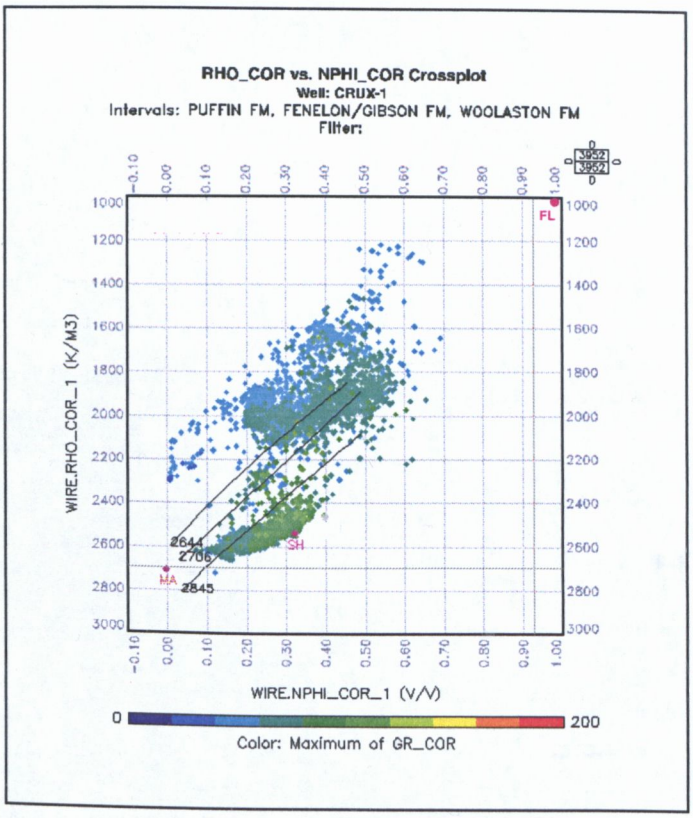

Figure 3.10. Example of shale point defined on a neutron-density crossplot: Upper section, Crux-1.

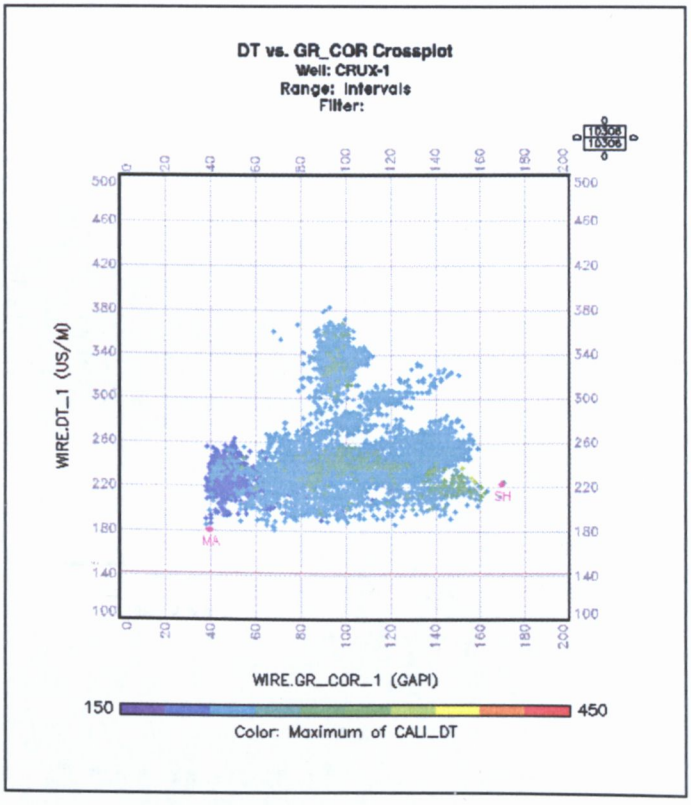

Figure 3.11. Example of shale sonic point determined on gamma ray-sonic crossplot: Upper Section, Crux-1.

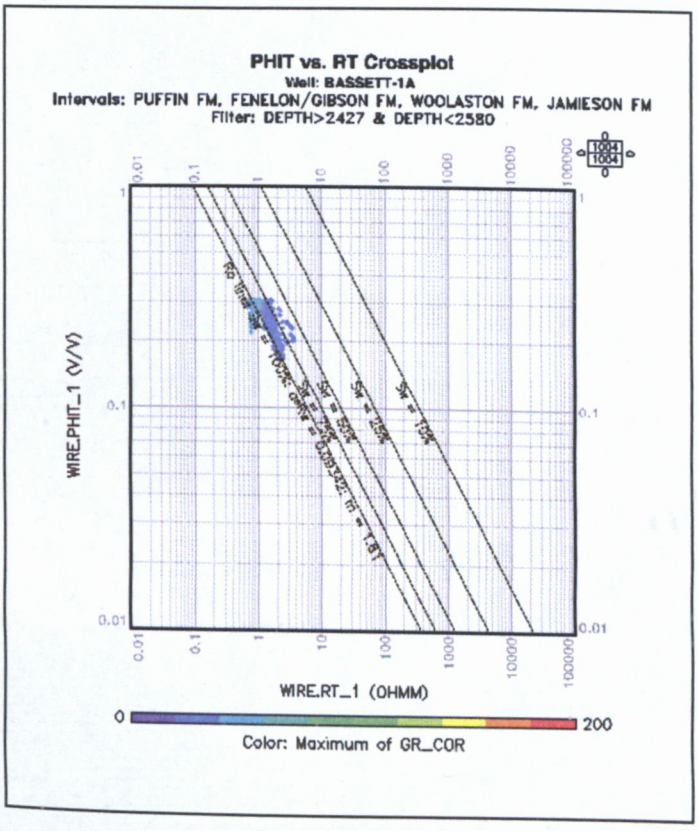

Figure 3.12. Example of formation water resistivity determined from Pickett plot in a wet zone: Basset-1A.

3.5.3 Shale Volume

The density-neutron combination is generally the best log indicator of shale volume (Rider, 2002) and was one method used here to calculate shale volume (Figure 3.10). The density and neutron porosity data are crossplotted over the selected intervals then the shale point is picked at the southeast extreme of the plot. The shale point, indicating 100% shale, is connected to a fluid point thus establishing a shale line (from 0 to 100% porosity). The zero porosity calcite/quartz matrix point is selected from its density and neutron porosity and connected to the fluid point creating a clean limestone/sandstone line. Here, a clean limestone line was used for the Upper Cretaceous section and a clean sandstone line for the Upper Triassic – Lower Cretaceous section.

This clean matrix line represents 0% of shale. With the triangle thus established (Figure 3.10), the shale volume and porosity of any point in the crossplot then can be estimated. However, it must be remembered that gas affects the calculation since the neutron reading is commonly low in gas zones (Bigelow, 1995).

The gamma ray log is often used quantitatively to calculate the shale volume. The simple calculation for a linear model is

$$Vsh = \frac{GR_{\log} - GR_{\min}}{GR_{\max} - GR_{\min}}$$

where GR_{max} is gamma ray value in 100% shale and GR_{min} is gamma ray value in clean sand (0% shale). Shale volume prediction from gamma ray is very straight forward but tends to overestimate the shale volume (Rider, 2002). GR_{max} and GR_{min} were picked from the gamma ray histogram (Figure 3.9).

In this study, shale volume was determined as the lowest of the gamma ray-derived volume and density-neutron-derived value. The gamma ray-derived value was used in bad hole sections, since density and neutron are more influenced by the borehole condition.

3.5.4 Porosity

Porosity is defined as the ratio of volume of pore space within a rock to the bulk volume of rock. It is expressed as a percentage or, in petrophysical calculations, as a fraction. Total porosity encompasses both interconnected and isolated pores. Effective porosity encompasses only the interconnected part of the total porosity.

Porosity can be calculated from log data using several different algorithms. In order to select the best method for this study, the results of several methods were compared to core porosity data measured from the core of Crux-1. The core data needed to be depth shifted by 6 m to match the log data (Figure 3.13).

The sonic log is a good porosity estimator in water and oil-filled rocks. The data needed for estimating porosity are the sonic response at the depth of interest and the response associated with the matrix. Typical matrix values are 55.5 μsec/ft for sandstone, 47.5 μsec/ft for limestone and 43.5 μsec/ft for dolomite.

The Wyllie equation, Raymer-Hunt-Gardner, and Acoustic Formation Factor methods were all used to transform sonic data to porosity. However, the correlation between the core-derived and the log-derived porosity is poor (Figure 3.14). The low correlation coefficients are to some extent due to the relatively small spread of porosity in the core data. Considering the core and log-derived porosities plotted against depth (Figure 3.15), the Raymer-Hunt-Gardner method provides reasonable porosity estimation, although exaggerating porosity in the shaly units and underestimating it by ~1-2% on average in the clean units, where porosity is 15-20%. The Raymer-Hunt-Gardner sonic porosity was used in this study.

The *Raymer-Hunt-Gardner* equation is an empirical approach developed from the statistical analysis of sonic measurements. The equation is

$$\phi_e = C\frac{\Delta t_l - \Delta t_{ma}}{\Delta t_l},$$

where Δt_l is the sonic value at the depth of interest, Δt_{ma} is the sonic value of the matrix, and C is a factor that varies between 0.625 and 0.7. The most widely used C-value is 0.67 but 0.6 is recommended for gas reservoirs (Morton-Thompson and Woods, 1992). The value of 0.67 was used for C in this study.

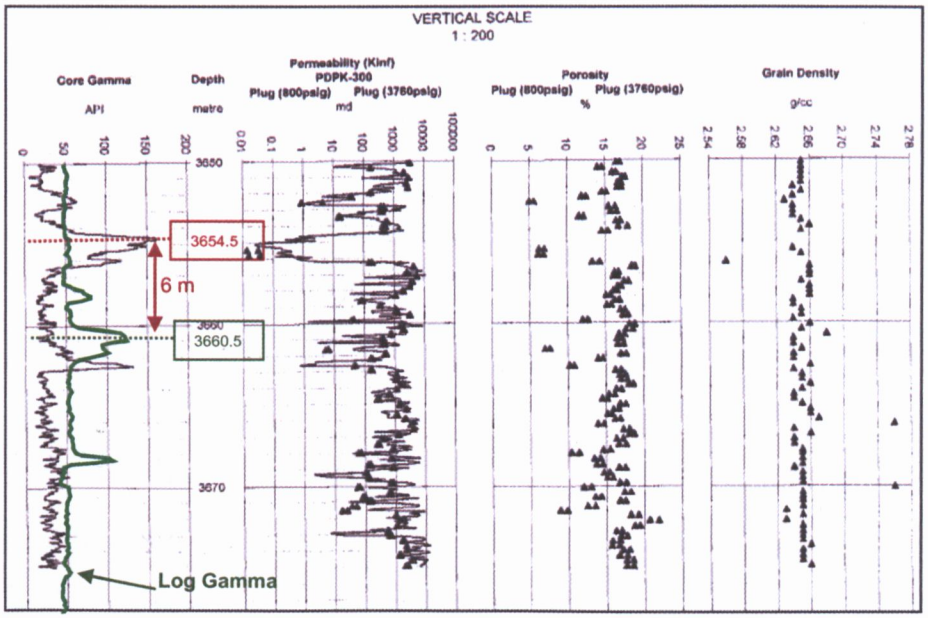

Figure 3.13. Core gamma for Crux-1 (from Well Completion Report) compared to the log reference gamma. The core data was off depth by about 6 metres .

The effective porosity is limited by choosing $\phi_{e\max}$, because the Raymer-Hunt-Gardner equation calculates unrealistic values occasionally (personal communication, Michael Wilson[1], 2007). Hence, the effective porosity should fulfill

$$\phi_e \leq \phi_{e\max}(1-Vsh).$$

The total porosity is calculated as

$$\phi_t = \phi_e + \phi_{cwb}, \text{ and}$$

$$\phi_{cwb} = Vsh\,\phi_{tsh},$$

where ϕ_{tsh} represents the volume of clay bound water, ϕ_e is effective porosity, ϕ_t is total porosity and ϕ_{cwb} is clay bound water porosity. In this study, $\phi_{e\max}$ and ϕ_{tsh} are assumed to 30% and 5% respectively.

[1] Chevron ASBU Petrophysicist

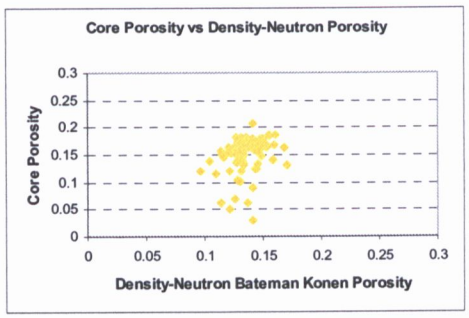

(a) Crossplot between core porosity and density-neutron porosity. R^2=0.307.

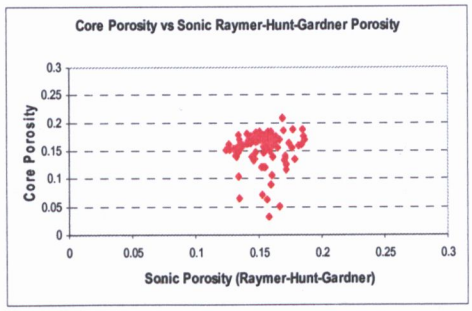

(b) Crossplot between core porosity and sonic porosity from Raymer-Hunt-Gardner equation. R^2=0.031.

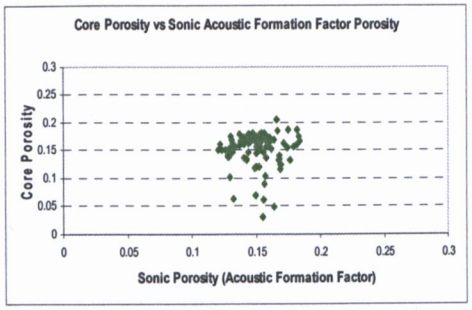

(c) Crossplot between core porosity and sonic porosity (Acoustic Formation Factor). R^2=0.024.

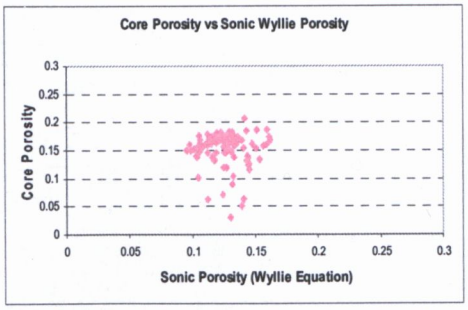

(d) Crossplot between core porosity and sonic porosity from Wyllie average equation. R^2=0.006.

Figure 3.14. Crossplot between core porosity and the log-derived porosity showing poor correlations.

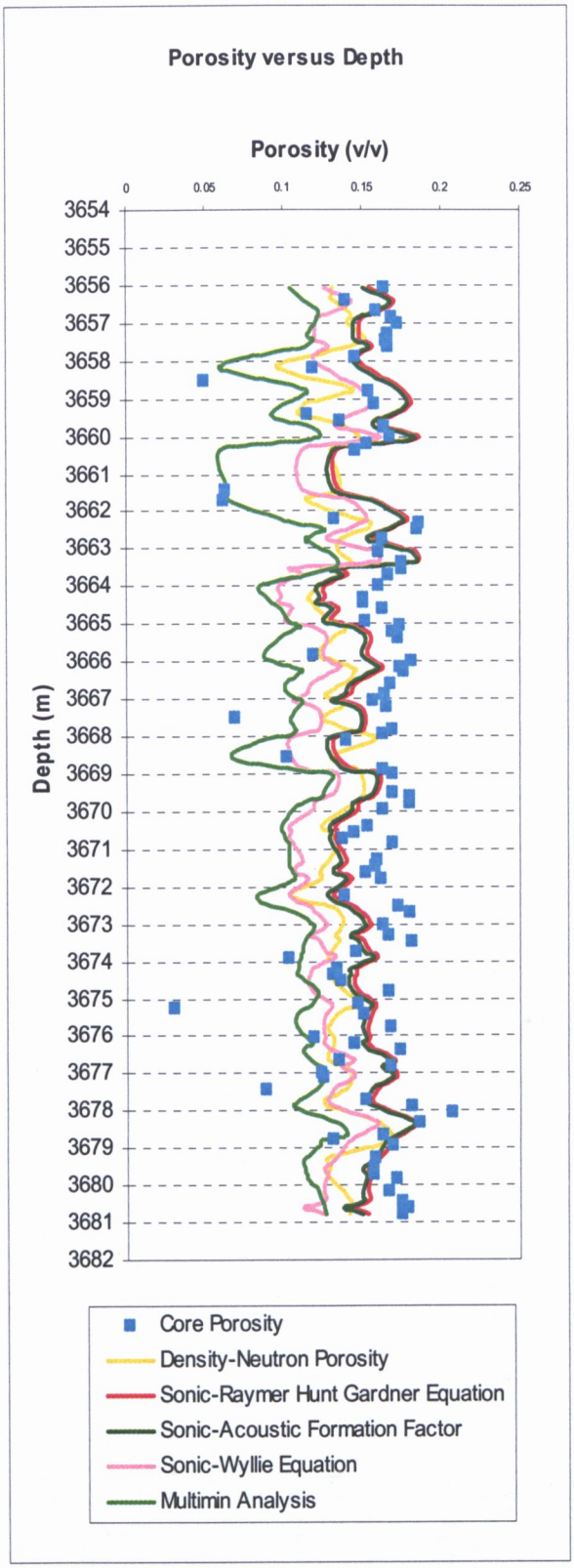

Figure 3.15. Core porosity and log-derived porosity versus depth.

3.5.5 Formation Water Resistivity Determination

Formation, connate or interstitial water is water, uncontaminated by drilling mud, which saturates the porous formation rock. The resistivity of this formation water, R_w, is an important parameter because it is needed for the saturation calculation.

The value of water resistivity, R_w, can be obtained directly from a sample of formation water. However, frequently the sample is contaminated by mud filtrate. R_w is therefore usually calculated. Here, formation water resisitivity is determined by the apparent formation water resitivity (R_{wa}) technique in an interpreted water zone, using a Pickett plot.

Pickett plots are crossplots of porosity against true formation resistivity. This plot is useful in wells with a minimum of petrophysical data. Knowledge of R_w and m, the cementation exponent, are not necessary, provided they are constants (Pickett, 1966).

Consider the Archie equation:

$$R_t = \frac{a R_w}{\phi^m S_w^n},$$

where R_t is true formation resistivity, a is a constant and (set equal to 1), ϕ is porosity, m is the cementation exponent (related to texture), S_w is water saturation and n is the saturation exponent. Pickett took the logarithms of both sides of the equation and converted it to the linear equation

$$\log R_t = -m \log \phi + \log\left(a R_w S_w^{-n}\right).$$

In a 100% water saturated formation, $R_t = R_0$, where R_0 is the wet resistivity, i.e. the true formation resistivity of the rock where the pore space is 100% saturated with brine of resistivity R_w. Hence, the equation becomes

$$\log R_0 = -m \log \phi + c,$$

where $c = \log a R_w$.

On a log-log plot of true resistivity against porosity, rocks with 100% water saturation is plot on a straight line of slope $-m$ and ordinate intercept $c = a\,R_w$. This line is called the R_0 line.

In this study, the R_0 line was determined from the Pickett plot in zone interpreted to be water saturated. R_w is obtained from the resistivity of the R_0 line for $\phi = 100\%$. The formation water resistivity was assumed to be the same through the entire Late Triassic-Late Cretaceous sequence analyzed in each well.

3.5.6 Water Saturation

Water saturation is defined as the ratio of formation water occupying pores to the total pore space. It is expressed as a percentage or in petrophysics analysis as a fraction. Hydrocarbon saturation is the complement of water saturation. The method used for determining water saturation in this study is the dual water model for shaly sand.

The dual water equation was designed for shaly sandstones with moderate amounts of dispersed clay (Morton-Thompson and Woods, 1992). The conductivity of clay is a result of its CEC (Cation Exchange Capacity) or the ability of the clay to exchange cations. The CEC is proportional to the surface area of the clays and it is a function of salinity and temperature.

In the dual water model, clay is composed of two components, bound water and clay minerals. The clay minerals are modeled as being electrically inert. The clay's electrical conductivity is modeled as being derived from the conductivity of the bound water (Serra, 1989). The conductivity of bound water depends on the surface area available in the clay; hence it is higher in the finer clays (montmorillonite) and lower in the coarser clays. In low salinity solutions, the diffuse layer expands, which increases the conductivity. The dual water equation is

$$C_t = \frac{\phi_t^{\,m} S_{wt}^{\,n}}{a} C_{we},$$

where a, m, and n are Archie constants, C_t is the conductivity of the uninvaded formation, C_{we} is the equivalent conductivity of the water in the pore space and S_{wt} is total water saturation (Serra, 1989).

The equivalent water conductivity is

$$C_{we} = \frac{V_w C_w + V_{wb} C_{wb}}{V_w + V_{wb}},$$

where V_w and V_{wb} are the bulk volumes of formation water and bound water, respectively, and C_w and C_{wb} are their conductivities (Serra, 1989). In terms of saturation, the equation becomes

$$C_{we} = C_w + \left(\frac{S_{wb}}{S_{wt}}\right)(C_{wb} - C_w),$$

where S_{wb} is the bound water saturation, the fraction of the total pore volume occupied by the bound water (Serra, 1989).

The porosity of the clean formation (nonclay) is then

$$\phi_e = \phi_t (1 - S_{wb}),$$

and the water saturation is

$$S_{we} = \frac{S_{wt} - S_{wb}}{1 - S_{wb}}.$$

In order to apply the dual water model, one needs to determine C_w or R_w, C_{wb} or R_{wb}, ϕ_t, and S_{wb}. The total porosity, ϕ_t, is calculated from the sonic porosity (the Raymer-Hunt-Gardner porosity equation). The conductivity of clay water bound, C_{wb}, is estimated from the salinity and formation water resistivity. The bound water saturation, S_{wb}, is calculated from the CEC to get the Q_v or the CEC of the rock per unit pore volume. Formation water resisitivity is determined by the R_{wa} technique in an interpreted water zone using the Pickett plot, as discussed previously.

The saturation equation parameters were taken from the core analysis report of Crux-1. The values 1.81 for the cementation exponent, m, and 1.77 for the saturation exponent, n, were

applied to all wells. The CEC of dry shale was assumed to be 0.15 *meq/g,* which was obtained from the core analysis of Buffon-1. There are large uncertainties here, since the values may not be constant throughout the study area.

3.5.7 Net Sand - Net Reservoir - Net Pay Summaries

The net sand-net reservoir-net pay summaries were based on the following definitions. Net sand requires $Vsh \leq 40\%$. Net reservoir is net sand with $\phi_e \geq 7\%$. Net pay is net reservoir with $S_{wt} \leq 60\%$.

4 Petrophysical Results

4.1 Formation Water Salinity

The calculated formation water resistivity for each well describes salinity within the region (Figure 4.1). Conversion from formation water resisitivity to salinity was performed using the resistivity of NaCl water solutions chart (Schlumberger, 2005). The salinity distribution shows a clear pattern across the region which is generally increasing from southwest to northeast. The lowest values of 12,000 ppm were encountered at Argus-1, Buffon-1, and Phrixus-1. The highest value of 70,000-80,000 ppm in Heywood-1, Crux-1 and Delta-1 are likely to be associated with the salt movement during the Early Miocene to late Middle Miocene (Struckmeyer et al., 1998).

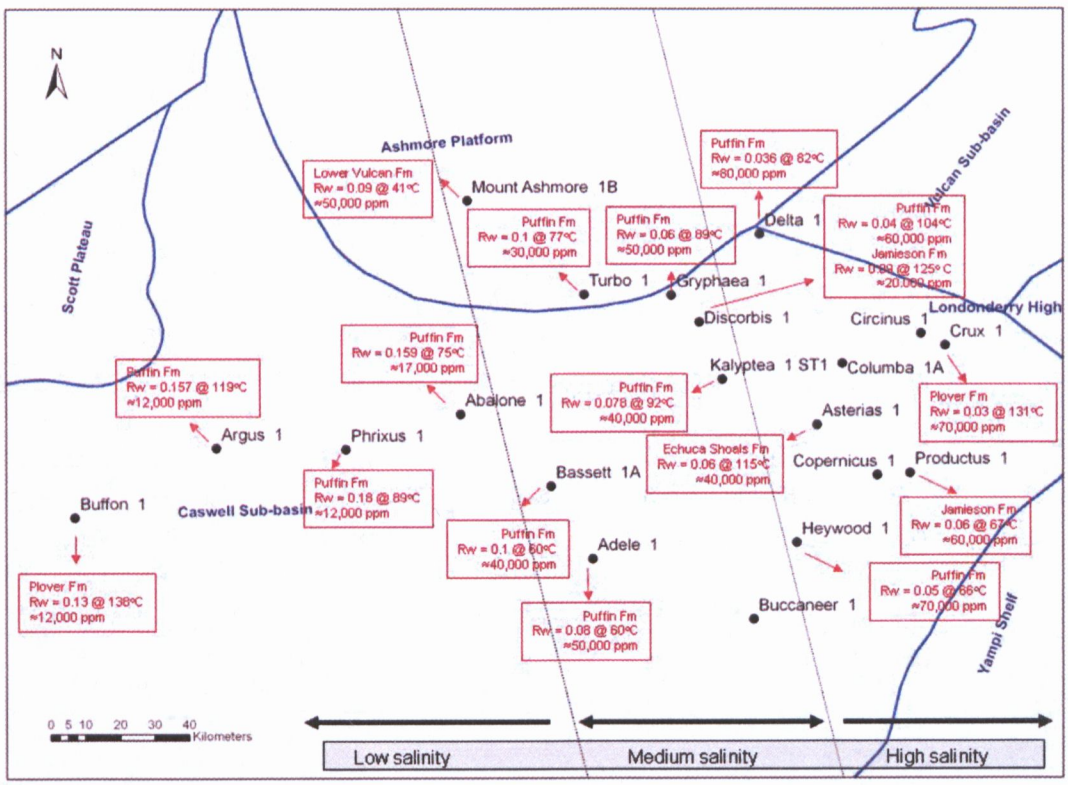

Figure 4.1. The distribution of formation water salinity within the study area calculated from *Rwa* data. The formation water is more saline in the northeast part of the region.

4.2 Petrophysical Properties within Each Formation

Although parameters such as shale and sand baselines were picked for the carbonate and clastic sequence, petrophysical analysis were repeated for nine separate formations. The net sand, reservoir and pay summaries and the composite logs of each well can be seen in Appendix 5 and 6 respectively. Cross-sections showing the sand, reservoir and pay intervals, were generated along the section shown in Figure 1.1.

Table 4.1 shows a summary of the potential net pay interpreted in each formation for each well. Phrixus-1 and Basset-1A did not encounter any potential net pay. Productus-1 and Turbo-1 contain potential net pay of 2 m in the Jamieson Formation and 3m in the Puffin Formation respectively, which are not significant. Hence, four out of the 16 analyzed wells do not have potential net pay thickness. The summary of the potential net pay encountered in each formation for each well is shown in Table 4.1.

Formation / Well	Puffin Formation	Fenelon/ Gibson Formation	Woolaston Formation	Jamieson Formation	Echuca Shoals Formation	Upper Vulcan Formation	Lower Vulcan Formation	Plover Formation	Nome Formation
Abalone-1	5.6	8.5	-	2.3	-	-	-	-	-
Adele-1	-	9.3	-	148.3	61	1.1	14.3	-	-
Argus-1	8.4	-	-	2.6	-	-	10.4	13.1	-
Asterias-1	1.5	-	-	15	15.1	143.1	-	-	-
Basset-1A	-	-	-	-	-	-	-	-	-
Buffon-1	-	-	-	-	-	-	-	44.7	-
Crux-1	-	-	-	-	-	19.1	-	-	167.3
Delta-1	28.8	-	-	-	-	-	-	-	-
Discorbis-1	51.4	67.4	24.1	1.8	-	-	-	-	-
Gryphaea-1	69.3	-	13.3	6.3	-	-	-	-	-
Heywood-1	31.2	4.5	-	47.6	12	430.8	34.2	-	-
Kalyptea-1ST1	127.4	-	-	6.3	16.5	33.4	-	-	-
Mt Ashmore-1B	12.6	-	-	-	2.6	-	-	-	-
Phrixus-1	-	-	-	-	-	-	-	-	-
Productus-1	-	-	-	1.2	-	-	-	-	-
Turbo-1	2.9	-	-	-	-	-	-	-	-

Table 4.1. Summary of potential net pay thickness (in meters) encountered in each formation for each well. The recognized hydrocarbon shows (from Table 2.1) are highlighted in grey.

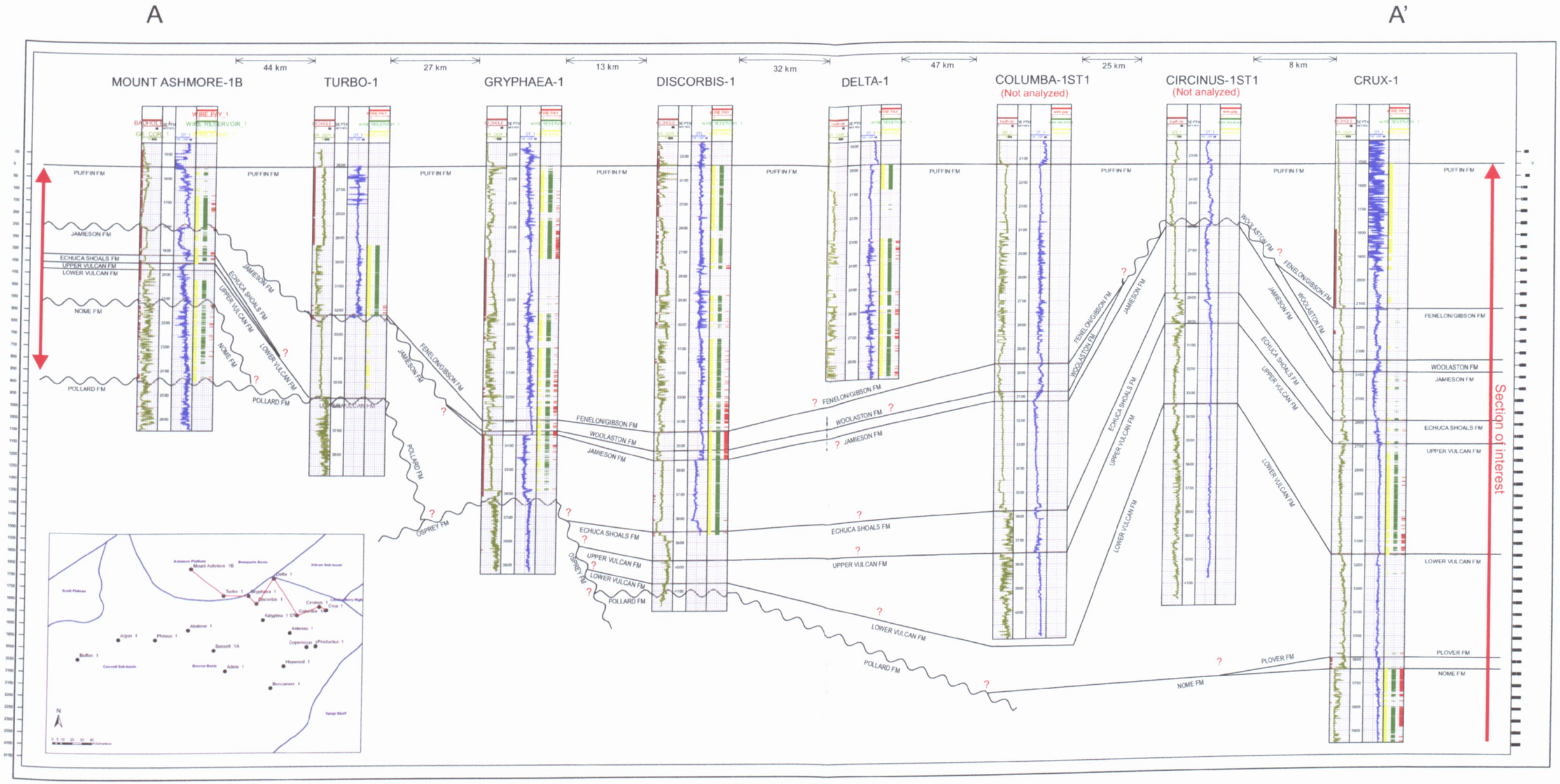

Figure 4.2. Log cross-section showing the pay, reservoir and sand intervals through the northern part of the study area. The data shown are:

track 1 - brown flag : bad hole indicator
- green curves : gamma ray logs (scale : 0 - 150, unit : GAPI)
track 2 - measured depth annotated at 100 m interval
track 3 - blue curves : sonic logs (scale: 140 - 40, unit : us/ft)
track 4 - yellow flag : net sand indicator
- green flag : net reservoir indicator
- red flag : net pay indicator

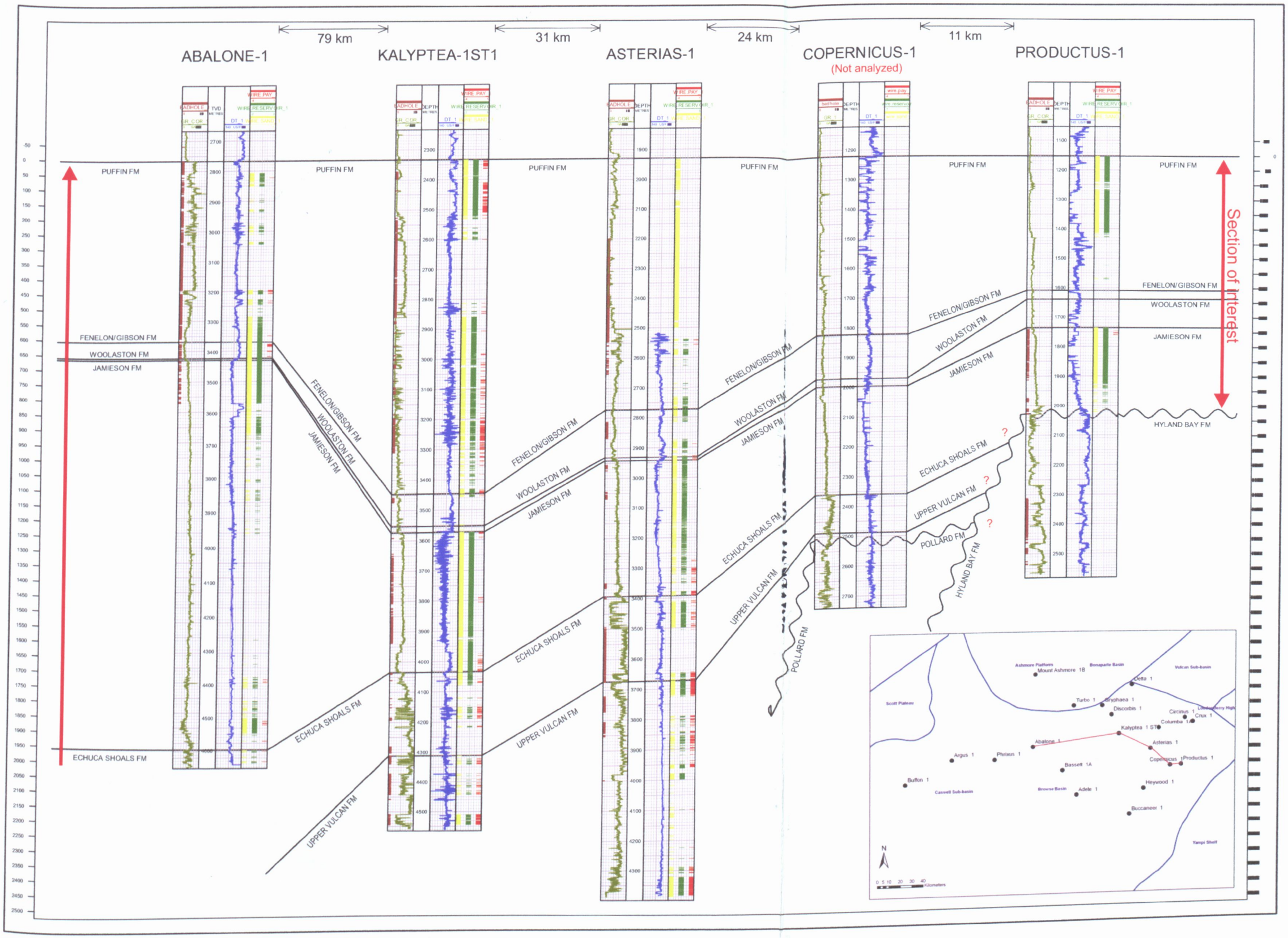

Figure 4.3. Log cross-section showing the pay, reservoir and sand intervals through the central part of the study area. The data shown are:

track 1 - brown flag : bad hole indicator
- green curves : gamma ray logs (scale : 0 - 150, unit : GAPI)
track 2 - measured depth annotated at 100 m interval, except for Abalone-1 in TVD
track 3 - blue curves : sonic logs (scale: 140 - 40, unit : us/ft)
track 4 - yellow flag : net sand indicator
- green flag : net reservoir indicator
- red flag : net pay indicator

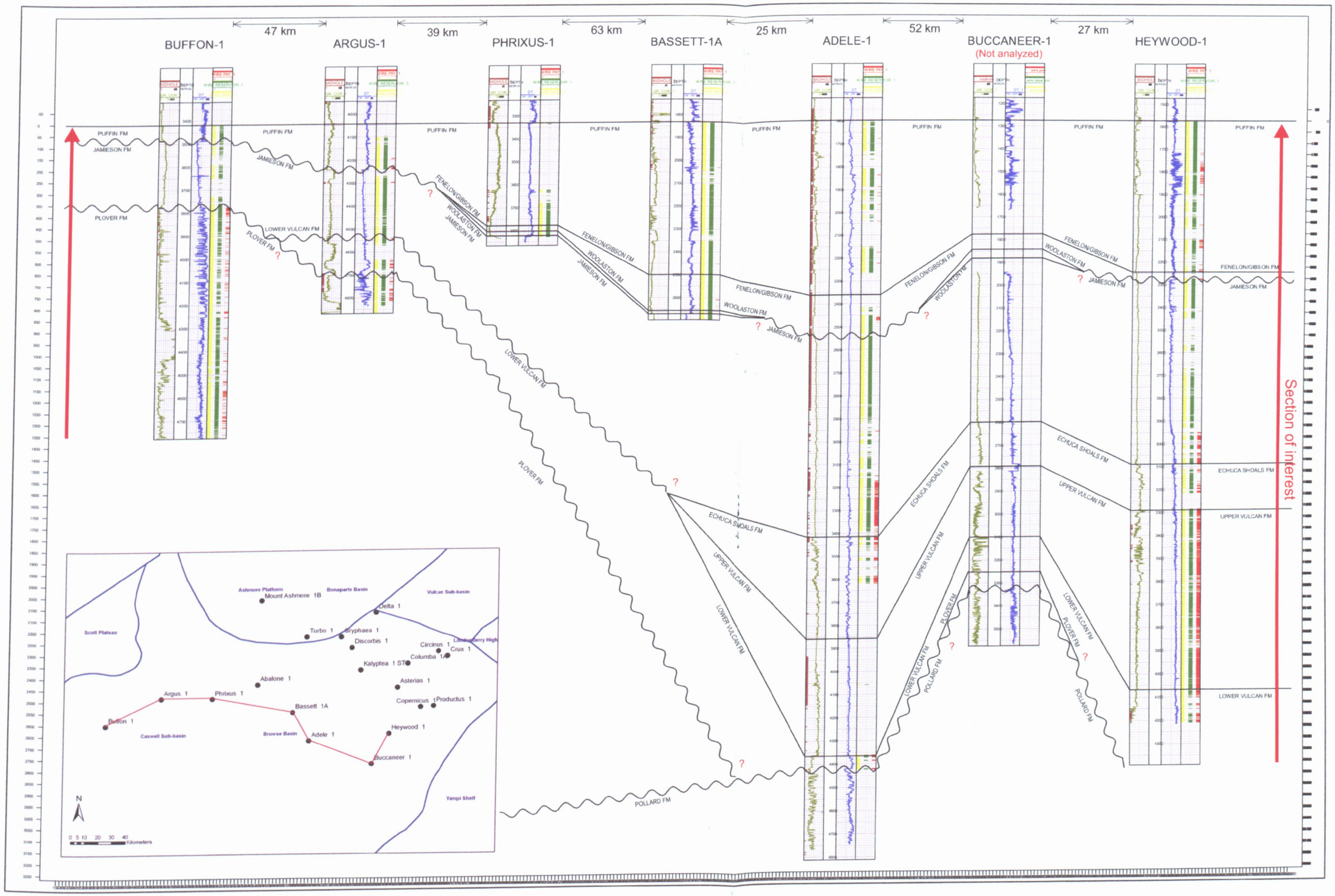

Figure 4.4. Log cross-section showing the pay, reservoir and sand intervals through the southern part of the study area. The data shown are:

track 1 - brown flag : bad hole indicator
- green curves : gamma ray logs (scale : 0 - 150, unit : GAPI)
track 2 - measured depth annotated at 100 m interval
track 3 - blue curves : sonic logs (scale: 140 - 40, unit : us/ft)
track 4 - yellow flag : net sand indicator
- green flag : net reservoir indicator
- red flag : net pay indicator

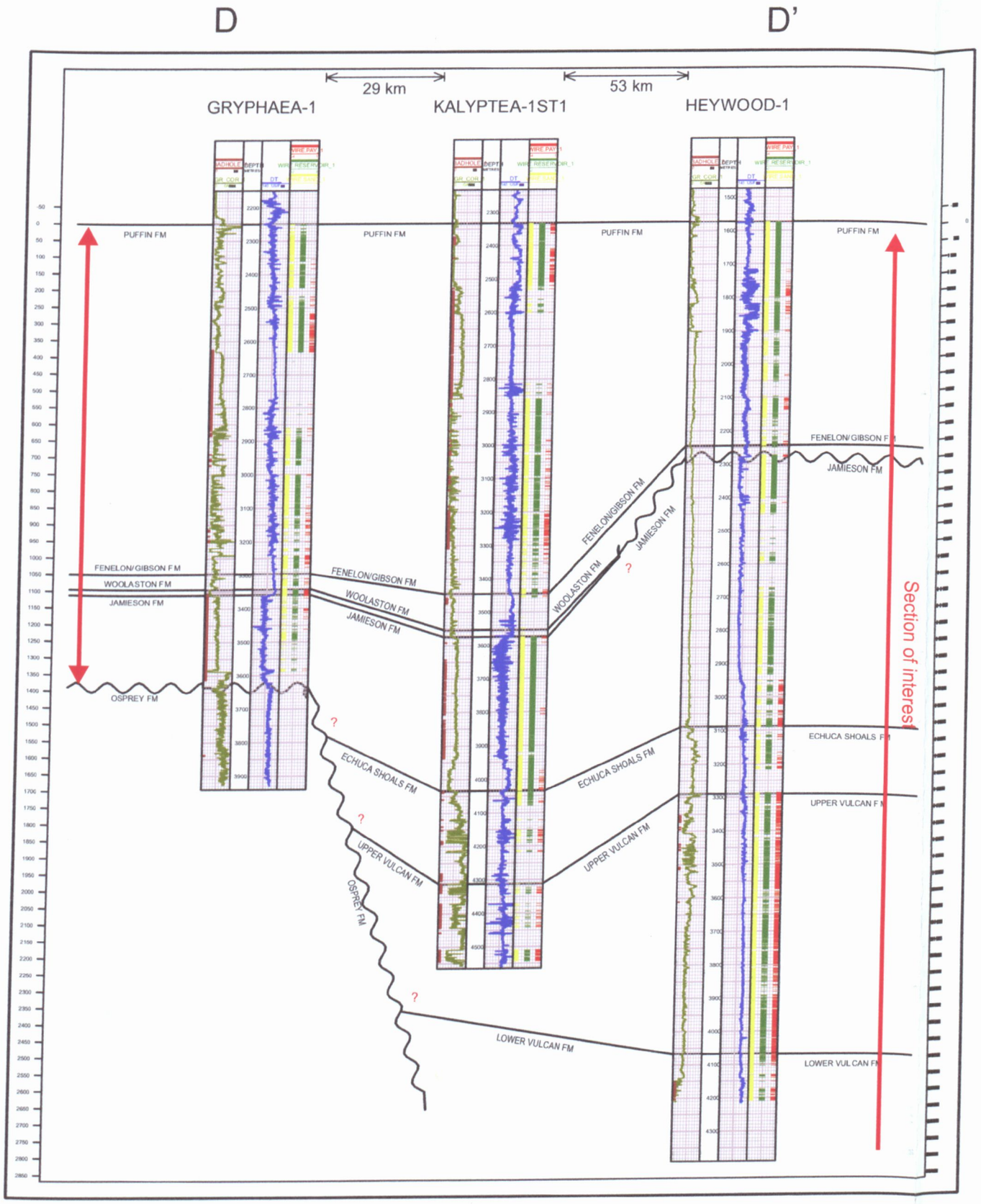

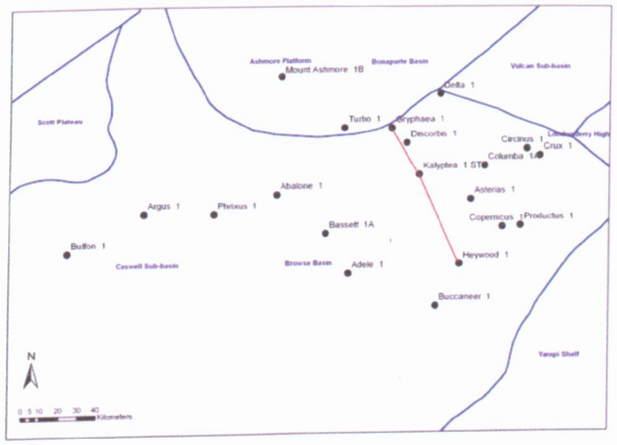

Figure 4.5. Log cross-section showing the pay, reservoir and sand intervals from north to south part of the study area. The data shown are:

track 1 - brown flag : bad hole indicator
- green curves : gamma ray logs (scale : 0 - 150, unit : GAPI)
track 2 - measured depth annotated at 100 m interval
track 3 - blue curves : sonic logs (scale: 140 - 40, unit : us/ft)
track 4 - yellow flag : net sand indicator
- green flag : net reservoir indicator
- red flag : net pay indicator

4.2.1 Puffin Formation

The Puffin Formation was identified in all analyzed wells. It comprises sandstones and limestones. The formation is the thickest unit of the formations being studied here. The thickness ranges from 69 m, in Buffon-1, to 1113 m, in Kalyptea-1ST1. It is thickest in the central part of the study area and thins to the west (Figure 3.2-3.4).

Potential net pay was recognized in 10 out of the 16 analyzed wells (Figure 4.6). An average of 20% porosity and 50% total water saturation across the pay was encountered. An area of thick potential net pay was identified in the northeast part of the study area in Gryphaea-1, Discorbis-1 and Kalyptea-1ST1. The thickest net pay section interpreted was 127 m in Kalyptea-1ST1, with approximately 16% porosity and 46% water saturation.

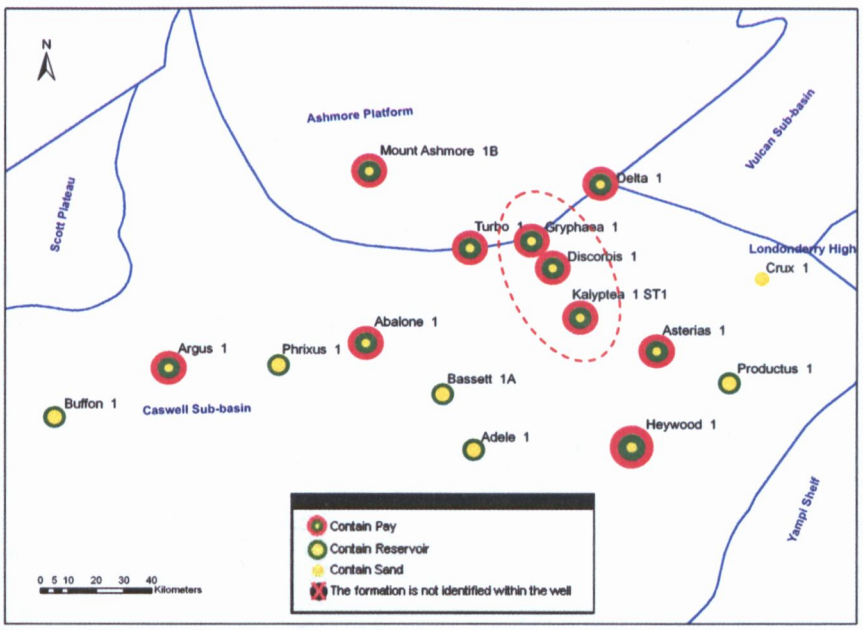

Figure 4.6. The identification of net pay, reservoir, and sand in the Puffin Formation. Gryphaea-1, Discorbis-1 and Kalyptea-1ST1 were interpreted to contain thick potential net pay.

Gas indications were obtained from this formation when drilling Abalone-1, Discorbis-1 and Gryphaea-1. This study indicates 69 m of potential net pay at 19% porosity and 54% water

saturation in Gryphaea-1, 51 m at 13% porosity and 51% water saturation in Discorbis-1, and only 5 m at 19% porosity and 39% water saturation in Abalone-1.

4.2.2 Fenelon/Gibson Formation

The Fenelon/Gibson Formation is a thin formation ranging from 12 m to 217 m. The formation thins to the northwest and is missing in three wells: Mount Ashmore-1B, Buffon-1 and Argus-1 and is dominantly limestone.

An average of 47 m of potential net reservoir was estimated for this formation. The greatest thickness of potential net reservoir was 156 m in Basset-1A at 24% total porosity and 80% water saturation. The thinnest was 4 m, identified in Kalyptea-1ST1 and Turbo-1, with approximately 9% porosity and 66% water saturation.

Four out of 12 wells have potential net pay (Figure 4.7) but only Discorbis-1 has a significant thickness, 67 m, while the others have less than 10 m. An average of 23% shale volume, 11% porosity and 51% water saturation was calculated across the pay in Discorbis-1.

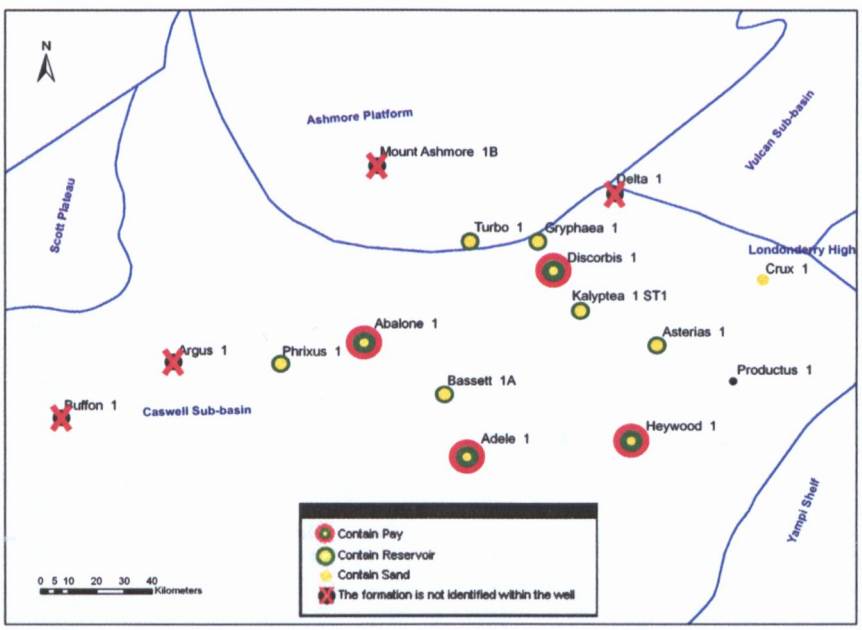

Figure 4.7. The identification of net pay, reservoir, and sand in the Fenelon/Gibson Formation.

4.2.3 Woolaston Formation

The Woolaston Formation is the thinnest formation encountered in this study. It thins to the west and south of the study region and is missing in seven of the analyzed wells (Figure 3.2-3.5). The greatest thickness, 96 m, was encountered in Productus-1 while the lowest, 7 m, was identified in Abalone-1. This formation comprises limestones.

Six out of nine wells that encountered this formation contain potential net reservoir ranging from 5 m to 23 m at approximately 15% porosity and 68% water saturation on average. Potential net pay was only interpreted in two wells (Figure 4.8); 24 m in Discorbis-1 and 13 m in Gryphaea-1. Gas was encountered from this formation while drilling Discorbis-1. This study analyzed approximately 21% shale volume, 10% porosity and 49% water saturation in Discorbis-1 for this formation.

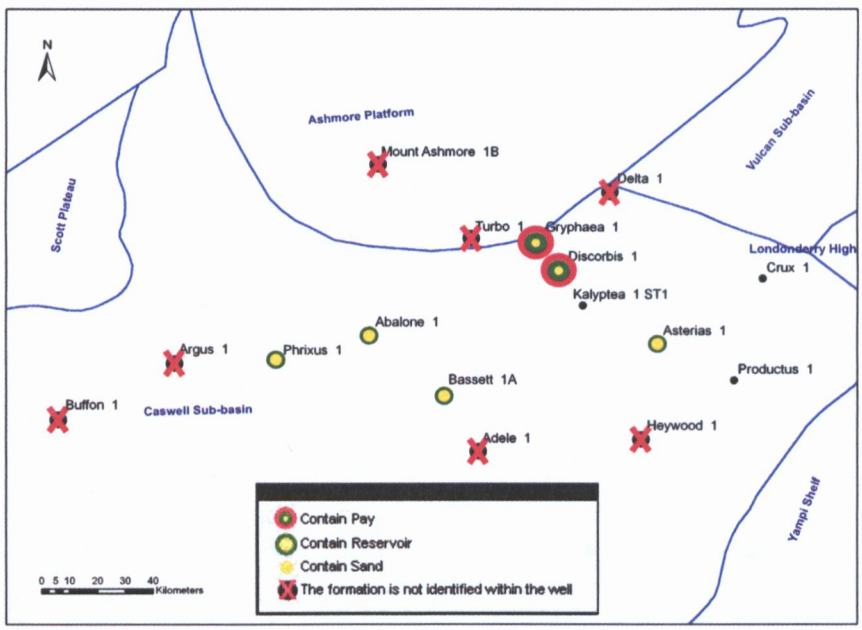

Figure 4.8. The identification of net pay, reservoir, and sand in the Woolaston Formation.

4.2.4 Jamieson Formation

The Jamieson Formation was identified in all of the wells except Delta-1. It is a thick sandstone formation. It is thickest at 1290 m in Abalone-1, and thinnest at 36 m in Bassett-1A.

Potential net sand was interpreted in all of the wells containing this formation, ranging from 6 m in Phrixus-1 and Crux-1 to 630 m in Adele-1. An average of 19% porosity and 85% water saturation were calculated for the sands within this formation.

More than half of the studied wells, nine out of 15 wells, have potential net pay (Figure 4.9). The southern part of the study area appears to be a zone of thick potential net pay, with Adele-1 and Heywood-1 having 148 m and 47 m respectively. The potential pay thickness thins to the north of the region with less than 15 m.

Gas bearing sand was encountered while drilling Adele-1. This study analyzed approximately 18% porosity and 53% water saturation across the pay in the well.

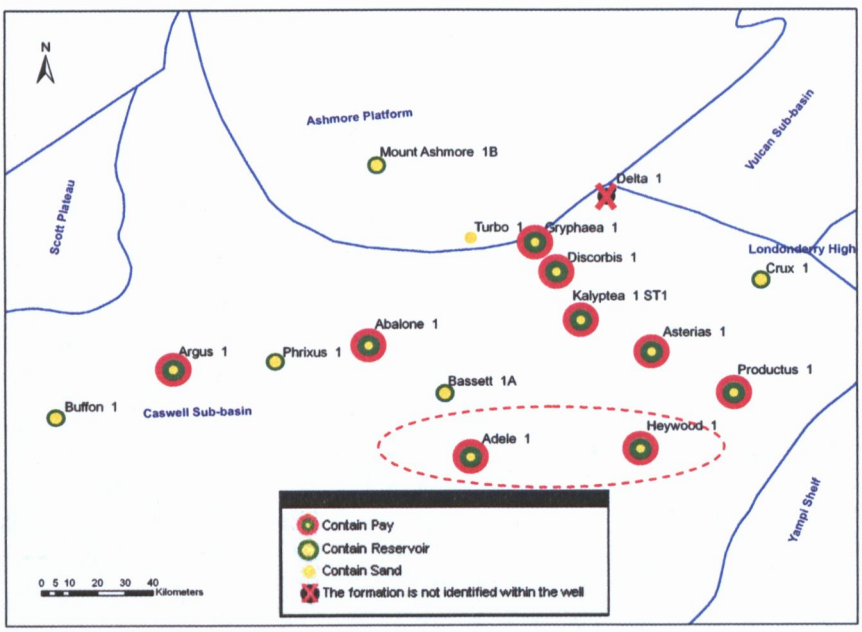

Figure 4.9. The identification of net pay, reservoir, and sand in the Jamieson Formation. Adele-1 and Heywood-1 were interpreted to contain thick potential net pay.

4.2.5 Echuca Shoals Formation

The Echuca Shoals Formation was encountered in eight wells, half of those analyzed. The sediment thickness ranges from 33 m, in Mount Ashmore-1B, to 440 m in Adele-1. It comprises sandstones.

Five out of eight wells have potential net pay (Figure 4.10), which averages 24% shale volume, 14% porosity and 44% water saturation. The thickest potential net pay was found in Adele-1 and Kalyptea-1ST1, with 61 m and 16 m respectively. The potential net pay thins to the northwest and southeast of these two wells.

Strong gas reading and fluorescence was encountered within this formation when drilling Adele-1. This study analyzed an average of 19% porosity and 38% water saturation across the pay in this well. Oil traces were also recorded in the lower Echuca Shoals Formation when drilling Copernicus-1. However, the logs from Copernicus-1 were not analyzed here.

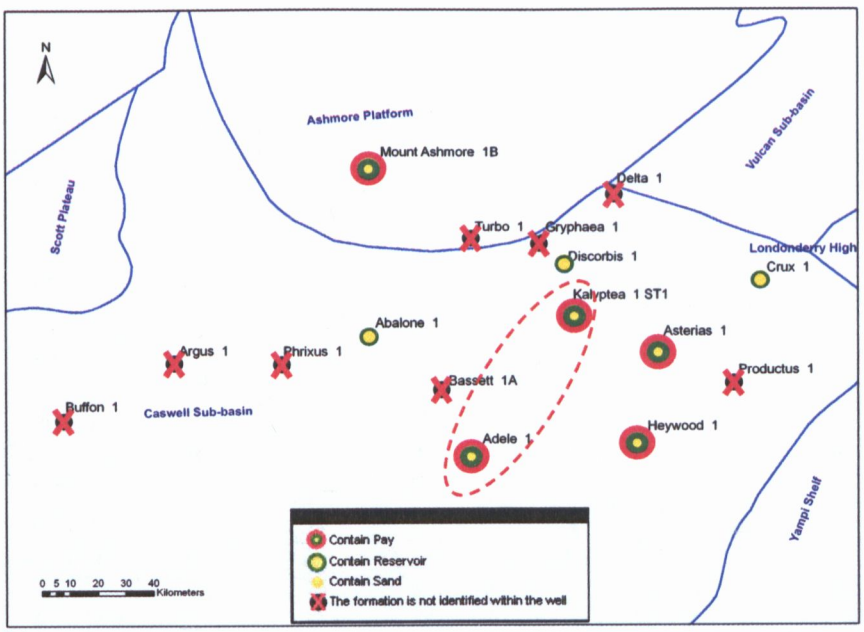

Figure 4.10. The identification of net pay, reservoir, and sand in the Echuca Shoals Formation. Adele-1 and Kalyptea-1ST1 were interpreted to contain thick potential net pay.

4.2.6 Upper Vulcan Formation

The Upper Vulcan Formation is primarily composed of sandstones. It was encountered in seven of the analyzed wells. Its thickness varies from 27 m in Discorbis-1 to 778 m in Heywood-1.

Five wells were interpreted to contain potential net pay (Figure 4.11), with the greatest thickness is in Heywood-1 and Asterias-1, at 430 m and 143 m respectively. The potential net pay thins to the west and east of these two wells, with thickness less than 30 m.

Oil and gas were indicated within this formation when drilling Heywood-1 and Asterias-1. These analyses gave average of 12% porosity and 32% water saturation across the pay in Asterias-1, and 9% porosity and 40% water saturation in Heywood-1. Oil and gas shows were also recorded when drilling Kalyptea-1ST1 and Buccaneer-1. In Kalyptea-1ST1, this study indicated 33 m potential net pay at 11% porosity and 21% water saturation. The logs from Buccaneer-1 were not evaluated here.

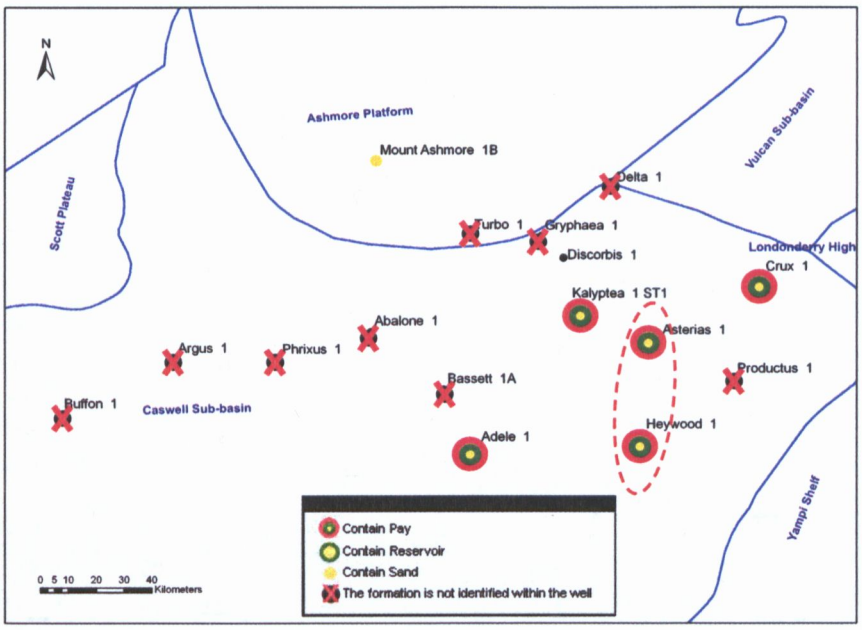

Figure 4.11. The identification of net pay, reservoir, and sand in the Upper Vulcan Formation. Heywood-1 and Asterias-1 were interpreted to contain thick potential net pay.

4.2.7 Lower Vulcan Formation

The Lower Vulcan Formation was identified in seven of the studied wells. The thickness of this formation varies from 9 m in Turbo-1, to 436 m in Crux-1. The formation thins to the west and is missing in Buffon-1. It is a clastic formation.

Potential net pay was only encountered in three out of seven wells (Figure 4.12). An average of 13% porosity and 29% water saturation were estimated for pay in this formation. The thickest potential net pay was in Heywood-1, where 34 m at approximately 8% porosity and 26% water saturation was indicated.

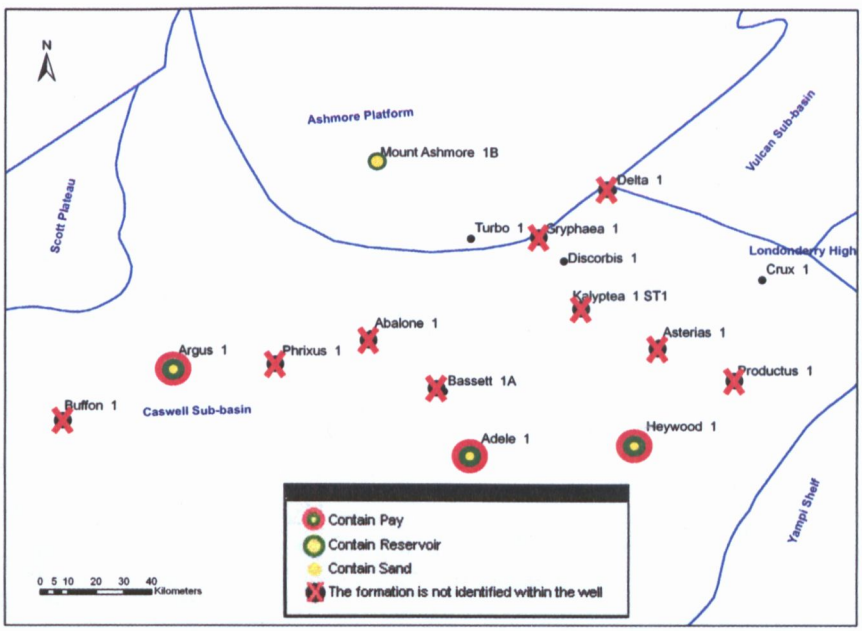

Figure 4.12. The identification of net pay, reservoir, and sand in the Lower Vulcan Formation.

4.2.8 Plover Formation

The Plover Formation contains the reservoirs for the giant gas accumulations at the Scott Reef and Brecknock Fields. However, this formation is only encountered in three of the analyzed

wells, Argus-1, Buffon-1 and Crux-1. It is thinnest, 49 m, in Crux-1 and thickest, 1011 m, in Buffon-1.

Potential net pay was only interpreted in Argus-1 and Buffon-1 (Figure 4.13). Argus-1 has approximately 13 m at 16% porosity and 43% water saturation. Buffon-1 has 44 m potential net pay at 17% porosity and 45% water saturation.

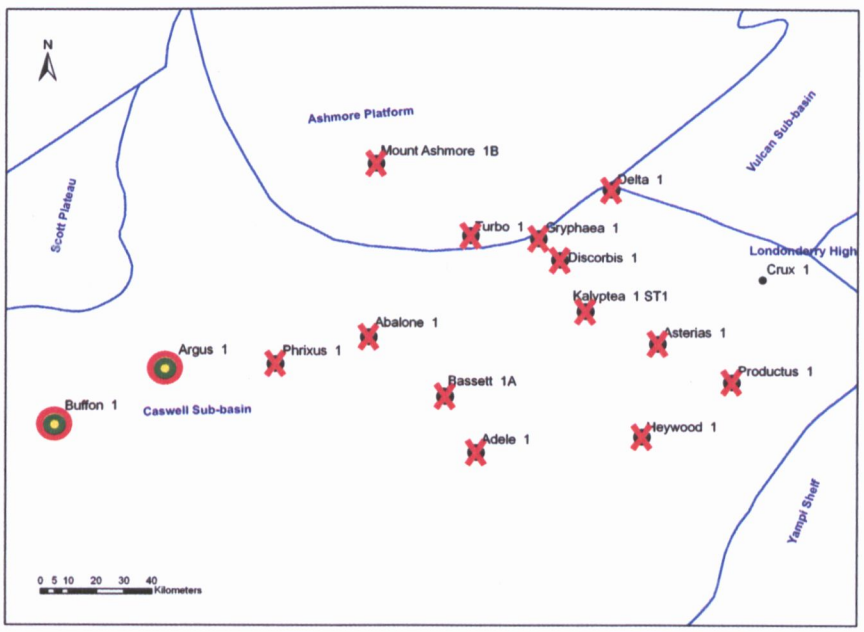

Figure 4.13. The identification of net pay, reservoir, and sand in the Plover Formation.

4.2.9 Nome Formation

The Nome Formation was only identified in Crux-1 and Mount Ashmore-1B. It comprises sandstones.

Potential net pay was only interpreted in Crux-1 (Figure 4.14). In Crux-1, the Nome Formation is a known reservoir containing gas accumulations. This analysis indicated 167 m of potential net pay in this well with approximately 12% porosity and 8% water saturation. Mount Ashmore-1B had approximately 74 m of potential reservoir sands at 12% porosity and 92% water saturation; hence no pay was calculated in this well.

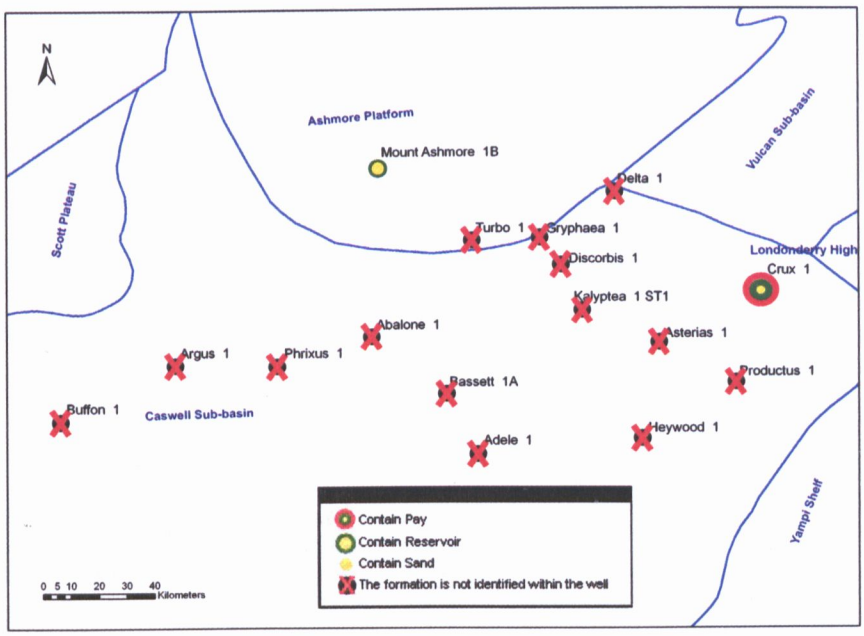

Figure 4.14 The identification of net pay, reservoir, and sand in the Nome Formation.

5 Discussion

5.1 Uncertainties

This was a reconnaissance study for possible unrecognized gas reservoirs in the Northern Browse Basin. Many of the petrophysical parameters would benefit from a more detailed, formation by formation determination, which was not possible in this regional study. This section briefly discusses these parameters.

Upper Cretaceous sediments were assumed to all have the same sand and shale gamma ray baselines and the same neutron-density shale point. However, the Upper Cretaceous comprises three different formations, the Puffin, Fenelon/Gibson, and Woolaston Formations and those parameters may vary between formations. A limestone matrix was assumed for these three formations, consistent with the calcite abundance in sample descriptions. However, the Puffin Formation does contain thick clastic intervals. The assumption of limestone instead of sandstone matrix in the Raymer-Hunt-Gardner equation might overestimate the porosity in this formation.

The sand and shale gamma ray baselines and neutron-density shale point were assumed to be the same throughout the Upper Triassic and Lower Cretaceous sediments. Again, these may vary because there are five Upper Triassic-Lower Cretaceous formations analyzed: Nome, Plover, Lower Vulcan, Upper Vulcan, Echuca Shoals and Jamieson Formations.

Even if this were not a regional study, it may be appropriate to 'lump' formations as above, especially where they are thin in some wells. If the formation is very thin then the range between the shale baseline and sand baseline might be too narrow. For example clean units would be erroneously assigned 100% shale at the shaliest point in that interval.

The selection of formation water resistivity (*Rw*) is a major uncertainty in this study. Formation water salinity was assumed to be the same through the entire Late Triassic-Late Cretaceous

sequence analyzed in each well. If *Rw* is too high, predicted water saturations are too high. This study has identified many possible gas reservoirs and follow-up study should focus on re-analyzing the intervals highlighted here, including where possible individual *Rw* estimates for different reservoirs.

The cementation exponent, *m*, and saturation exponent, *n*, were obtained from the analysis of core cut in the Nome Formation in Crux-1, and applied to all wells within the study area. However, this *m*-value of 1.81 is supported by the Pickett plots for Basset-1A (Figure 3.12) and Abalone-1, Buffon-1, Mount Ashmore-1B and Asterias-1 (Figure 5.1).

5.2 Multimin Method

The Multimin module in Geolog 6.6 was used as an alternate method of analysis. Compared to the deterministic approach discussed above, Multimin uses an optimization method to find a model, which gives the best match between the measured data and the predicted log response. The response equations for each logging tool are built into the module in order to define the effect on each tool of the mineral and fluid volumes. Those response equations, together with the mineral and fluid parameters are then used to reconstruct the actual logging measurement. Hence, the volumes of the minerals and fluids present in the reservoir can be approximated. The method simultaneously solves the response equations to determine the various volumes which best match actual log measurement.

The procedure for using Multimin analysis is as follows. First, determine the minerals and fluids parameters as well as consider any mud invasion effects on log responses. Then, build a multimin model and review the analysis results. All available knowledge must be integrated when building the Multimin model. All sources of data, i.e. wireline logs, rock and fluid data, core analysis, fluid sampling and any chemical analysis should be considered when deciding the correct minerals, fluids and the parameters. Minerals and fluid parameters may be varied to improve the match, provided the responses are within the range of known values for those minerals and fluids.

The Multimin method was applied to the Nome Formation in Crux-1. The formation water resistivity was estimated to be 0.1 ohmm at 25 °C from Pickett plots over the Plover Fm. The gas gravity is 0.712 (air = 1.00) or equivalent to 0.24 g/cc, determined from the DST report. Standard values were used for the various known minerals and fluids (Figure 5.2).

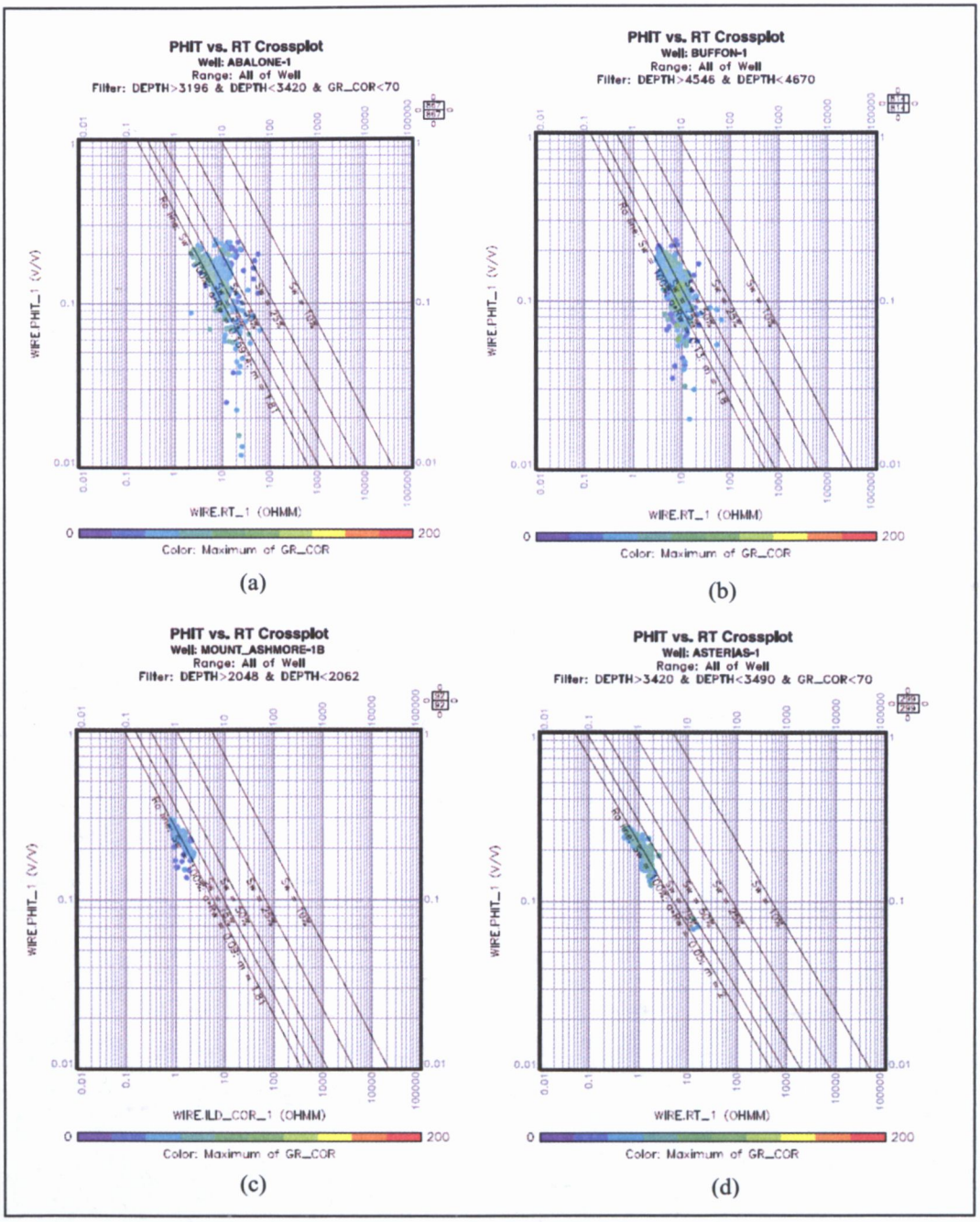

Figure 5.1. The Pickett plots of Abalone-1 (a), Buffon-1 (b), Mount Ashmore-1B (c) and Asterias-1 (d) show that the slope of the family lines are 1.81.

Multimin analysis calculated a volume of wet clay as opposed to a volume of shale. It calculates the total porosity as a combination of the individual fluid components which are in the unflushed zone. The dual water equation is used in the Multimin method. The values of 1.81 and 1.77 were used for cementation exponent, *m*, and saturation exponent, *n*, respectively.

```
MODELS:
   Type     Name              Cond# Cutoff Expression

   Primary  NOME              2.842  10.0

FORMATION FLUID PARAMETERS:
   Fluid properties option = DEPTH
   Oil Gravity Degrees API = 30.00 dapi    Gas specific gravity = 0.700
   Rws = 0.0300  @ 131.00 degC              Cwbs = -  @ - degC                 Rmfs = 0.0790  @ 24.00 degC

BOREHOLE PARAMETERS:
   Mud base = WATER                         Mud density = 1.160 g/cc           KCl concentration of mud = 0.00 %
   SHT = -                                  BHT = 133.00 degC
   Rms = 0.0890  @ 25.00 degC               Rmcs = 0.090  @ 22.00 degC         Total depth = - metres

   Average temperature of 128.27 degC by TLI/BLI method.
   Average pressure of 43229.27 kpa by MUD_DENS method.

                     ------------------------------------------------------------------------
           Component |QUARTZ |ILLITE |KAOLIN | XGAS  |XBNDWAT|XFREWAT| UGAS  |UBNDWAT|UFREWAT|
 Error of prediction | 0.0344| 0.0439| 0.0674| 0.0172| 0.0104| 0.0272| 0.0333| 0.0194| 0.0322|
                     ------------------------------------------------------------------------
EQUATION RESPONSES:
   Log        Method      Uncertainty
                     ------------------------------------------------------------------------
Formation density [G/CC]    RHO_COR_UNC |      3|      3|      3|      0|      1|      1|      0|      0|      0|
   RHO_COR    Linear                    |-------|-------|-------|-------|-------|-------|-------|-------|-------|
Neutron [V/V]               TNPH_COR_UNC | -0.020|  0.400|  0.400|  0.519|  0.914|  0.914|  0.000|  0.000|  0.000|
   NPHI_COR   Linear                    |-------|-------|-------|-------|-------|-------|-------|-------|-------|
Sonic transit time [US/F]        DT_UNC |   54.9|   95.3|   95.3|  250.0|  199.0|  199.0|    0.0|    0.0|    0.0|
   DT         Linear                    |-------|-------|-------|-------|-------|-------|-------|-------|-------|
Photoelectric absorption [B/C?]   U_UNC |   5.00|  11.73|   4.44|   0.03|   0.78|   0.78|   0.00|   0.00|   0.00|
   U          Linear                    |-------|-------|-------|-------|-------|-------|-------|-------|-------|
Total gamma [GAPI]          GR_COR_UNC |   40.0|  200.0|  150.0|    0.0|    0.0|    0.0|    0.0|    0.0|    0.0|
   GR_COR     Linear                    |-------|-------|-------|-------|-------|-------|-------|-------|-------|
Degree Kelvin                   0.1717I|   0.00|   0.00|   0.00|   0.00|   0.00|   0.00|   0.00|  40.81|  22.74|
   CT         Dual-water nonlinear      |-------|-------|-------|-------|-------|-------|-------|-------|-------|
Flushed conductivity [MH/M]     0.1937I|   0.00|   0.00|   0.00|   0.00|  40.81|  41.67|   0.00|   0.00|   0.00|
   CXO        Dual-water nonlinear      ------------------------------------------------------------------------
```

Figure 5.2. Model data used in the Multimin method.

Although the condition number for the model was mathematically good (2.842 is within good interval (Figure 5.2)) and the analysis showed good quality (Figure 5.3), the porosity obtained from the Multimin method was too pessimistic. It underestimated the porosity compared to the core porosity and deterministically-derived porosity (Figure 5.3 and Figure 3.15). That could be caused by the inappropriate logging response for the known minerals and Cation Exchange Capacity (CEC) component. A further study needs to be performed regarding to those.

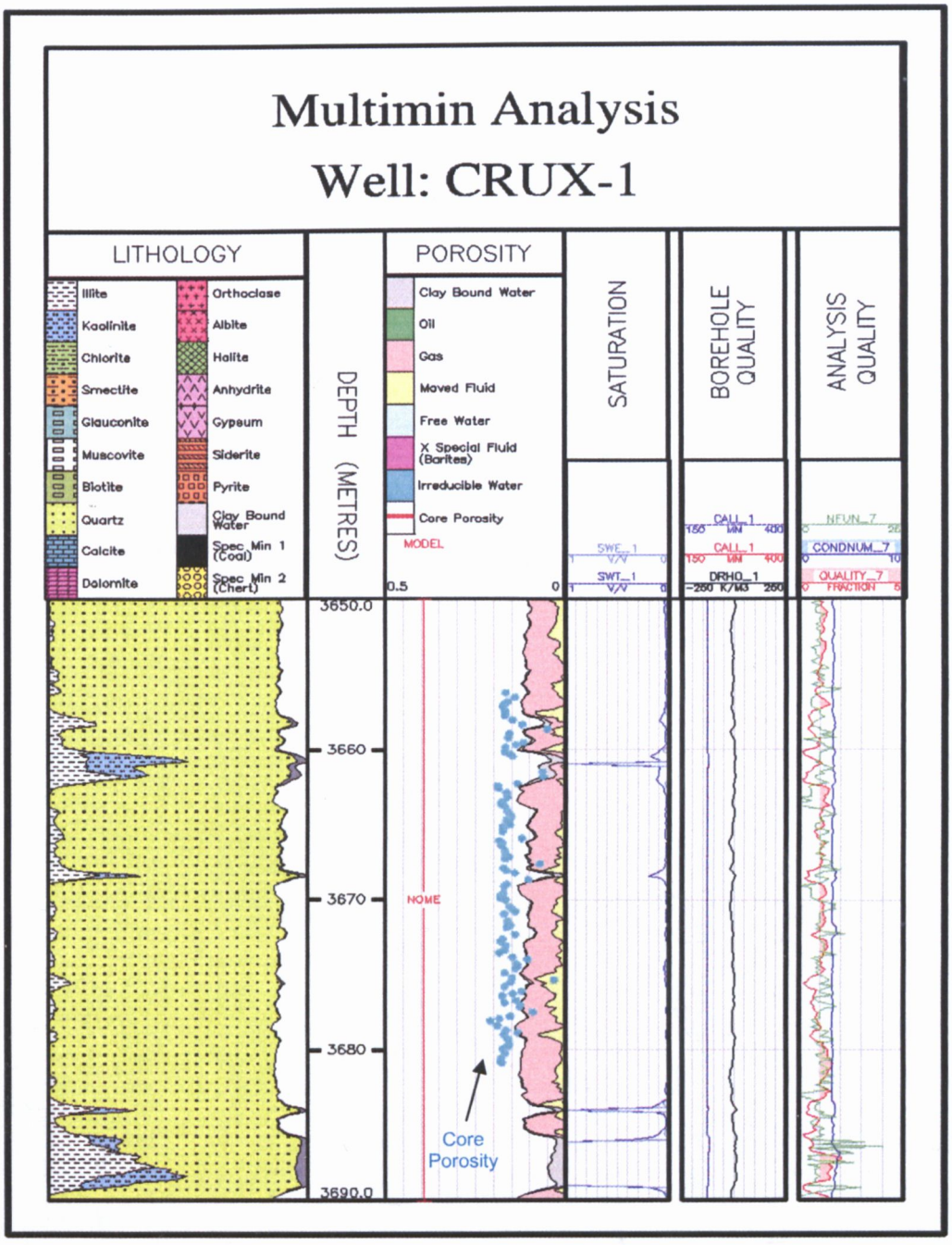

Figure 5.3. The result of Multimin method. The porosity is too low compared to the core porosity.

6 Conclusions and Recommendations

6.1 Conclusions

The following are the conclusions of this project:

- The petrophysical study of the Northern Browse Basin covered twenty wells within the study area. Sixteen wells were analyzed in order to calculate the shale volume, porosity, and water saturation while the others do not have complete data to be examined. The main stratigraphic interval of interest was from the Late Triassic to Late Cretaceous sections covering the Nome, Plover, Lower Vulcan, Upper Vulcan, Echuca Shoals, Jamieson, Woolaston, Fenelon/Gibson and Puffin Formations.

- The sequence of interest was split into two units for parameter picking. (1) the Upper Cretaceous sequence which comprises the Puffin, Fenelon/Gibson and Woolaston Formations. This section is carbonate-dominated. (2) The Late Triassic-Early Cretaceous section which encompasses the Jamieson, Echuca Shoals, Upper Vulcan, Lower Vulcan, Plover and Nome Formations. This section is clastic-dominated. Some of these formations are missing in some wells.

- Formation water resistivity was determined using the Pickett plots and assumed to be the same through the entire Late Triassic-Late Cretaceous sequence analyzed in each well. The resultant *Rw* values describe the salinity distribution within the study area and show a pattern across the region, generally increasing from southwest to northeast, with a range from 12,000 to 80,000 ppm.

- The water saturation was determined using the dual water equation for shaly sand. The saturation equation parameters were taken from the core analysis of Crux-1. The values 1.81 for cementation exponent, *m*, and 1.77 for saturation exponent, *n*, were applied to all wells. The *m* value used is supported by the slope of family lines in the Pickett plots for other wells.

- Twelve out of the 16 analyzed wells were interpreted to contain potential net pay. Potential net pay was encountered in the Puffin, Jamieson, Echuca Shoals and Upper Vulcan Formations while the other units contain only insignificant net pay.

- The Puffin Formation yielded high potential net pay thicknesses in Gryphaea-1, Discorbis-1 and Kalyptea-1ST1, with the thickest being 127 m identified in Kalyptea-1ST1. This formation has good reservoir quality with an average of 17% shale volume, 20% porosity and 50% water saturation.

- The Jamieson Formation encountered an average of 25 m net pay thickness and 20% porosity. The thickest net pay was encountered in Adele-1 and Heywood-1, with 148 m and 47 m respectively. Pay thicknesses decrease to the north of the region.

- Half of wells that intersect the Echuca Shoals Formation contain potential net pay with the greatest thickness (61 m) being encountered in Adele-1. The identified net pay was spread evenly among the wells in the southeast part of the region. This formation has good reservoir quality with an average of 24% shale volume, 14% porosity and 44% water saturation.

- A very significant 430 m of potential net pay was encountered in the Upper Vulcan Formation in Heywood-1. With an average of 125 m net pay thickness and 10% porosity from five out of seven wells, this formation has good reservoir quality across the study area.

- This project was a reconnaissance study for possible unrecognized reservoirs in the Northern Browse Basin. It has identified many possible potential reservoirs and follow-up study should focus on re-analyzing the intervals highlighted here.

6.2 Recommendations for Further Work

Further research would enhance the level of understanding of the petrophysics in the Northern Browse Basin. Some suggestions are as follows:

- Reservoir by reservoir analysis instead of per well analysis, especially when picking the parameters such as formation water resistivity.

- MDT analysis for pressure and temperature gradient to determine the formation pressure and temperature trends of the area.

- Better knowledge of the saturation parameters such as cementation exponent, m, and saturation exponent, n, used in the dual water equation. Facies and lithology analysis could be useful in order to determine those parameters. Creating the trend model of clean and shaly sand and extrapolating to other wells and lithologies could be a better method to approach these parameters.

- A probabilistic method (e.g. Multimin) might be a better approach when considering the proper log response of the known minerals and CEC factor. This would have to take into consideration the complex lithology in each formation.

References

Australian Government, Department of Industry, Tourism and Resources, 2004, 2004 Offshore Acreage Release.

Australian Government, Department of Industry, Tourism and Resources, 2005, 2005 Offshore Acreage Release.

Australian Government, Department of Industry, Tourism and Resources, 2006, 2006 Offshore Acreage Release.

Australian Government, Department of Industry, Tourism and Resources, 2007, 2007 Offshore Acreage Release.

Benson, J. M., Brealey, S.J., Luxton, C.W., Walshe, P.F., & Tupper, N.P., 2004, Late Cretaceous Ponded Turbidite Systems: A New Stratigraphic Play Fairway in the Browse Basin: APPEA Journal, v. 44(1), p. 269-285.

Bigelow, E. L., 1995, Introduction to Wireline Log Analysis, Western Atlas International.

Blevin, J. E., Struckmeyer, H.I.M., Cathro, D.L., Totterdell, J.M., Boreham C.J., Romine, K.K., Loutit, T.S. & Sayers, J., 1998, Tectonostratigraphic Framework and Petroleum System of the Browse Basin, North West Shelf: Proceedings of the Petroleum Exploration Society of Australia Symposium, p. 369-395.

Chevron, 2007, Chevron Australia Exploration and Production, http://www.chevron.com/countries/australia/?view=3.

Doré, A. G., Stewart, I., 2002, Similarities and Differences in the Tectonics of Two Passive Margins: The Northeast Atlantic Margin and the North West Shelf: The Sedimentary Basins of Western Australia 3: Proceedings of the Petroleum Exploration Society of Australia Symposium.

Edwards, D. S., Preston, J.C., Kennard, J.M., Boreham, C.J., Van Aarssen, B.K.J., Summons, R.E., & Zumberge, J.E., 2004, Geochemical Characteristics of Hydrocarbons from the Vulcan Sub-basin, western Bonaparte Basin, Australia: Proceedings of the Timor Sea Symposium, 19-20 June 2003, p. 169-201.

Paradigm, 2006, Geolog 6.6.1 Manual.

Longley, I. M., Buessenschuett, C., Clydsdale, L., Cubitt, C.J., Davis, R.C., Johnson, M.K., Marshall, N.M., Murray, A.P., Somerville R., Spry, T.B., Thompson, N.B., 2002, The North West Shelf of Australia - a Woodside Prospective: The Sedimentary Basins of Western Australia 3: Proceedings of the Petroleum Exploration Society of Australia Symposium.

Maung, T. U., Cadman, S., & West, B., 1994, A Review of the Petroleum Potential of the Browse Basin, The Sedimentary Basins of Western Australia: Proceedings of the Petroleum Exploration Society of Australia Symposium, p. 333-346.

Morthon-Thompson, D., Woods, AM, 1992, Development Geology Reference Manual: AAPG Methods in Exploration Series, v. 10.

Pickett, G. R., 1966, A Review of Current Techniques for Determination of Water Saturation from Logs: paper SPE 1446: SPE Journal of Petroleum Tech. (Nov 1966), p. 1425-1435.

Rider, M., 2002, The Geological Interpretation of Well Logs (2nd Edition), Rider-French Consulting Ltd.

Schlumberger, 2005, Log Interpretation Charts.

Serra, O., 1989, Schlumberger Log Interpretation Principles/Applications, Schlumberger.

Struckmeyer, H. I. M., Blevin, J.E., Sayers, J., Totterdell, J.M., Baxter, K. & Cathro, D.L., 1998, Structural Evolution of the Browse Basin, North West Shelf : New concepts from deep-seismic data: The Sedimentary Basins of Western Australia 2: Proceedings of Petroleum Exploration Society of Australia Symposium, p. 345-367.

Symonds, P. A., Collins, C.D.N., & Bradshaw, J., 1994, Deep Structure of the Browse Basin: Implications for Basin Development and Petroleum Exploration: The Sedimentary Basins of Western Australia: Proceedings of the Petroleum Exploration Society of Australia Symposium, p. 315-331.

Appendix 1

Abbreviations

Tools Mnemonics

AGS	:	Aluminium Gamma Ray Spectroscopy Sonde
AMS	:	Auxiliary Measurement Sonde
BCS	:	Borehole Compensated Sonic
BHC	:	Borehole Compensated Sonic
BHCS	:	Borehole Compensated Sonic
CAL	:	Caliper
CCL	:	Casing Colar Locator
CDL	:	Compensated Density Log
CN	:	Compensated Neutron Log
CNL	:	Compensated Neutron Log
CSAT	:	Combined Seismic Acquisition Tool
CST	:	Core Sample Taker
DFIL	:	Dipmeter Fracture Identification Log
DIL	:	Dual Induction
DLL	:	Dual Laterolog
DSI	:	Dipole Shear Sonic
DSL	:	Digital Spectralog
DSLT	:	Digitizing Sonic Logging Tool
FDC	:	Fluid Density Tool
FMI	:	Formation Microresisitivity Imager
GR	:	Gamma Ray
HALS	:	HILT Azimuthal Laterolog Sonde
HDIL	:	High Definition Induction Log
IND	:	Induction Log
ISFL	:	Induction Spherically Focused Log
LDL	:	Litho-Density Log
MDT	:	Modular Formation Dynamic Tester
ML	:	Minilog
MLL	:	Microlaterolog Tool
MSCT	:	Mechanical Sidewall Coring Tool
MSFL	:	Micro-spherically-focused Resistivity
NCS	:	Nuclear Combination Sonde
NGS	:	Natural Gamma Ray Spectrometry Sonde
NGT	:	Natural Gamma Ray Spectrometry Tool
NL	:	Neutron Lifetime Log
PEX	:	Platform Express
SDT	:	Sonic Digital Tool
SLS	:	Sonic Logging Sonde
SONIC	:	Sonic
SP	:	Spontaneous Potential
XMAC	:	Cross Multipole Array Acoustilog
ZDEN	:	Compensated Bulk Density
ZDL	:	Z-Density Log

Curves Mnemonics

BADHOLE	:	Badhole flag
BS	:	Bit size (*inch*)
CALI	:	Caliper (*inch*)
CALS	:	Caliper sonic (*inch*)
DRHO	:	Bulk density correction factor (*gr/cc*)
DT	:	Sonic transit time (*us/ft*)
GR_COR	:	Gamma ray corrected (*GAPI*)
LLD_COR	:	Borehole corrected deep laterolog resistivity (*ohmm*)
LLS_COR	:	Borehole corrected shallow laterolog resistivity (*ohmm*)
NPHI_COR	:	Correcter NPHI (*v/v*)
PAY	:	Net pay flag
PEF	:	Photoelectric factor
PHIE	:	Effective porosity (*v/v*)
PHIT	:	Total porosity (*v/v*)
RESERVOIR	:	Net reservoir flag
RHO_COR	:	Density corrected (*gr/cc*)
RT	:	True formation resistivity (*ohmm*)
RXO	:	Flushed zone resisitivity (ohmm)
SAND	:	Net sand flag
SP	:	Spontaneous potential (*mV*)
SWE	:	Effective water saturation (*v/v*)
SWT	:	Total water saturation (*v/v*)
VOL_UWAT	:	Unflushed zone volume of water (*v/v*)
VSH_MINDET	:	Shale volume (*v/v*)

Appendix 2

Pre-Calculation Data for Each Well

ABALONE-1

Elevation	25 m (RT)
WD	406 m below MSL
TD	4795 m

Pre-Calculation Data

Top Log Temperature (TLT)	10 degC at seabed
Bottom Log Temperature (BLT)	82 degC at 3605 m

	Unit	Suite 1
TLI	m	406
BLI	m	3605
BS	in	12.25
DFD	gr/cm3	1.14
RMS	ohmm	0.1
MST	degc	28
RMFS	ohmm	0.092
MFST	degc	23
RMCS	ohmm	0.131
MCST	degc	28
Logging		DLL-DSI-MSFL-LDL-CNL-GR-CAL-SP

Environmental Corrections

Logging Service Company : Schlumberger
Corrections were applied to GR, NPHI, FDC, MSFL and DLL

ADELE-1

Elevation	22 m (DF)
WD	243 m below LAT
TD	4822 m

Pre-Calculation Data

Top Log Temperature (TLT)	14.4 degC at seabed*
Bottom Log Temperature (BLT)	147 degC at TD*

	Unit	Suite 1	Suite 2	Suite 3
TLI	m	857	2547	3934
BLI	m	2506	3934	4822
BS	in	17.5	12.25	8.5
DFD	gr/cm3	1.09	1.29	1.19
RMS	ohmm	0.22	0.18	0.29
MST	degc	39	48	35
RMFS	ohmm			
MFST	degc			
RMCS	ohmm			
MCST	degc			
Logging		DFIL/MLL/XMAC/GR/	DIL/CAL/XMAC/GR/	MLL/HDIL/XMAC/ZDL/CN/DSL
		ZDEN/CN/DSL	ZDL/CN/DSL/GR	

Environmental Corrections

Logging Service Company : Schlumberger
Corrections were applied to GR, NPHI, FDC, MSFL and DLL

* Data assumption

ARGUS-1

Elevation	22 m (RT)
WD	572 m below LAT
TD	4878 m

Pre-Calculation Data

Top Log Temperature (TLT)	10 degC at seabed*
Bottom Log Temperature (BLT)	139 degC at 4876.5 m

	Unit	Suite 1	Suite 2	Suite 3	Suite 4
TLI	m	10			
BLI	m	4294.9	4560	4695.5	4876.5
BS	in	8.5	6	6	6
DFD	gr/cm3	1.19		1.19	1.19
RMS	ohmm	0.129		0.094	0.097
MST	degc	24		27	31
RMFS	ohmm	0.109		0.066	0.067
MFST	degc	24		27	31
RMCS	ohmm	0.18		1.97	0.16
MCST	degc	24		27	31
Logging		DLL-MSFL-LDL-CNL-DSI-GR-SP-CSAT	CAL	DLL-MSFL-DLL-GR-SP-CAL	LDL-CNL-MSFL-DLL-GR-SP-CAL
		MDT-GR	CCL	FMI-LDL-CNL-GR	MDT-GR
		MSCT-GR		MDT-GR	FMI-BHC-GR
		CST-GR		CSAT	CSAT-CST

Environmental Corrections

Logging Service Company : Schlumberger
Corrections were applied to GR, NPHI, FDC, MSFL and DLL

** Data assumption*

ASTERIAS-1

Elevation	17 m (KB)
WD	194.4 m below MSL
TD	4402 m

Pre-Calculation Data

Top Log Temperature (TLT)	15.75 degC at seabed*
Bottom Log Temperature (BLT)	147 degC at TD

	Unit	Suite 1	Suite 2	Suite 3	Suite 4	Suite 5
TLI	m	1306	1850	2516	2516	3998
BLI	m	2217	2482	3612	3998	4400
BS	in	17.5	12.25	8.5	8.5	6
DFD	gr/cm3	*1.03*		*1.14*	*1.14*	*1.24*
RMS	ohmm	0.55		0.07	0.075	0.123
MST	degc	28		30	32	37
RMFS	ohmm	0.404		0.055	0.061	0.084
MFST	degc	27		27	27	29
RMCS	ohmm	0.54		0.095	0.092	0.211
MCST	degc	27		25	23	27
Logging		DLL-SDT-CAL-AMS-GR	SDT-GR-AMS	DLL-MSFL-BHC-GR-SP-CAL-AMS	DLL-MSFL-SDT-GR-SP-CAL-AMS	DLL-MSFL-BHC-GR-SP-CAL-AMS
		SLS-GR-AMS				

Environmental Corrections

Logging Service Company : Schlumberger
Corrections were applied to GR, NPHI, FDC, MSFL and DLL

** Data assumption*

BASSET-1A

Elevation	8 m (RT)
WD	372 m below MSL
TD	2706 m

Pre-Calculation Data

Top Log Temperature (TLT)	9.5 degC at seabed*
Bottom Log Temperature (BLT)	65 degC at TD

	Unit	Suite 1	Suite 2	Suite 3	Suite 4	Suite 5
TLI	m	702	1165	1381.5	2035	2438
BLI	m	1338	1390	2035	2515	2700
BS	in	17.5	17.5	12.25	8.5	8.5
DFD	gr/cm3	1.06	1.06	1.07	1.25	1.3
RMS	ohmm	0.339	0.345	0.25	0.27	0.37
MST	degc	28	28	25.5	26.6	25.5
RMFS	ohmm	0.331	0.333	0.25	0.23	0.26
MFST	degc	28	28	24.4	25.5	23.3
RMCS	ohmm	0.505	0.513	0.08	0.52	0.82
MCST	degc	28	28	24.4	25.5	23.3
Logging		IND/SONIC/GR/SP	FDC/CNL/GR/CAL	DLL/MSFL/GR/SP/CAL	IND/SONIC/GR/SP/CAL	IND/GR/SP
		FDC/CNL/GR/CAL	BHCS/GR	FDC/CNL/GR/CAL	BHCS/GR	BHC SONIC/GR
		BHCS/GR		BHCS/GR	ISFL/GR	ISFL/GR
				MLL/ML/GR	FDC/CNL/GR/CAL	FDC/CNL/GR/CAL

Environmental Corrections

Logging Service Company : Schlumberger
Corrections were applied to GR, NPHI, FDC, MSFI, DLL, and ILD

** Data assumption*

BUFFON-1

Elevation	10.36 m (RT)
WD	533 m below MSL
TD	4787 m

Pre-Calculation Data

Top Log Temperature (TLT)	9 degC at seabed*
Bottom Log Temperature (BLT)	143 degC at TD

	Unit	Suite 1	Suite 2	Suite 3	Suite 5	Suite 6
TLI	m	830	2724	3637	4020	4400
BLI	m	1843	3651	4286	4487	4777
BS	in	17.5	8.5	6	6	6
DFD	gr/cm3	1.08	1.18	1.53	1.52	1.53
RMS	ohmm	0.34	0.072	0.09	0.079	0.075
MST	degc	26	30	27	25	26
RMFS	ohmm	0.26	0.051	0.075	0.049	0.051
MFST	degc	26	35	28	25	31
RMCS	ohmm	0.4	0.091	0.43	0.11	0.305
MCST	degc	26	35	25	25	28
Logging		FDC-CNL-GR-CAL	FDC-CNL-GR-CAL	FDC-CNL-GR-CAL	FDC-CNL-GR-CAL	FDC-CNL-GR-CAL
		ISF-SONIC-SP-GR	ISF-SONIC-SP-GR	ISF-SONIC-MSFL-GR-SP-CAL	MSFL-DLL-GR-SP-CAL	MSFL-DLL-GR-SP-CAL
					BHCS-GR	BHCS-GR

Environmental Corrections

Logging Service Company : Schlumberger
Corrections were applied to GR, NPHI, FDC, MSFI, and DLL

** Data assumption*

CRUX-1

Elevation	26.5 m (RT)
WD	168 m below MSL
TD	3955 m

Pre-Calculation Data

Top Log Temperature (TLT)	18 degC at seabed
Bottom Log Temperature (BLT)	133.5 degC at 3255.5 m

	Unit	Suite 1	Suite 2
TLI	m	100	3450
BLI	m	3450	3951
BS	in	8.5	8.5
DFD	gr/cm3	1.16	1.16
RMS	ohmm	0.089	0.083
MST	degc	25	37
RMFS	ohmm	0.079	0.084
MFST	degc	24	27
RMCS	ohmm	0.09	0.096
MCST	degc	22	23
Log Type		LDL/CNL/NGT	LDL/CNL/NGT
		MSFL-DLL-GR	MSFL-DLL-GR
		MDT-GR	MDT-GR

Environmental Corrections

Logging Service Company : Schlumberger
Corrections were applied to GR, NPHI, LDT, MSFL, and DLL

DELTA-1

Elevation	25 m (KB)
WD	205 m below MSL
TD	2888 m

Pre-Calculation Data

Top Log Temperature (TLT)	40 degC at 450 m*
Bottom Log Temperature (BLT)	94 degC at 2900 m

	Unit	Suite 1
TLI	m	230
BLI	m	2900
BS	in	17.5
DFD	gr/cm3	1.1
RMS	ohmm	0.273
MST	degc	30.6
RMFS	ohmm	0.214
MFST	degc	30
RMCS	ohmm	0.361
MCST	degc	30
Log Type		

Environmental Corrections

Logging Service Company : Schlumberger
Corrections were applied to GR, NPHI, FDC, MSFL, and DLL

** Data assumption*

DISCORBIS-1

Elevation	22 m (KB)
WD	156 m below MSL
TD	4196 m

Pre-Calculation Data

Top Log Temperature (TLT)	18 degC at seabed
Bottom Log Temperature (BLT)	135 degC at TD

	Unit	Suite 1	Suite 2	Suite 3	Suite 4	Suite 5
TLI	m	226	1620	2020	2771	3860
BLI	m	1733	2035	2775	3965	4165
BS	in			13.375	9.625	7
DFD	gr/cm3			1.029	1.199	1.25
RMS	ohmm			0.291	0.091	0.05
MST	degc			38	20	30
RMFS	ohmm			0.269	0.076	0.042
MFST	degc			26	24	30
RMCS	ohmm			0.301	0.116	0.099
MCST	degc			26	20	30
Log Type				DLL-MSFL-SDT-GR-AMS	DLL-MSFL-SDT-GR-AMS	DLL-MSFL-BHC-GR-AMS
				LDL-CNL-ML-NCS-AMS	LDL-CNL-ML-NCS-AMS	LDL-CNL-NGS

Environmental Corrections

Logging Service Company : Schlumberger
Corrections were applied to GR, NPHI, FDC, MSFL, and DLL

** Data assumption*

GRYPHAEA-1

Elevation	17 m (KB)
WD	200 m below MSL
TD	3950 m

Pre-Calculation Data

Top Log Temperature (TLT)	15.5 degC at seabed*
Bottom Log Temperature (BLT)	116 degC at TD

	Unit	Suite 1	Suite 2	Suite 3	Suite 4
TLI	m	459	1280	1723.5	2631
BLI	m	1303.5	1700	2641.5	3940
BS	in	20	17.5	12.25	8.5
DFD	gr/cm3	1.031	1.031	1.06	1.17
RMS	ohmm			0.271	0.098
MST	degc			27	29
RMFS	ohmm			0.232	0.086
MFST	degc			26	28
RMCS	ohmm			0.38	0.15
MCST	degc			26	26
Log Type		DLL-MSFL-SLS-SP-GR	GR-AMS (CASED HOLE)	DLL-MSFL-SDT-SP-GR	DLL-MSFL-SLS-SP-GR
					LDL-CNL-NGS

Environmental Corrections

Logging Service Company : Schlumberger
Corrections were applied to GR, NPHI, FDC, MSFL, and DLL

** Data assumption*

HEYWOOD-1

Elevation	10 m (RT)
WD	35 m below MSL
TD	4572 m

Pre-Calculation Data

Top Log Temperature (TLT)	18 degC at seabed
Bottom Log Temperature (BLT)	128 degC at 4240 m

	Unit	Suite 1	Suite 2	Suite 3	Suite 4
TLI	m	387	1308	3338	4100
BLI	m	1308	3360	4212	4240
BS	in	17.5	12.25	8.5	8.5
DFD	gr/cm3	1.05	1.38	1.15	1.12
RMS	ohmm	0.232	0.04	0.093	0.21
MST	degc	26	26	22	26
RMFS	ohmm	0.205	0.04	0.077	0.17
MFST	degc	26	26	22	26
RMCS	ohmm	0.26	0.05	0.11	0.44
MCST	degc	26	26	22	26
Log Type		DLL-GR-CAL-BHC	DLL-GR-CAL-BHC	DLL-GR-CAL-BHC	DLL-GR-CAL-BHC
			FDC-GR-CAL		

Environmental Corrections

Logging Service Company : Schlumberger
Corrections were applied to GR, NPHI, FDC, MSFL, and DLL

KALYPTEA-1ST1

Elevation	17.7 m (KB)
WD	215 m below MSL
TD	4575 m

Pre-Calculation Data

Top Log Temperature (TLT)	15 degC at seabed*
Bottom Log Temperature (BLT)	140 degC at TD*

	Unit	Suite 1	Suite 2	Suite 3	Suite 4
TLI	m	215	1682	3457	3288
BLI	m	1313	3458	4090	4568
BS	in	17.5	12.25	8.5	8.5
DFD	gr/cm3	1.15	1.15	1.15	1.15
RMS	ohmm	0.292	0.225	0.054	0.051
MST	degc	28.5	29.8	27.6	29
RMFS	ohmm	0.25	0.102	0.04	0.041
MFST	degc	26.5	29.7	29.2	27.5
RMCS	ohmm	0.159	0.055	0.116	0.072
MCST	degc	27.5	28.1	26.1	27
Log Type		DLL-MSFL-BHC-GR-SP-CAL-AMS	DLL-MSFL-SDT-GR-SP-CAL-AMS	DLL-MSFL-SDT-GR-SP-CAL-AMS	DLL-MSFL-SDT-GR-SP-CAL-AMS
					LDL-CNL-MGT-NL-CAL-AMS

Environmental Corrections

Logging Service Company : Schlumberger
Corrections were applied to GR, NPHI, FDC, MSFL, and DLL

** Data assumption*

MOUNT ASHMORE-1B

Elevation	11 m (RT)
WD	623 m below MSL
TD	2655 m

Pre-Calculation Data

Top Log Temperature (TLT)	7 degC at seabed*
Bottom Log Temperature (BLT)	56 degC at TD

	Unit	Suite 1	Suite 2	Suite 3
TLI	m	1021	1225	1952
BLI	m	1503	1944	2652
BS	in	14.75	12.25	8.5
DFD	gr/cm3	1.025	1.15	1.18
RMS	ohmm	0.188	0.098	0.094
MST	degc	25	29	28
RMFS	ohmm		0.081	0.07
MFST	degc		30	29
RMCS	ohmm		0.143	0.358
MCST	degc		27	30
Log Type		FDC/GR/CAL	FDC/GR/CAL	FDC/CNL/GR/CAL
		ISF/SONIC/FDC/GR/SP	ISF/SONIC/GR/SP	ISF/MSFL/SONIC/GR/SP/CAL

Environmental Corrections

Logging Service Company : Schlumberger
Corrections were applied to GR, NPHI, FDC, MSFL, and DLL

** Data assumption*

PHRIXUS-1

Elevation	26 m (RT)
WD	407 below LAT
TD	3874 m

Pre-Calculation Data

Top Log Temperature (TLT)	11 degC at seabed*
Bottom Log Temperature (BLT)	92 degC at TD

	Unit	Suite 1	Suite 2	Suite 3	Suite 4	Suite 5	Suite 6
TLI	m		1680	1838	2634	3031	3257
BLI	m		1838	2634	3031	3257	3866
BS	in		12.25	12.25	12.25	12.25	8.5
DFD	gr/cm3		1.15	1.11	1.12	1.12	1.15
RMS	ohmm		0.0931	0.0826	0.0854	0.0979	0.092
MST	degc		28	26	27	27	20
RMFS	ohmm		0.0675	0.0788	0.0672	0.0745	0.091
MFST	degc		28	26	27	27	20
RMCS	ohmm		0.1382	0.1377	0.1246	0.1447	0.102
MCST	degc		28	26	27	27	20
Log Type			HALS/PEX/DSLT/GR/SP				

Environmental Corrections

Logging Service Company : Schlumberger
Corrections were applied to GR, NPHI, FDC, MSFL, and DLL

** Data assumption*

PRODUCTUS-1

Elevation	22 m (DF)
WD	142 m below MSL
TD	2590 m

Pre-Calculation Data

Top Log Temperature (TLT)	30 degC at seabed*
Bottom Log Temperature (BLT)	94 degC at TD

	Unit	Suite 1	Suite 2
TLI	m	755	1741
BLI	m	1761	2591
BS	in	17.5	12.25
DFD	gr/cm3	1.059	1.199
RMS	ohmm	0.289	0.148
MST	degc	28	35
RMFS	ohmm	0.228	0.111
MFST	degc	26	25
RMCS	ohmm	0.374	0.247
MCST	degc	27	26
Log Type		DLL-MSFL-SLS-GR-SP-CAL-AMS	DLL-MSFL-SLS-GR-SP-CAL-AMS
			LDL-CNL-AGS

Environmental Corrections

Logging Service Company : Schlumberger
Corrections were applied to GR, NPHI, FDC, MSFL, and DLL

** Data assumption*

TURBO-1

Elevation	25 m (RT)
WD	299 m below MSL
TD	3900 m

Pre-Calculation Data

Top Log Temperature (TLT)	11 degC at seabed
Bottom Log Temperature (BLT)	96 degC at TD

	Unit	Suite 1
TLI	m	2535
BLI	m	3244
BS	in	8.5
DFD	gr/cm3	1.24
RMS	ohmm	0.078
MST	degc	30
RMFS	ohmm	0.067
MFST	degc	26
RMCS	ohmm	0.136
MCST	degc	30
Log Type		DLL-MSFL-BHC-CAL-GR-SP-
		CNL-LDL

Environmental Corrections

Logging Service Company : Schlumberger
Corrections were applied to GR, NPHI, FDC, MSFL, and DLL

Appendix 3

Documentation of Log Editing in Each Well

No	Well	Log Data Editing	Bad Hole
1	Abalone-1	Spliced wireline and LWD of gamma ray, resistivity and sonic at 3566 m.	Badhole was identified by caliper and DRHO (density correction).
2	Adele-1	Edited the sonic and density curves.	Badhole was identified by caliper and DRHO (density correction). Missing sections of resistivity at 3930-4060 m and 2500-2550 m.
3	Argus-1	Spliced the sonic curve at 4652 m.	Badhole was identified by caliper and DRHO (density correction).
4	Asterias-1	-	Badhole was identified by caliper and DRHO (density correction). No sonic encountered at 1929-2517 m, hence the porosity and water saturation can not be computed.
5	Basset-1A	Spliced lateralog with induction resistivity at 2035 m	Badhole was identified by caliper and DRHO (density correction). Caliper reading is uncertain.
6	Buffon-1	Spliced laterolog and induction resistivity at 3640 m; Curve inserted of missing gamma ray, density, neutron, and sonic at 3925 m, 4752 m, 4340 m, 3511 m.	Badhole was identified by caliper and DRHO (density correction).
7	Crux-1	Wireline GR was spliced to different run of wireline log at 1810 m MD. Spike removal of sonic due to bad reading.	Badhole was identified by caliper and DRHO (density correction). Bad data quality at 1509-2100 m; bad sonic, bad resistivity, no density, and no neutron curves
8	Delta-1	No caliper log, so gamma ray, neutron, density and induction resistivity can not be environmentally corrected. Corrected the MSFL	Badhole can not be identified since there is no DRHO (density correction) and caliper.
9	Discorbis-1	Sonic was edited at 3850-3870 m	Badhole was identified by caliper and DRHO (density correction).
10	Gryphaea-1	-	Badhole was identified by caliper sonic in the Puffin Formation and by caliper and DRHO (density correction) in the other formations.
11	Heywood-1	-	DRHO (density correction) was used to identify badhole
12	Kalyptea-1ST1	-	Badhole was defined by caliper sonic until depth 3457 m and by DRHO (density correction) and caliper from depth 3457 m to well bottom.
13	Mount Ashmore-1B	-	No DRHO (density correction), so badhole was defined from caliper.
14	Phrixus-1	DT was spliced at 3257 m	Badhole was identified by caliper and DRHO (density correction).
15	Productus-1	-	Badhole was identified by caliper and DRHO (density correction) and encoountered mostly througout the borehole
16	Turbo-1	GR and resistivity were spliced between LWD and wireline at 3220 m	Badhole was identified by caliper and DRHO (density correction). No porosity curves in the Jamieson and Upper Vulcan Formation.

Appendix 4

Documentation of Parameter Picking in Each Well

No	Well	Shale Volume		Porosity		Water Saturation
		Limestones Matrix	Sandstones Matrix	Limestones Matrix	Sandstones Matrix	
1	Abalone-1	Calculated using the gamma ray (linear) due to badhole		Used the sonic Raymer-Hunt-Gardner equation. RHOfl = 1 gr/cc; PHITsh = 5%; PHIE was limited by 30%x(1-Vsh);		Used dual water model with m = 1.81, n =1.77, a = 1 and CEC = 0.15 meq/g. Rw was determined using Pickett plots from water zone at 3196-3420 m. Rw = 0.15974 @ 75 degC was picked.
		Puffin, Fenelon/Gibson and Woolaston Formations : GRmax=150;GRmin=25	**Jamieson and Echuca Shoals Formations** : GRmax =160; GRmin=50;	**Puffin, Fenelon/Gibson and Woolaston Formations**: DTsh=89 us/ft	**Jamieson and Echuca Shoals Formations**: DTsh=85.6 us/ft	
2	Adele-1	Calculated using the gamma ray (linear) due to badhole		Used the sonic Raymer-Hunt-Gardner equation. RHOfl = 1 gr/cc; PHITsh = 5%; PHIE was limited by 30%x(1-Vsh);		Used dual water model with m = 1.81, n =1.77, a = 1 and CEC = 0.15 meq/g. Rw was determined using Pickett plots from water zone at 1810-1990 m. Rw = 0.083 @ 60 degC was picked.
		Puffin and Fenelon/Gibson Formations: GRmax=80;GRmin=25	**Jamieson, Echuca Shoals, Upper Vulcan and Lower Vulcan Formations**: GRmax =140; GRmin=40;	**Puffin and Fenelon/Gibson Formations**: DTsh=92.5 us/ft	**Jamieson, Echuca Shoals, Upper Vulcan and Lower Vulcan Formations**: DTsh=94.5 us/ft	
3	Argus-1	Calculated using the minimum of shale volume obtained from gamma ray (linear) and density/neutron. The gamma ray (linear) was used in badhole.		Used the sonic Raymer-Hunt-Gardner equation. RHOfl = 1 gr/cc; PHITsh = 5%; PHIE was limited by 30%x(1-Vsh);		Used dual water model with m = 1.81, n =1.77, a = 1 and CEC = 0.15 meq/g. Rw was determined using Pickett plots from water zone at 4190-4242 m. Rw = 0.15675 @ 119 degC was picked.
		Puffin Formation: GRmax=120;GRmin=25; RHOsh=2.595 gr/cc and NPHIsh=0.329	**Jamieson, Lower Vulcan and Plover Formations**: GRmax =173; GRmin=4; RHOsh=2.824 gr/cc and NPHIsh=0.372	**Puffin Formation** : DTsh=91.4 us/ft	**Jamieson, Lower Vulcan and Plover Formations**: DTsh=94.5 us/ft	
4	Asterias-1	Calculated using the minimum of shale volume obtained from gamma ray (linear) and density/neutron. The gamma ray (linear) was used in badhole.		Used the sonic Raymer-Hunt-Gardner equation. RHOfl = 1 gr/cc; PHITsh = 5%; PHIE was limited by 30%x(1-Vsh);		Used dual water model with m = 1.81, n =1.77, a = 1 and CEC = 0.15 meq/g. Rw was determined using Pickett plots from water zone at 3420-3490 m. Rw = 0.06 @ 115 degC was picked.
		Puffin and Fenelon/Gibson Formation : GRmax =131; GRmin=7; RHOsh=2.588 gr/cc and NPHIsh=0.317. Unless at the upper part of the Puffin Formation where there was no density/neutron curve, the shale volume was calculated using the gamma ray (linear). The gamma ray (linear) was used in badhole	**Jamieson, Echuca Shoals, and Upper Vulcan Formations** : GRmax =200; GRmin=40; RHOsh=2.652 gr/cc and NPHIsh=0.334.	**Puffin, Fenelon/Gibson and Woolaston Formation** : DTsh=95.7 us/ft but no sonic from the top of Puffin Formation to 2517 m.	**Jamieson, Echuca Shoals and Upper Vulcan Formations** : DTsh=70.7 us/ft	
5	Basset-1A	Calculated using the minimum of shale volume obtained from gamma ray (linear) and density/neutron. The gamma ray (linear) was used in badhole.		Used the sonic Raymer-Hunt-Gardner equation. RHOfl = 1 gr/cc; PHITsh = 5%; PHIE was limited by 30%x(1-Vsh);		Used dual water model with m = 1.81, n =1.77, a = 1 and CEC = 0.15 meq/g. Rw was determined using Pickett plots from water zone at 2427-2580 m. Rw = 0.1 @ 60 degC was picked.
		Puffin, Fenelon/Gibson and Woolaston Formations : GRmax =92; GRmin=6; RHOsh=2.598 gr/cc and NPHIsh=0.404	**Jamieson Formation**: Since the tool reading in Jamieson Formation was only 15 m, so the parameters used are the same as the overlying sediment.	**Puffin, Fenelon/Gibson and Woolaston Formations** : DTsh=86.8 us/ft	**Jamieson Formation** : DTsh=86.8 us/ft	
6	Buffon-1	Calculated using the minimum of shale volume obtained from gamma ray (linear) and density/neutron. The gamma ray (linear) was used in badhole.		Used the sonic Raymer-Hunt-Gardner equation. RHOfl = 1 gr/cc; PHITsh = 5%; PHIE was limited by 30%x(1-Vsh);		Used dual water model with m = 1.81, n =1.77, a = 1 and CEC = 0.15 meq/g. Rw was determined using Pickett plots from water zone at 4546-4670 m. Rw = 0.13 @ 138 degC was picked.
		Puffin Formation : GRmax =57; GRmin=12; RHOsh=2.661 gr/cc and NPHIsh=0.226	**Jamieson and Plover Formations** : GRmax =200; GRmin=7; RHOsh=2.84 gr/cc and NPHIsh=0.38	**Puffin, Fenelon/Gibson and Woolaston Formation** : DTsh=92.6 us/ft	**Jamieson and Plover Formations** : DTsh=77.7 us/ft	

No	Well	Shale Volume		Porosity		Water Saturation
		Limestones Matrix	Sandstones Matrix	Limestones Matrix	Sandstones Matrix	
7	Crux-1	Calculated using the minimum of shale volume obtained from gamma ray (linear) and density/neutron. The gamma ray (linear) was used in badhole.		Used the sonic Raymer-Hunt-Gardner equation. RHOfl = 1 gr/cc; PHITsh = 5%; PHIE was limited by 30%x(1-Vsh);		Used dual water model with m = 1.81, n =1.77, a = 1 and CEC = 0.15 meq/g. Rw was determined using Pickett plots from water zone at 3893-3915 m. Rw = 0.03 @ 131 degC was picked.
		Puffin, Fenelon/Gibson and Woolaston Formations : GRmax =115; GRmin=26; RHOsh=2.542 gr/cc and NPHIsh=0.324	**Jamieson, Echuca Shoals, Upper Vulcan, Lower Vulcan, Plover and Nome Formations** : GRmax =171; GRmin=38; RHOsh=2.756 gr/cc and NPHIsh=0.389	**Puffin, Fenelon/Gibson and Woolaston Formations** : DTsh=100 us/ft; Uncertain of the quality of sonic reading in Puffin Formation, analysis has not done yet.	**Jamieson, Echuca Shoals, Upper Vulcan, Lower Vulcan, Plover and Nome Formations** : DTsh=77 us/ft	
8	Delta-1	**Puffin Formation** : GRmax =110; GRmin=6; Sandstones matrix; RHOsh=2.595 gr/cc and NPHIsh=0.337. The shale volume was calculated using the minimum of the shale volume obtained from gamma ray (linear) and density/neutron.The gamma ray (linear) was used in badhole.	-	**Puffin Formation**: Used the sonic Raymer-Hunt-Gardner equation. RHOfl = 1 gr/cc; PHITsh = 5%; PHIE was limited by 30%x(1-Vsh). DTsh=94.2 us/ft,	-	Used dual water model with m = 1.81, n =1.77, a = 1 and CEC = 0.15 meq/g. Rw was determined using Pickett plots from water zone at 2390-2570 m. Rw = 0.036 @ 82 degC was picked.
9	Discorbis-1	Calculated using the gamma ray (linear) due to badhole		Used the sonic Raymer-Hunt-Gardner equation. RHOfl = 1 gr/cc; PHITsh = 5%; PHIE was limited by 30%x(1-Vsh);		Used dual water model with m = 1.81, n =1.77, a = 1 and CEC = 0.15 meq/g. Rw was determined using Pickett plots from predicted water zone at 3060-3200 m and 3550-3855 m. Rw = 0.04 @ 104 degC was picked for the Puffin, Fenelon/Gibson and Woolaston Formation. Rw = 0.09 @ 125 degC was picked for the Jamieson, Echuca Shoals, Upper Vulcan, and Lower Vulcan Formation.
		Puffin, Fenelon/Gibson and Woolaston Formations: GRmax =140; GRmin=9;	**Jamieson, Echuca Shoals, Upper Vulcan and Lower Vulcan Formations**: GRmax =180; GRmin=25;	**Puffin, Fenelon/Gibson and Woolaston Formations** : DTsh=82.6 us/ft	**Jamieson, Echuca Shoals, Upper Vulcan and Lower Vulcan Formations**: DTsh=101.8 us/ft	
10	Gryphaea-1	Calculated using the gamma ray (linear) due to badhole		Used the sonic Raymer-Hunt-Gardner equation. RHOfl = 1 gr/cc; PHITsh = 5%; PHIE was limited by 30%x(1-Vsh);		Used dual water model with m = 1.81, n =1.77, a = 1 and CEC = 0.15 meq/g. Rw was determined using Pickett plots from water zone at 2900-2950 m. Rw = 0.06 @ 89 degC was picked.
		Puffin, Fenelon/Gibson and Woolaston Formations : GRmax =125; GRmin=15;	**Jamieson Formation** : GRmax =180; GRmin=26;	**Puffin, Fenelon/Gibson and Woolaston Formations** : DTsh=81.5 us/ft	**Jamieson Formation** : DTsh=77.7 us/ft	
11	Heywood-1	Calculated using the minimum of shale volume computed from gamma ray (linear) and density/neutron. The gamma ray (linear) was used in badhole.		Used the sonic Raymer-Hunt-Gardner equation. RHOfl = 1 gr/cc; PHITsh = 5%; PHIE was limited by 30%x(1-Vsh);		Used dual water model with m = 1.81, n =1.77, a = 1 and CEC = 0.15 meq/g. Rw was determined using Pickett plots from water zone at 1870-1900 m. Rw = 0.05 @ 66 degC was picked.
		Puffin and Fenelon/Gibson Formations: GRmax = 72; GRmin=8; RHOsh=2.709 gr/cc and NPHIsh=0.415	**Jamieson, Echuca Shoals, Upper Vulcan and Lower Vulcan Formations** : GRmax =125; GRmin=15; RHOsh=2.843gr/cc and NPHIsh=0.348	**Puffin and Fenelon/Gibson Formations**: DTsh=92 us/ft	**Jamieson, Echuca Shoals, Upper Vulcan and Lower Vulcan Formations** : DTsh=73.5 us/ft	
12	Kalyptea-1ST1	Calculated using the gamma ray (linear) due to badhole		Used the sonic Raymer-Hunt-Gardner equation. RHOfl = 1 gr/cc; PHITsh = 5%; PHIE was limited by 30%x(1-Vsh);		Used dual water model with m = 1.81, n =1.77, a = 1 and CEC = 0.15 meq/g. Rw was determined using Pickett plots from water zone at 2860-2982 m. Rw = 0.078 @ 92 degC was picked.
		Puffin, Fenelon/Gibson, and Woolaston Formations : GRmax =100; GRmin=8;	**Jamieson, Echuca Shoals and Upper Vulcan Formations** : GRmax =205; GRmin=42;	**Puffin, Fenelon/Gibson and Woolaston Formations** : DTsh=79.6 us/ft	**Jamieson, Echuca Shoals and Upper Vulcan Formations** : DTsh=81.4 us/ft	

No	Well	Shale Volume		Porosity		Water Saturation
		Limestones Matrix	Sandstones Matrix	Limestones Matrix	Sandstones Matrix	
13	Mount Ashmore-1B	**Puffin Formation** : GRmax =110; GRmin=10; The shale volume was calculated using the gamma ray (linear) method since there is no density/neutron curves.	**Jamieson, Echuca Shoals, Upper Vulcan, Lower Vulcan and Nome Formations** : GRmax =150; GRmin=5; RHOsh=2.702 gr/cc and NPHIsh=0.42. The shale volume was calculated using the minimum of shale volume from gamma ray (linear) and density/neutron. The gamma ray (linear) method was used in badhole	Used the sonic Raymer-Hunt-Gardner equation. RHOfl = 1 gr/cc; PHITsh = 5%; PHIE was limited by 30%x(1-Vsh); **Puffin Formation** : DTsh=98.2 us/ft,	**Jamieson, Echuca Shoals, Upper Vulcan, Lower Vulcan and Nome Formations** : DTsh=92 us/ft	Used dual water model with m = 1.81, n =1.77, a = 1 and CEC = 0.15 meq/g. Rw was determined using Pickett plots from water zone at 2048-2062 m. Rw = 0.09 @ 41 degC was picked.
14	Phrixus-1	**Puffin, Fenelon/Gibson and Woolaston Formations** : GRmax =140; GRmin=22; RHOsh=2.67 gr/cc and NPHIsh=0.345. The shale volume was calculated using the minimum of shale volume from gamma ray (linear) and density/neutron. The gamma ray (linear) method was used in badhole.	**Jamieson Formation** : GRmax =147; GRmin=68; The shale volume was calculated using the gamma ray (linear) method since there is no density/neutron curves.	Used the sonic Raymer-Hunt-Gardner equation. RHOfl = 1 gr/cc; PHITsh = 5%; PHIE was limited by 30%x(1-Vsh); **Puffin, Fenelon/Gibson and Woolaston Formations** : DTsh=87 us/ft,	**Jamieson Formation** : DTsh=103 us/ft	Used dual water model with m = 1.81, n =1.77, a = 1 and CEC = 0.15 meq/g. Rw was determined using Pickett plots from water zone at 3740-3780 m. Rw = 0.18 @ 89 degC was picked.
15	Productus-1	**Puffin, Fenelon/Gibson and Woolaston Formations** : GRmax =60; GRmin=10; The shale volume was calculated using the gamma ray (linear) method since there is no density/neutron curves.	**Jamieson Formation** : GRmax =130; GRmin=40; RHOsh=2.618 gr/cc and NPHIsh=0.309. The shale volume was calculated using the minimum of gamma ray (linear) and density/neutron. The gamma ray (linear) was used in badhole.	Used the sonic Raymer-Hunt-Gardner equation. RHOfl = 1 gr/cc; PHITsh = 5%; PHIE was limited by 30%x(1-Vsh); **Puffin, Fenelon/Gibson and Woolaston Formations** : DTsh=103 us/ft,	**Jamieson Formation** : DTsh=67 us/ft	Used dual water model with m = 1.81, n =1.77, a = 1 and CEC = 0.15 meq/g. Rw was determined using Pickett plots from water zone at 1280-1910 m. Rw = 0.06 @ 67 degC was picked.
16	Turbo-1	**Puffin and Fenelon/Gibson Formations** : GRmax =135; GRmin=30; RHOsh=2.662 gr/cc and NPHIsh=0.326. Calculated using the minimum of shale volume computed from gamma ray (linear) and density/neutron. The gamma ray (linear) was used in badhole.	**Jamieson and Upper Vulcan Formations** : GRmax =160; GRmin=60; The shale volume was calculated using the gamma ray (linear) since there is no density/neutron curves.	**Puffin and Fenelon/Gibson Formations** : Used the sonic Raymer-Hunt-Gardner equation. RHOfl = 1 gr/cc; PHITsh = 5%; PHIE was limited by 30%x(1-Vsh); DTsh=103 us/ft,	**Jamieson and Upper Vulcan Formations** : - (no porosity curves)	Puffin Formation and Fenelon/Gibson Formation : Used dual water model with m = 1.81, n =1.77, a = 1 and CEC = 0.15 meq/g. Rw was determined using Pickett plots from water zone at 3077-3177 m. Rw = 0.1 @ 77 degC was picked. Jamieson Formation and Upper Vulcan Formation : No sonic curve hence no porosity and water saturation were calculated.

Appendix 5

Net Pay-Reservoir-Sand Summaries

Well	Depth (m)		Gross Thickness (m)	Potential Net Pay					Potential Net Reservoir					Potential Net Sand				
	Top	Base		Thickness (m)	Net to Gross	Shale Volume Average	Effective Porosity Average	Total Water Saturation Average	Thickness	Net to Gross	Shale Volume Average	Effective Porosity Average	Total Water Saturation Average	Thickness (m)	Net to Gross	Shale Volume Average	Effective Porosity Average	Total Water Saturation Average
Puffin Formation																		
Abalone-1	2767	3370	603.00	5.64	0.01	0.14	0.19	0.39	141.03	0.23	0.25	0.16	0.87	152.91	0.25	0.25	0.16	0.87
Adele-1	1597	2361	764.00	0.00	0.00	-	-	-	364.39	0.48	0.16	0.25	0.98	364.39	0.48	0.16	0.25	0.98
Argus-1	4044	4242	198.00	8.40	0.04	0.01	0.26	0.49	111.43	0.56	0.24	0.19	0.89	111.43	0.56	0.24	0.19	0.89
Asterias-1	1929	2773	844.00	1.52	0.00	0.02	0.30	0.59	23.62	0.03	0.16	0.16	0.91	511.91	0.61	0.18	0.14	0.90
Bassett-1A	1832	2499.5	667.50	0.00	0.00	-	-	-	545.81	0.82	0.14	0.23	0.96	548.70	0.82	0.14	0.23	0.97
Buffon-1	3419	3488	69.00	0.00	0.00	-	-	-	44.75	0.65	0.25	0.17	0.99	44.90	0.65	0.25	0.17	0.99
Crux-1	1509	2120	611.00	0.00	0.00	-	-	-	0.00	0.00	-	-	-	387.39	0.63	0.23	-	-
Delta-1	1980	2888	908.00	28.80	0.03	0.13	0.21	0.41	576.79	0.64	0.03	0.26	0.93	581.52	0.64	0.03	0.26	0.93
Discorbis-1	2339	3443	1104.00	51.36	0.05	0.34	0.13	0.51	598.32	0.54	0.22	0.21	0.91	614.63	0.56	0.22	0.20	0.91
Gryphaea-1	2249	3297.5	1048.50	69.34	0.07	0.25	0.19	0.54	523.95	0.50	0.20	0.21	0.82	534.01	0.51	0.20	0.21	0.82
Heywood-1	1572	2244	672.00	31.24	0.05	0.23	0.20	0.52	424.35	0.63	0.17	0.23	0.88	433.49	0.65	0.17	0.23	0.88
Kalyptea-1ST1	2333	3446	1113.00	127.41	0.11	0.14	0.16	0.46	558.70	0.50	0.15	0.20	0.82	571.81	0.51	0.15	0.20	0.82
Mount Ashmore-1B	1553	1805	252.00	12.62	0.05	0.21	0.18	0.57	142.12	0.56	0.15	0.17	0.77	152.08	0.60	0.16	0.16	0.77
Phrixus-1	3330	3779	449.00	0.00	0.00	-	-	-	84.44	0.19	0.21	0.19	0.91	85.05	0.19	0.21	0.19	0.91
Productus-1	1153	1610	457.00	0.00	0.00	-	-	-	231.78	0.51	0.14	0.26	1.00	231.78	0.51	0.14	0.26	1.00
Turbo-1	2609	3220	611.00	2.90	0.01	0.20	0.20	0.53	250.30	0.41	0.14	0.21	0.97	253.85	0.42	0.14	0.20	0.97
		Average	**648.19**	**33.92**	**0.04**	**0.17**	**0.20**	**0.50**	**308.12**	**0.48**	**0.17**	**0.21**	**0.91**	**348.74**	**0.54**	**0.18**	**0.20**	**0.91**
Fenelon/Gibson Formation																		
Abalone-1	3370	3424	54.00	8.53	0.16	0.12	0.16	0.54	54.00	1.00	0.16	0.14	0.72	54.00	1.00	0.16	0.14	0.72
Adele-1	2361	2540	179.00	9.30	0.05	0.17	0.25	0.57	92.81	0.52	0.22	0.23	0.72	92.81	0.52	0.22	0.23	0.72
Asterias-1	2773	2931	158.00	0.00	0.00	-	-	-	39.62	0.25	0.32	0.11	0.84	48.89	0.31	0.31	0.10	0.84
Bassett-1A	2499.5	2656	156.50	0.00	0.00	-	-	-	156.50	1.00	0.11	0.24	0.80	156.50	1.00	0.11	0.24	0.80
Crux-1	2120	2337	217.00	0.00	0.00	-	-	-	0.00	0.00	-	-	-	1.68	0.01	0.37	0.06	0.97
Discorbis-1	3443	3521	78.00	67.36	0.86	0.23	0.11	0.51	70.05	0.90	0.23	0.11	0.51	78.00	1.00	0.23	0.10	0.52
Gryphaea-1	3297.5	3342	44.50	0.00	0.00	-	-	-	19.36	0.44	0.25	0.10	0.71	27.27	0.61	0.27	0.08	0.75
Heywood-1	2244	2279	35.00	4.51	0.13	0.24	0.17	0.53	5.57	0.16	0.26	0.17	0.55	5.57	0.16	0.26	0.17	0.55
Kalyptea-1ST1	3446	3553	107.00	0.00	0.00	-	-	-	4.27	0.04	0.35	0.09	0.66	4.27	0.04	0.35	0.09	0.66
Phrixus-1	3779	3803	24.00	0.00	0.00	-	-	-	24.00	1.00	0.07	0.20	-	24.00	1.00	0.07	0.20	-
Productus-1	1610	1640	30.00	0.00	0.00	-	-	-	0.00	0.00	-	-	-	0.00	0.00	-	-	-
Turbo-1	3220	3232	12.00	0.00	0.00	-	-	-	4.45	0.37	0.11	0.15	-	4.85	0.40	0.11	0.15	-
		Average	**91.25**	**22.42**	**0.30**	**0.19**	**0.17**	**0.53**	**47.06**	**0.57**	**0.21**	**0.15**	**0.69**	**45.26**	**0.55**	**0.22**	**0.14**	**0.72**

Well	Depth (m)		Gross Thickness (m)	Potential Net Pay					Potential Net Reservoir					Potential Net Sand				
	Top	Base		Thickness (m)	Net to Gross	Shale Volume Average	Effective Porosity Average	Total Water Saturation Average	Thickness	Net to Gross	Shale Volume Average	Effective Porosity Average	Total Water Saturation Average	Thickness (m)	Net to Gross	Shale Volume Average	Effective Porosity Average	Total Water Saturation Average
Woolaston Formation																		
Abalone-1	3424	3431	7.00	0.00	0.00	-	-	-	7.00	1.00	0.25	0.20	0.87	7.00	1.00	0.25	0.20	0.87
Asterias-1	2931	2942	11.00	0.00	0.00	-	-	-	5.02	0.46	0.31	0.12	0.70	7.04	0.64	0.32	0.11	0.71
Bassett-1A	2656	2670	14.00	0.00	0.00	-	-	-	13.24	0.95	0.26	0.18	0.85	13.24	0.95	0.26	0.18	0.85
Crux-1	2337	2388	51.00	0.00	0.00	-	-	-	0.00	0.00	-	-	-	0.00	0.00	-	-	-
Discorbis-1	3521	3560	39.00	24.08	0.62	0.21	0.10	0.49	23.17	0.59	0.21	0.11	0.48	29.54	0.76	0.23	0.10	0.50
Gryphaea-1	3342	3359	17.00	13.33	0.78	0.10	0.12	0.49	16.53	0.97	0.10	0.11	0.51	17.00	1.00	0.10	0.11	0.51
Kalyptea-1ST1	3553	3574	21.00	0.00	0.00	-	-	-	0.00	0.00	-	-	-	0.00	0.00	-	-	-
Phrixus-1	3803	3822	19.00	0.00	0.00	-	-	-	18.85	0.99	0.13	0.18	-	18.85	0.99	0.13	0.18	-
Productus-1	1640	1736	96.00	0.00	0.00	-	-	-	0.00	0.00	-	-	-	0.00	0.00	-	-	-
		Average	**30.56**	**18.70**	**0.70**	**0.16**	**0.11**	**0.49**	**13.97**	**0.83**	**0.21**	**0.15**	**0.68**	**15.44**	**0.89**	**0.21**	**0.15**	**0.69**
Jamieson Formation																		
Abalone-1	3431	4724	1293.00	2.29	0.00	0.20	0.21	0.53	250.60	0.19	0.28	0.19	0.94	272.70	0.21	0.28	0.18	0.94
Adele-1	2540	3415	875.00	148.29	0.17	0.36	0.18	0.53	634.82	0.73	0.34	0.19	0.76	634.82	0.73	0.34	0.19	0.76
Argus-1	4242	4536	294.00	2.59	0.01	0.27	0.22	0.44	192.22	0.65	0.34	0.19	0.98	192.22	0.65	0.34	0.19	0.98
Asterias-1	2942	3392	450.00	15.04	0.03	0.35	0.15	0.51	181.17	0.40	0.36	0.19	0.78	181.17	0.40	0.36	0.19	0.78
Bassett-1A	2670	2706	36.00	0.00	0.00	-	-	-	29.69	0.83	0.08	0.28	1.00	29.69	0.83	0.08	0.28	1.00
Buffon-1	3488	3776	288.00	0.00	0.00	-	-	-	54.62	0.19	0.33	0.20	0.97	55.23	0.19	0.33	0.20	0.97
Crux-1	2388	2591.5	203.50	0.00	0.00	-	-	-	6.71	0.03	0.36	0.14	0.66	6.71	0.03	0.36	0.14	0.66
Discorbis-1	3560	3855	295.00	1.83	0.01	0.17	0.22	0.53	208.60	0.71	0.29	0.18	0.94	208.60	0.71	0.29	0.18	0.94
Gryphaea-1	3359	3636	277.00	6.25	0.02	0.25	0.20	0.54	41.23	0.15	0.33	0.19	0.68	46.26	0.17	0.31	0.18	0.69
Heywood-1	2279	3089	810.00	47.63	0.06	0.35	0.17	0.47	404.77	0.50	0.36	0.19	0.79	404.77	0.50	0.36	0.19	0.79
Kalyptea-1ST1	3574	4035	461.00	6.25	0.01	0.25	0.20	0.51	427.01	0.93	0.29	0.18	0.81	434.32	0.94	0.29	0.17	0.81
Mount Ashmore-1B	1805	1921	116.00	0.00	0.00	-	-	-	39.37	0.34	0.29	0.17	0.81	54.97	0.47	0.23	0.14	0.82
Phrixus-1	3822	3866	44.00	0.00	0.00	-	-	-	6.21	0.14	0.23	0.22	-	6.21	0.14	0.23	0.22	-
Productus-1	1736	2028	292.00	1.22	0.00	0.09	0.27	0.59	177.09	0.61	0.30	0.21	0.92	182.12	0.62	0.30	0.20	0.92
Turbo-1	3232	3567	335.00	0.00	0.00	-	-	-	0.00	0.00	-	-	-	31.50	0.09	0.23	-	-
		Average	**404.63**	**25.71**	**0.04**	**0.25**	**0.20**	**0.52**	**189.58**	**0.46**	**0.30**	**0.19**	**0.85**	**193.56**	**0.47**	**0.29**	**0.19**	**0.85**

Well	Depth (m)		Gross Thickness (m)	Potential Net Pay					Potential Net Reservoir					Potential Net Sand				
	Top	Base		Thickness (m)	Net to Gross	Shale Volume Average	Effective Porosity Average	Total Water Saturation Average	Thickness	Net to Gross	Shale Volume Average	Effective Porosity Average	Total Water Saturation Average	Thickness (m)	Net to Gross	Shale Volume Average	Effective Porosity Average	Total Water Saturation Average
Echuca Shoals Formation																		
Abalone-1	4724	4790	66.00	0.00	0.00	-	-	-	4.42	0.07	0.32	0.14	0.65	8.83	0.13	0.27	0.10	0.68
Adele-1	3415	3858	443.00	60.99	0.14	0.22	0.19	0.38	64.34	0.15	0.22	0.19	0.39	64.34	0.15	0.22	0.19	0.39
Asterias-1	3392	3674	282.00	15.09	0.05	0.24	0.15	0.34	85.04	0.30	0.12	0.18	0.74	88.09	0.31	0.12	0.18	0.73
Crux-1	2591.5	2690	98.50	0.00	0.00	-	-	-	8.53	0.09	0.26	0.13	0.84	10.06	0.10	0.26	0.11	0.84
Discorbis-1	3855	3974	119.00	0.00	0.00	-	-	-	13.60	0.11	0.29	0.13	0.93	13.60	0.11	0.29	0.13	0.93
Heywood-1	3089	3290	201.00	11.95	0.06	0.33	0.13	0.51	75.73	0.38	0.33	0.14	0.69	77.71	0.39	0.33	0.14	0.69
Kalyptea-1ST1	4035	4312	277.00	16.46	0.06	0.09	0.15	0.43	45.59	0.17	0.20	0.14	0.62	53.36	0.19	0.21	0.13	0.61
Mount Ashmore-1B	1921	1954	33.00	2.58	0.08	0.31	0.09	0.52	11.25	0.34	0.35	0.09	0.78	32.24	0.98	0.24	0.05	0.82
		Average	**189.94**	**21.41**	**0.08**	**0.24**	**0.14**	**0.44**	**38.56**	**0.20**	**0.26**	**0.14**	**0.70**	**43.53**	**0.30**	**0.24**	**0.13**	**0.71**
Upper Vulcan Formation																		
Adele-1	3858	4365	507.00	1.07	0.00	0.34	0.12	0.54	2.29	0.01	0.34	0.14	0.54	2.29	0.01	0.34	0.14	0.54
Asterias-1	3674	4400	726.00	143.09	0.20	0.20	0.12	0.32	158.17	0.22	0.20	0.12	0.32	190.94	0.26	0.22	0.11	0.33
Crux-1	2690	3154.5	464.50	19.05	0.04	0.35	0.08	0.55	195.53	0.42	0.33	0.09	0.69	293.98	0.63	0.33	0.08	0.70
Discorbis-1	3974	4070	96.00	0.00	0.00	-	-	-	0.00	0.00	-	-	-	0.00	0.00	-	-	-
Heywood-1	3290	4068	778.00	430.77	0.55	0.23	0.09	0.40	453.33	0.58	0.22	0.10	0.44	686.26	0.88	0.23	0.09	0.44
Kalyptea-1ST1	4312	4570	258.00	33.38	0.13	0.21	0.11	0.21	28.19	0.11	0.20	0.12	0.20	50.29	0.20	0.22	0.09	0.23
Mount Ashmore-1B	1954	1981	27.00	0.00	0.00	-	-	-	0.00	0.00	-	-	-	2.62	0.10	0.29	0.00	-
		Average	**408.07**	**125.47**	**0.18**	**0.27**	**0.10**	**0.40**	**167.50**	**0.27**	**0.26**	**0.11**	**0.44**	**204.40**	**0.35**	**0.27**	**0.08**	**0.45**
Lower Vulcan Formation																		
Adele-1	4365	4424	59.00	14.26	0.24	0.19	0.15	0.11	14.80	0.25	0.20	0.15	0.13	50.92	0.86	0.25	0.06	0.23
Argus-1	4536	4700	164.00	10.36	0.06	0.00	0.15	0.50	55.58	0.34	0.08	0.16	0.69	65.95	0.40	0.08	0.15	0.70
Crux-1	3154.5	3591	436.50	0.00	0.00	-	-	-	0.00	0.00	-	-	-	0.00	0.00	-	-	-
Discorbis-1	4070	4110	40.00	0.00	0.00	-	-	-	0.00	0.00	-	-	-	0.00	0.00	-	-	-
Heywood-1	4068	4220	152.00	34.23	0.23	0.17	0.08	0.26	31.48	0.21	0.17	0.08	0.25	132.07	0.87	0.17	0.05	0.25
Mount Ashmore-1B	1981	2120	139.00	0.00	0.00	-	-	-	58.98	0.42	0.22	0.18	0.92	68.99	0.50	0.23	0.15	0.92
Turbo-1	3567	3576	9.00	0.00	0.00	-	-	-	0.00	0.00	-	-	-	0.00	0.00	-	-	-
		Average	**142.79**	**19.62**	**0.18**	**0.12**	**0.13**	**0.29**	**40.21**	**0.31**	**0.17**	**0.14**	**0.50**	**79.48**	**0.66**	**0.18**	**0.10**	**0.52**
Plover Formation																		
Argus-1	4700	4877	177.00	13.11	0.07	0.21	0.16	0.43	101.80	0.58	0.26	0.15	0.78	160.48	0.91	0.20	0.13	0.78
Buffon-1	3776	4787	1011.00	44.65	0.04	0.14	0.17	0.45	588.51	0.58	0.17	0.14	0.78	934.91	0.93	0.15	0.10	0.79
Crux-1	3591	3640	49.00	0.00	0.00	-	-	-	0.00	0.00	-	-	-	0.00	0.00	-	-	-
		Average	**412.33**	**28.88**	**0.06**	**0.17**	**0.16**	**0.44**	**345.16**	**0.58**	**0.22**	**0.15**	**0.78**	**547.70**	**0.92**	**0.18**	**0.11**	**0.79**
Nome Formation																		
Crux-1	3640	3961	321.00	167.34	0.52	0.07	0.12	0.08	204.83	0.64	0.06	0.11	0.21	264.72	0.83	0.10	0.10	0.24
Mount Ashmore-1B	2120	2444	324.00	0.00	0.00	-	-	-	74.18	0.23	0.14	0.12	0.92	171.76	0.53	0.21	0.07	0.93
		Average	**322.50**	**167.34**	**0.52**	**0.07**	**0.12**	**0.08**	**204.83**	**0.64**	**0.06**	**0.11**	**0.21**	**264.72**	**0.83**	**0.10**	**0.10**	**0.24**